Stony Brook University

Study of Phosphatidylinositol 3-Kinase in the Regulation of Autophagy

A Dissertation Presented

by

Zhixun Dou

to

The Graduate School

in Partial Fulfillment of the

Requirements

for the Degree of

Doctor of Philosophy

in

Molecular and Cellular Biology

Stony Brook University

August 2012

Stony Brook University

The Graduate School

Zhixun Dou

We, the dissertation committee for the above candidate for the

Doctor of Philosophy degree, hereby recommend

acceptance of this dissertation.

Dr. Wei-Xing Zong, Dissertation Advisor
Associate Professor, Department of Molecular Genetics and Microbiology

Dr. Richard Z. Lin, Chairperson of Defense
Professor, Department of Medicine

Dr. Deborah A. Brown
Associate Professor, Department of Biochemistry and Cell Biology

Dr. Michael A. Frohman
Professor, Department of Pharmacological Sciences

Dr. Howard C. Crawford
Associate Professor, Department of Research, Cancer Biology
Mayo Clinic

This dissertation is accepted by the Graduate School

Charles Taber
Interim Dean of the Graduate School

Abstract of the Dissertation

Study of Phosphatidylinositol 3-Kinase in the Regulation of Autophagy

by

Zhixun Dou

Doctor of Philosophy

in

Molecular and Cellular Biology

Stony Brook University

2012

Autophagy is an evolutionarily conserved membrane trafficking process that maintains cell and tissue homeostasis. Autophagy plays essential roles in response to starvation and stress, and is involved in organelle homeostasis. Dysregulation of autophagy is implicated in diseases such as neurodegeneration and cancer. The induction of autophagy depends on phosphatidylinositol 3-phosphate (PI(3)P), the product of the Class III Phosphatidylinositol 3-Kinase (PI3K), Vps34. In metazoans, autophagy is thought to be inhibited by Class I PI3Ks, which are activated by cell surface trophic factor receptors and produce $PI(3,4,5)P_3$ that activates the Akt-TOR kinase cascade and negatively regulates autophagy. Class IA PI3Ks are heterodimeric proteins consisting of an 85-kD regulatory subunit and a 110-kD catalytic subunit. During the course of my dissertation research, I discovered a previously unknown role of the Class IA p110β catalytic subunit as a positive regulator of autophagy. Upon trophic factor limitation, p110β dissociates from trophic factor receptor complexes, and increases its interaction with the small GTPase Rab5. This p110β-Rab5 association sequesters Rab5 from its GTPase activating proteins and enhances the Rab5-Vps34 interaction, which in turn activates Vps34 and promotes autophagy. Genetic deletion of p110β results in impaired autophagy in mouse embryonic fibroblasts, liver, and heart. This p110β-mediated autophagy is independent of the Akt-TOR pathway. These results unveiled a previously unknown function for p110β as a positive regulator of autophagy, and suggested a new mechanism of autophagy induction in response to trophic factor limitation.

Dedication Page

I would like to dedicate this dissertation to my wife, Dr. Peiwen Zheng. Her love and support have always been of tremendous help of my research. She is a successful scientist and a great person who helped me through the hard time and inspired my passion of exploring the unknown.

Table of Contents

List of Figures

List of Abbreviations

3-MA	3-methyladenine
AMPK	AMP-activated protein kinase
Atg	autophagy-related gene
Baf A1	bafilomycin A1
DFCP1	double FYVE domain-containing protein 1
EGF	epidermal growth factor
ER	Endoplasmic Reticulum
FBS	fetal bovine serum
GAP	GTPase activating protein
GEF	guanine nucleotide exchange factor
GFP	green fluorescent protein
GPCR	G-protein-coupled-receptor
IGF	Insulin-like growth factor
IRS	insulin receptor substrate
KO	knockout
LC3	microtubule-associated protein 1 light chain 3
LPA	lysophosphatidic acid
MEF	mouse embryonic fibroblast
PDGF	Platelet-derived growth factor
PE	phosphatidylethanolamine
PH domain	pleckstrin homology domain
PI	phosphatidylinositol
PI3K	Phosphatidylinositol 3-Kinase
PTEN	phosphatase and tensin homologue deleted on chromosome ten
R5BD	Rab5-binding domain
ROS	Reactive oxygen species
RTK	receptor tyrosine kinase
TAC	Transverse aortic constriction
TCA	trichloroacetic acid
TEM	transmission electron microscopy
TOR	target of rapamycin
WT	wild-type

Acknowledgments

I would like to acknowledge Dr. Wei-Xing Zong for giving me the great opportunity to work in his lab, and for his constant advice and support. I thank the past lab members Dr. Jennifer Guerriero for her guidance during my lab rotation and for her assistance on animal experiments, Dr. Erica Ullman for help on autophagy assays, and Dr. Yongjun Fan for his patient help on a variety of experiments. I would also like to thank the current lab members, Dr. Ji-An Pan for his tremendous support throughout the project and making the lab an enjoyable place to work in, Juei-Suei Chen for her kind assistance, Joseph Catanzaro, Namratha Sheshadri, Nadia Jaber and Jennifer DeLeon for technical assistance and fruitful discussions.

I thank Dr. Richard Lin and his lab for wonderful advice and support. My work on PI3K would be impossible without their input. Specially, I thank Dr. Lisa Ballou for her critical assistance on PI3K and Rab5 activity assays, Dr. Ya-Ping Jiang for heart experiments, Dr. Chia-Yen Wu for technical help, and the past member Elzbieta Selinger and Dr. Mohar Chattopadhyay for liver experiments. I feel very lucky to have such great collaboration during my thesis research.

I would like to thank my thesis committee members Dr. Howard Crawford for many constructive and critical input of my research and for the help from his laboratory, Dr. Deborah Brown for advice and sharing reagents, Dr. Michael Frohman for the encouragement and discussions. I also thank members of the microscopy center, Susan Van Horn and Dr. Guowei Tian for assistance on imaging. I specially thank Susan for her excellent expertise on electron microscopy. My work on autophagy cannot be done without her help.

In addition, I thank collaborators outside Stony Brook, Dr. Zhenyu Yue for sharing ideas and many reagents, Dr. Jonathan Backer and his laboratory for help on PI3K assays, Dr. Guangpu Li for reagents and assays on Rab5.

Moreover, I thank my previous mentors Dr. Youjia Cao and Dr. Zhuo Zhou for their guidance and advice. My undergraduate training in Dr. Cao's laboratory inspired my motivation for scientific research and well prepared me for graduate study.

I would never forget my first biology teacher in my senior high school, Yanhui Liu, who lightened my strong interest in biology and spent a lot of extra time on training me. I was determined to pursue biology since then.

Last but not the least, I thank my parents for their caring, understanding and confidence on me. I would have never completed my Ph.D. study without their support.

Publications

Dou Z, Pan J-A, Dbouk HA, Ballou LM, DeLeon JL, Fan Y, Chen J-S, Li G, Backer JM, Lin RZ, Zong W-X. Class IA phosphoinositide 3-kinase p110β subunit promotes autophagy through Rab5 small GTPase in response to trophic factor limitation. *Manuscript submitted*.

Jaber N, **Dou Z**, Lin RZ, Zhang J, Zong W-X. Mammalian PIK3C3/VPS34: The key to autophagic processing in liver and heart. **Autophagy**. 2012 Apr 1;8(4).

Jaber N, **Dou Z**, Chen J-S, Catanzaro JM, Jiang Y-P, Ballou LM, Selinger E, Ouyang X, Lin RZ, Zhang J, Zong W-X. The Class III PI3K Vps34 plays an essential role in autophagy and in the heart and liver function. **Proc Natl Acad Sci U S A**. 2012 Feb 7;109(6):2003-8.

Pan J-A, Ullman E, **Dou Z**, Zong W-X. Inhibition of protein degradation induces apoptosis through an LC3-mediated activation of caspase-8 at intracellular membranes. **Mol Cell Biol**. 2011 Aug;31(15):3158-70.

Dou Z, Pan J-A, Lin RZ, Zong W-X. The beta identity of class I PtdIns3K: A positive role of p110β in autophagy revealed. **Autophagy**. 2011 Feb;7(2):246-7.

Dou Z, Chattopadhyay M, Pan J-A, Guerriero JL, Jiang Y-P, Ballou LM, Yue Z, Lin RZ, Zong W-X. The Class IA phosphatidylinositol 3-kinase p110β subunit is a positive regulator of autophagy. **J Cell Biol**. 2010 Nov 15;191(4):827-43.

I. Introduction

1) Introduction to phosphatidylinositol 3-kinases (PI3Ks)

Phosphatidylinositol 3-kinases (PI3Ks) are lipid kinases that phosphorylate the 3'-hydroxyl group of phosphatidylinositol and phosphoinositides (Cantley, 2002; Fruman et al., 1998). The generated phospholipids are critical signaling molecules that bind to a variety of proteins containing lipid binding domains (Engelman et al., 2006; Fruman et al., 1998). The interaction with phospholipids generally recruits proteins to specific cellular membranes, e.g., plasma membrane, endosome, endoplasmic reticulum (ER). In addition, phospholipids may serve as structure components of cellular membranes that are critical for membrane morphologies and functions. As such, the phospholipids produced by PI3Ks regulate a large array of cellular functions as diverse as vesicle trafficking, cytoskeletal organization, metabolism, survival, proliferation and differentiation.

Based on substrate specificity and sequence homology, PI3Ks are grouped into three classes: Class I, Class II, and Class III (Domin and Waterfield, 1997; Engelman et al., 2006), which utilizes different lipid substrates and possess diverse cellular activities. The following three sections will describe each class of PI3K with respect to their substrate preference, structure, and function.

(1) Class I PI3Ks

The in vivo preferred substrate of Class I PI3Ks is thought to be $PI(4,5)P_2$, and Class I PI3K phosphorylate it into $PI(3,4,5)P_3$ (Carpenter et al., 1990). In some in vitro assays, Class I PI3Ks are able to phosphorylate PI and PI(4)P. However, the in vivo relevance of these activities is not clear. Class I PI3Ks are further divided into two groups, Class IA and Class IB. Class IA PI3Ks respond to both receptor tyrosine kinases (RTKs) and G-protein-coupled-receptor (GPCRs), and are composed of a p85 regulatory subunit and a p110 catalytic subunit (p110α, β, δ). Class IB PI3Ks respond only to GPCRs and consist of a p101 regulatory subunit and p110γ catalytic subunit (Engelman et al., 2006). Among these p110 catalytic subunits, p110α and p110β isoforms are ubiquitously expressed, whereas the p110δ and p110γ expressions are restricted and mainly function in hematopoietic cells (Engelman et al., 2006; Vanhaesebroeck et al., 2012). The p110 catalytic subunit possesses an N-terminal p85 binding domain, a Ras binding domain, a C2 domain, a helical domain, and a C-terminal catalytic domain. The p85 regulatory subunit is composed of an N-terminal SH3 domain, a BH domain, and the p110 binding domain flanked by two SH2 domains. The interaction of p110s with p85s stabilizes p110s, and inactivates their catalytic activity (Yu et al., 1998). In vivo, p110s are obligated heterodimers with p85s (Geering et al., 2007). Upon trophic factor receptor activation, e.g., through RTKs, the SH2 domain of p85 associates with activated receptor and recruits p110s to the localized plasma membrane. The p110-p85 interaction with receptor relieves p110s from the inhibition posed by p85, which produce $PI(3,4,5)P_3$ in the localized plasma membrane microdomains (Vadas et al., 2011). The mechanisms of recruitment and activation of p110-p85 by GPCRs are relatively less well understood. This interaction may be mediated through direct heterodimeric G proteins binding to p110.

Once $PI(3,4,5)P_3$ is present, it serves as a second messenger to recruit a number of downstream effector proteins to the plasma membrane, such as PDK1 and Akt (Franke et al., 1997). Plasma membrane-bound Akt is phosphorylated by PDK1, and activates a number of targets, including glucose transporters that mediates glucose uptake, FOXO family transcription

factors that regulates cell cycle and metabolism, and tuberous sclerosis complex (TSC) that regulates activation of mammalian target of rapamycin (mTOR) (Cantley, 2002). mTOR complex activation leads to phosphorylation of S6 and 4-EBP which ultimately promote protein synthesis (Sarbassov et al., 2005).

Class I PI3Ks/Akt/mTOR pathways are frequently altered in cancers. PTEN, a phosphatase that converts $PI(3,4,5)P_3$ to $PI(4,5)P_2$ and thus antagonizes Class I PI3K signalings, is a tumor suppressor that is commonly lost or down-regulated in a large panel of cancers (Li et al., 1997). Mutation or amplification of the p110α catalytic subunit is common in human cancers such as in colon and breast (Isakoff et al., 2005; Sartore-Bianchi et al., 2009). Gain of function mutation of p85 has recently been found in endometrial cancers that have altered the PTEN-PI3K pathways (Urick et al., 2011). Akt mutation is frequently observed in breast and ovary cancers (Altomare et al., 2004; Bose et al., 2006). Loss of function of TSC1/2 is associated with tuberous sclerosis (Green et al., 1994). In addition, many other oncogenic signaling pathways, such as those mediated by Ras, EGFR, are intimately connected with the Class I PI3Ks/Akt/mTOR cascades (Engelman et al., 2006; Kodaki et al., 1994; Sartore-Bianchi et al., 2009). Pharmacological inhibition of Class I PI3Ks is therefore under intensive investigation in clinic.

As a central mediator of cell activation, Class I PI3Ks are regulated at multiple layers. In addition to the activation by trophic factor receptors, p110s are known to be regulated by small GTPase, such as Ras and Rab (Christoforidis et al., 1999b; Kodaki et al., 1994). Ras has been shown to directly associate with p110α and p110γ through the Ras-binding domain, and potentiates the kinase activities of p110 (Castellano and Downward, 2011). The association of p110α and Ras appeared to be critical for certain scenarios of oncogenesis (Gupta et al., 2007). Point mutations of p110α in the Ras-binding domain that abrogated the Ras association impaired Akt activation and tumor initiation in the lung driven by Ras (Gupta et al., 2007). In addition, p110β is regulated by Rab5 (Christoforidis et al., 1999b), as described in later sections. Class I PI3Ks are also down-regulated by several mechanisms. The activation of mTOR complex 1 (mTORC1) negatively regulates growth factor receptors and Class I PI3K activation, providing a necessary negative feedback for cellular activation (Jaeschke et al., 2002; Werner et al., 2004; Zhang et al., 2003). In response to stress, such as amino acids deprivation, IKK phosphorylates p85 and inhibits the receptor association of p85, leading to diminished p110 catalytic activities (Comb et al., 2012). Persistent PKC and PKD activation also phosphorylate p85 and inhibit PI3K signalings (Lee et al., 2011). Moreover, calpain, a calcium-dependent protease, is recently shown to cleave p110α and suppress the activation of Akt (Beltran et al., 2011).

While the importance of PI3Ks has been demonstrated by PI3K inhibitors, such as wortmannin, the specific roles of Class I PI3Ks are not established until the genetic modification of individual p110 and p85 isoforms. Mice homozygous for p110α or p110β gene deletion are embryonic lethal (Bi et al., 2002; Graupera et al., 2008), whereas genetic deletion of p110δ or p110γ mainly showed defects in leukocyte functions (Ali et al., 2004; Chang et al., 2007). Mice with both alleles of p110α kinase-dead knockin are embryonic lethal, which is attributed to the deficiency in embryonic angiogenesis (Graupera et al., 2008). Mice with one allele of p110α kinase-dead knockin showed growth retardation and metabolic disorders such as glucose intolerance (Foukas et al., 2006). Tissue-specific knockout of p110α in the heart results in smaller heart and reduced contractility (Lu et al., 2009). Deletion of p110α in the liver leads to

insulin resistance (Chattopadhyay et al., 2011; Sopasakis et al., 2010). These results suggest a specific and pivotal role of p110α in growth factor mediated activation of Akt under physiological conditions. In contrary to p110α kinase-dead knockin mice, p110β kinase-dead knockin mice are viable, but showed growth retardation (Ciraolo et al., 2008). As the p110β knockout mice are lethal, this observation strongly supports a kinase-independent function of p110β. The mechanism of the kinase-independent activity is not understood and will be one of the questions to address in this dissertation. Liver-specific deletion of p110β leads to hyperglycemia and insulin resistance (Chattopadhyay et al., 2011; Jia et al., 2008). Deletion of p110β blocks prostate cancer driven by PTEN loss (Jia et al., 2008). These physiological and pathological roles of p110β may be exerted through both its kinase activity and kinase-independent activity.

Genetic deletion of p110 isoforms in mice also revealed divergent roles of p110α and p110β catalytic subunits. Besides the phenotypes described above, p110α-deficient cells showed impaired activation of Akt by RTKs, while the activation by GPCRs remained intact (Guillermet-Guibert et al., 2008; Jia et al., 2008; Zhao et al., 2006). By contrast, p110β seems to play a major role under GPCR-mediated activation, and that the stimulation of Akt by RTK is largely intact (Guillermet-Guibert et al., 2008; Jia et al., 2008), although the p110β kinase-dead knockin cells showed minor deficiency in sustained insulin-mediated Akt activation (Ciraolo et al., 2008). The crystal structure of p110β-p85 complex revealed a stronger inhibition of p85 on p110β catalytic activities under conditions stimulated by RTK, e.g., by phospho-peptides, which may attribute to the less sensitivity of p110β to RTK stimulations (Zhang et al., 2011). In addition to the different responses to trophic factors, the scaffold activity of p110β is also noted. The kinase-dead p110β is able to rescue some defects of the p110β-deficient cells in cell growth, endocytosis, and mTOR activation (Ciraolo et al., 2008; Jia et al., 2008). Moreover, it is noteworthy that activation mutations of p110α are frequently observed in human cancer (Engelman et al., 2006), while such mutations of p110β have not been reported.

(2) Class II PI3Ks

Class II PI3Ks are composed of three members, PIK3C2α, β, and γ. The expression of C2α and β are ubiquitous, whereas that of C2γ is high in liver and prostate (Falasca and Maffucci, 2012). They are large monomeric enzymes that share certain sequence homology with Class I PI3K p110 catalytic subunits, but are characterized by an extra C-terminal PX and C2 domain and the lack of regulatory subunit binding domains. In vitro, they can phosphorylate PI, PI(4)P, and PI(5)P, but not PI(4,5)P_2. In vivo, the preferred substrate is suggested to be PI (Falasca and Maffucci, 2012). Downregulation of Class II PI3Ks in mammalian cells blocked growth factor stimulation-induced plasma membrane translocation of GFP-FYVE, a probe for PI(3)P (Maffucci et al., 2005). Genetic deletion of Class II PI3K in Drosophila resulted in decrease cellular PI(3)P (Velichkova et al., 2010). Class II PI3Ks bind to clathrin coated pits, and play a role in endocytosis and membrane trafficking (Domin et al., 2000; Gaidarov et al., 2001). Class II PI3Ks are also reported to be activated by membrane receptors (Arcaro et al., 2000; Gaidarov et al., 2001; Wheeler and Domin, 2001). Although studies in cell lines revealed multiple functions of Class II PI3Ks, in vivo evidence supporting these roles are not fully established.

Mice lacking C2α and C2β have recently been described. Unlike Class IA PI3K p110α and p110β knockouts, the PIK3C2α deficient mice do not show defects in embryonic

development, but show postnatal lethality (Harris et al., 2011). The C2α-deficient mice are smaller in size and showed progressive renal failure, due to glomerulonephropathy and podocyte injury (Harris et al., 2011). Although possessing an altered hematological profile, the mice showed essentially normal immune response, suggesting that C2α is dispensable for leukocyte activation (Harris et al., 2011). The mechanisms underlying the renal failure and podocyte injury are not fully understood, but are suggested to be through altered membrane trafficking and endocytosis. The C2β-deficient mice were viable and fertile and did not display major noticeable defects (Harada et al., 2005). Despite a role of C2β in epidermal cells as indicated in cell lines, the C2β-deficient mice displayed normal epidermal growth, differentiation, and functions, such as would healing, indicating that C2β is not essential for epidermal differentiation (Harada et al., 2005). The exact roles of C2β in vivo remained to be identified. To my knowledge, no C2γ knockout mice have been reported to date.

(3) Class III PI3K

Class III PI3K consists of only one member, Vps34. Its only substrate is PI, both in vitro and in vivo. Vps34 phosphorylates PI into PI(3)P. Vps34 is the only PI3K so far reported to be evolutionary conserved from yeast to mammals. It is composed of an N-terminal C2 domain, a helical domain, and the kinase domain (Backer, 2008). Unlike Class I or Class II PI3Ks, Vps34 does not possess a Ras-binding domain. Instead, it associates with its regulatory subunit Vps15, which regulates its catalytic activity and directs it to diverse cellular membranes (Backer, 2008; Yan et al., 2009). Vps34 was first identified in a yeast mutant that is defective in vacuole protein sorting (Herman and Emr, 1990). Since then Vps34 was found to play important roles in higher eukaryotes in membrane trafficking events, such as endocytosis, endosomal maturation, and autophagy (Backer, 2008; Kihara et al., 2001b; Vieira et al., 2001).

Vps34 exerts its diverse function via its association with various binding partners. The Vps34-Vps15 association with Beclin 1 and Atg14L diverts it to the precursor autophagosome membrane where it produces localized PI(3)P, which recruits PI(3)P binding proteins to this specific membrane for autophagosome biogenesis (Itakura et al., 2008; Matsunaga et al., 2009; Sun et al., 2008; Zhong et al., 2009). This will be further described in greater details in the introduction to autophagy section. The Vps34-Vps15 interaction with UVRAG or Rubicon diverts it to the late endosome/lysosome where it regulates endocytosis and autophagosome maturation (Itakura et al., 2008; Liang et al., 2008; Matsunaga et al., 2009; Zhong et al., 2009). The interaction with Rab5 recruits the Vps34-Vps15 complex to the early endosome where localized PI(3)P is produced and recruits effector such as EEA1 to facilitate endosome sorting and maturation (Christoforidis et al., 1999b; Murray et al., 2002).

In addition to its distinct localizations, Vps34 kinase activity is regulated by multiple mechanisms. The association with its regulatory subunit Vps15 potentiates Vps34 activity (Yan et al., 2009). Unlike Class I PI3K, in which the association with p85 is mandatory for p110 stability, Vps15 acts mainly to stimulate Vps34 catalytic activity. Overexpressed Vps34 by itself possesses little activity, while co-expression of Vps15 significantly enhances its kinase activity (Yan et al., 2009). For the Vps34-Beclin 1 interaction, it is found that while all Beclin 1 associates with Vps34, only 50% of Vps34 associates with Beclin 1 (Kihara et al., 2001a). This evidence strongly suggests an autophagy-independent function of Vps34. The interaction of Beclin 1, Atg14L, and UVRAG with Vps34 has been shown to potentiate Vps34 kinase activity (Liang et al., 2006; Matsunaga et al., 2009; Zhong et al., 2009), whereas the interaction with

Rubicon inhibits it (Zhong et al., 2009). In addition, small GTPase, such as Rab5 and Rab7, has also been suggested to stimulate Vps34 in the endosomal environment, which is required for downstream effector docking to the membrane (Christoforidis et al., 1999b; Shin et al., 2005). Furthermore, Vps34 is regulated by phosphorylation, such as Cdk5, that responds to different growth factor and cell cycle clues (Furuya et al., 2010). Moreover, Vps34 activity is suggested to be regulated by calcium and amino acids, which may be implicated in amino acids stimulation of mTOR (Gulati et al., 2008). However, the mechanism by which Vps34 acts on mTOR is not fully understood.

While Vps34 clearly plays an essential role in membrane trafficking in yeast, its role in the mammalian system is not well understood. Due to the lack of specificity, the commonly used pharmacological inhibitors of Vps34, such as wortmannin or 3-methyladenine (3-MA), do not accurately indicate a specific role of Vps34. The recent generations of Vps34 knockout mice have greatly facilitated our understanding in Vps34 function in physiological settings. Homozygous deletion of Vps34 is embryonic lethal, and that the mTOR activity in the embryos are largely deficient (Zhou et al., 2011). Tissue specific deletion of Vps34 in sensory neuron leads to impaired PI(3)P production, as indicated by FYVE-GFP puncta, and neurodegeneration and lethality (Zhou et al., 2010). It was suggested that while the endosomal trafficking is severely impaired, the autophagosome formation is not (Zhou et al., 2010). Deletion of Vps34 in MEFs, liver and heart, however, indicates that Vps34 is essential for both endocytic trafficking and autophagosome formation (Jaber et al., 2012). Electron microscope analysis revealed that Vps34 deficient MEFs, liver and heart are unable to form double-membraned autophagosome (Jaber et al., 2012). Deletion of Vps34 in the liver leads to liver steatosis and hepatomegaly; deletion of Vps34 in the heart causes cardiomegaly and reduced contractility (Jaber et al., 2012). While the underlying detailed mechanisms are still under investigation, these results strongly support an essential role of Vps34 in regulating membrane trafficking events in mammals.

2) Introduction to macroautophagy

Macroautophagy (hereafter referred to as autophagy) is an evolutionary conserved process in eukaryotes. It is a catabolic membrane trafficking event that delivers molecules and organelles to lysosome for degradation (Levine and Kroemer, 2008). Autophagy starts with the formation of the double-membrane structure, termed autophagosome, that encloses cellular constituents (range from protein, lipid to mitochondrion and peroxisome) then later fuse with acidified late endosomes or lysosomes, where the enclosed content is degraded by the hydrolyses (Levine and Kroemer, 2008). In the next several paragraphs, I will briefly describe its physiological and pathological roles and its regulation at the molecular level.

(1) Physiological and pathological roles of autophagy

Autophagy is upregulated in starving cells and tissues, which digests self-content so as to provide nutrients in response to starvation. In neonates, autophagy is essential for maintaining energy homeostasis during neonatal starvation period when nutrient supply is suddenly disrupted at birth (Kuma et al., 2004). In adults, autophagy is detected between meals and plays a role in maintaining blood amino acid levels (Mizushima et al., 2008). In addition to nutrient supply, autophagy is also involved in resolving intracellular insult, such as ER stress and DNA damage, and is essential for organelle and cellular homeostasis (Levine and Kroemer, 2008; Mizushima et

al., 2008). Disruption of autophagy can cause multiple cellular anomalies, including accumulation of deformed mitochondria and elevated reactive oxygen species (ROS) level, aberrant organization of ER and ribosomes, and buildup of peroxisomes and ubiquitin aggregates in cell lines and in tissues (Komatsu et al., 2005). Moreover, autophagy has been shown as a host defense mechanism against microbial infection (Levine et al., 2011).

The importance of autophagy in physiological settings has been demonstrated in mice with genetic inactivation of genes essential for autophagy. Genetic knockout of Atg5 or Atg7 (autophagy-related genes necessary for autophagosome formation, as described in later section) leads to postnatal lethality. Forced milk feeding can largely rescue the early death (Kuma et al., 2004). Tissue specific deletion of Atg5 or Atg7 reveals essential roles of autophagy in various tissues. In liver, deficiency in autophagy causes hepatomegaly, liver steatosis, liver injury, and hepatoma (Komatsu et al., 2005). Ultra-structural analysis by electron microscope unveiled that the KO livers displayed impaired mitochondria clearance, accumulation of lipid droplets, and abnormal ER tubule (Komatsu et al., 2005). Disruption of autophagy in the heart leads to cardiomyopathy and a deficient response to pressure overload (Nakai et al., 2007). Disruption of autophagy in the muscle leads to muscle degeneration and reduced workload (He et al., 2012; Masiero et al., 2009). Genetic inactivation of autophagy in pancreatic β cells leads to insulin secretion deficiency (Jung et al., 2008). In adipose tissue, disruption of autophagy causes defective white adipose tissue development (Singh et al., 2009). Suppression of autophagy in the nervous system leads to neurodegeneration (Wong and Cuervo, 2010). Moreover, deficiency in Beclin 1, a component of the Class III PI3K Vps34 complex, leads to spontaneous tumorigenesis (Liang et al., 1999).

While the use of genetic knockout strategy provides important information on the roles of autophagy, the results from those knockout mice should be interpreted with caution. It is noteworthy that the phenotypes from knocking out different autophagy-related genes do not perfectly resemble each other. For example, while Atg5 or Atg7 knockout mice showed postnatal lethality (Kuma et al., 2004), the Beclin 1 knockout mice are embryonic lethal (Yue et al., 2003). Downregulation of Beclin 1 leads to tumor formation in multiple tissues (Yue et al., 2003), whereas mosaic deletion of Atg5 only causes liver hepatoma (Takamura et al., 2011). One possible explanation is that the autophagy-related genes may have autophagy-independent functions. Indeed, Beclin 1 has been shown to play a role in endocytosis and endosomal maturation (Liang et al., 2008; Ruck et al., 2011). Recent reports have indicated that Beclin 1 positively regulates p53 protein stability (Liu et al., 2011), and that Atg7 regulates p53 activity that controls cell cycle and stress response (Lee et al., 2012). Mice with double deficiency of Atg7 and Chk2, a p53 effector, are able to survive through the neonatal starvation period (Lee et al., 2012).

Autophagy has been implicated in human diseases. Dysfunctional autophagy has been implicated in cancer, neurodegeneration and myopathies (Mizushima et al., 2008). Alzheimer's disease and Parkinson's disease patients showed reduced Beclin 1 protein level and impaired autophagy in the brain (Cheung and Ip, 2009; Moreira et al., 2010; Pickford et al., 2008). It is acknowledged that autophagy plays an essential role in the degradation of pathogenic mutant proteins/aggregates. It is therefore of great interest to enhance autophagy for treating neurodegenerative diseases (Cheung and Ip, 2009; Santos et al., 2010). In addition, autophagy has been viewed as a tumor suppressive mechanism (Mathew et al., 2007a). Defective

autophagy leads to cellular stress, impaired mitochondria turnover, chromosome instability, and DNA damage, which ultimately promotes tumorigenesis (Inami et al., 2011; Mathew et al., 2007b; Takamura et al., 2011). At molecular level, impaired autophagy causes accumulation of its substrate SQSTM1/p62 that stimulates NFκB and other oncogenic and inflammatory pathways that facilitate tumor initiation (Mathew et al., 2009). In contrary to tumor formation, chemotherapy and radiotherapy often induce autophagy, which serves as a protective mechanism for cancer cells that leads to tumor resistance and recurrence (Amaravadi and Thompson, 2007; Amaravadi et al., 2007; Livesey et al., 2009). It is therefore reasonable to suppress cancer cell autophagy for tumor therapeutics. For example, a number of reports have shown that combining traditional chemotherapeutic reagents with autophagy inhibitor can lead to more efficient tumor killing, both in vitro and in vivo (Amaravadi and Thompson, 2007; Amaravadi et al., 2007; Livesey et al., 2009).

Designing autophagy inhibitors and activators are of great interests in clinic. As mentioned above, activators of autophagy is likely to benefit patients with neurodegenerative diseases. In addition, boosting autophagy is also potentially beneficial to obesity and diabetes and may lead to longevity. So far, reagents reported to stimulate autophagy largely go through inhibition of Class I PI3K/Akt/mTOR pathways, such as rapamycin (Berger et al., 2006; Ravikumar et al., 2002), or the stimulation of AMP-activated protein kinase (AMPK), such as metformin and resveratrol (Buzzai et al., 2007; Morselli et al., 2010; Opipari et al., 2004). Drugs that directly target autophagy machinery, to my knowledge, have not been well characterized and widely accepted. Trehalose, a natural component formed by an α,α-1,1-glucoside bond between two α-glucose units, has been shown to stimulate autophagy through an mTOR-independent mechanism (Sarkar et al., 2007). However, the exact mechanism by which trehalose stimulates autophagy and the pharmacokinetics are not fully understood. In contrast to autophagy activators, autophagy inhibitors are of strong potentials in treating diseases like cancer. Chloroquine, a widely used drug for the treatment of malaria, is a well-tolerated drug that also inhibits autophagy flux through inhibition of lysosome function (Fedorko, 1967; Mizushima et al., 2010). Co-administration of chemotherapeutic reagents and chloroquine has shown promising results in curing cancers in animal models (Amaravadi and Thompson, 2007; Amaravadi et al., 2007; Livesey et al., 2009). Other autophagy inhibitors have not been reported to be safe in humans. It should be noted that systematic inhibition of autophagy may lead to severe side effects, including diabetes and cardiomyopathy, as demonstrated in animal models of autophagy deficiencies.

(2) Autophagy regulation at molecular level

a. ULK1 complex integrates growth factor signals and nutrient availability to modulate autophagy

Autophagy is regulated at multiple steps. Some mechanisms are evolutionarily conserved from yeasts to mammals. One major mechanism is through the regulation of TOR pathways. TOR is regulated by nutrients, such as amino acids, and growth factor signalings (Zoncu et al., 2011). Once TOR is activated, for example, in the nutrient rich condition, autophagy is suppressed by TOR, through direct interaction and phosphorylation of the Atg1/ULK1 and inhibits its kinase activity (Kamada et al., 2000; Kamada et al., 2010). Atg1/ULK1 is one of the

first autophagy-related genes identified through a yeast genetic screen (Kamada et al., 2000). It is a serine-threonine kinase that is thought to be one of the most upstream factors for autophagy initiation (Itakura and Mizushima, 2010). Unlike yeast, whose autophagy and TOR is mainly regulated by nutrient availability, mammalian cells are often bathed in a nutrient rich condition, and their nutrient uptake is regulated by the growth factor signaling, especially the Class I PI3K/Akt cascade, which activates mTOR (Lum et al., 2005). Therefore, growth factor signaling acts to suppress autophagy. In response to nutrient starvation or growth factor deprivation, the TOR pathway is inactivated, and the ULK1 complex activity is relieved, which promotes downstream events for autophagy (Kamada et al., 2000; Kamada et al., 2010). Another important mechanism involves the sensing of cellular ATP level. When AMP/ATP ratio is high, AMPK is activated, which in turn suppressed mTOR and directly associates and phosphorylates ULK1. The phosphorylation by AMPK is stimulatory to ULK1 activity (Egan et al., 2011; Kim et al., 2011). This mechanism plays a major role in response to glucose shortage. In addition to phosphorylation by mTOR and AMPK, ULK1 is also regulated by acetylation, by the GSK3β-TIP60 pathways that respond to growth factor signalings (Lin et al., 2012).

It is necessary to point out that, through a hierarchy analysis that utilized various genetic knockout cells, ULK1 complex is placed at the most upstream of the autophagy pathways (Itakura and Mizushima, 2010). Study of ULK1 modifications and localizations will greatly facilitate our understanding of several fundamental questions for autophagy, including the source of autophagosome membrane.

b. Ubiquitin-like conjugation system for autophagosome formation

The immediate downstream or substrate of ULK1 complex is poorly understood. Via a largely unknown mechanism, ULK1 complex signals to two events that is required for autophagosome formation: the Class III Vps34 complex that produces PI(3)P on the nascent precursor membrane, and the ubiquitin-like conjugation system that lipidates Atg8/ microtubule-associated protein 1 light chain 3 (LC3) and is required for vesicle elongation and closure (Mizushima et al., 2011). LC3 is a ubiquitin-like protein that undergoes a series of processing, first of which is the cleavage at the C-terminus by the cysteine protease Atg4. Through a ubiquitin-like conjugation system, the processed LC3 is activated by the E1-like enzyme Atg7, transferred to the E2-like enzyme Atg3, and finally covalently linked the phosphatidylethanolamine (PE) group through the E3-like enzyme Atg5-Atg12 complex (Hemelaar et al., 2003; Kabeya et al., 2000; Mizushima et al., 1998; Nemoto et al., 2003). The site of LC3 lipidation is determined by Atg16L that associates with the Atg5-Atg12 complex and directs its localization (Fujita et al., 2008). The key concepts of the ubiquitin-like conjugation system were verified through the use of genetic knockout cells and animals. For example, Atg7 knockouts showed lack of conjugation of Atg5-Atg12, and abrogated LC3 lipidation (Komatsu et al., 2005). Similarly, Atg5 or Atg12 knockout showed no LC3 lipidation and greatly impaired autophagosome formation (Kuma et al., 2004).

LC3 is widely used as a molecular marker for autophagy. The un-lipidated LC3 form is termed LC3-I, which is cytoplasmic, and the lipidated LC3 form is named LC3-II, which associates with the autophagosome membrane, and migrates faster on SDS-PAGE gel, thus allowing an indirect measurement of autophagy using LC3 immunoblotting (Kabeya et al., 2000). Experimentally, GFP-tagged LC3 is commonly used as a molecular marker for autophagy. In the fed condition, GFP-LC3 appeared as a diffuse pattern in the cell. Upon

autophagic induction, GFP-LC3 associates with the autophagosome membrane, and forms punctate pattern, allowing a visualization of autophagosome formation (Kabeya et al., 2000). It should be noted that upon fusion with lysosomes, the autophagosomal content, including LC3, is degraded, thus complicating the results of LC3 immunoblotting and the GFP-LC3 analysis. It is therefore necessary to include a lysosomal inhibitor, such as chloroquine or bafilomycin A1, to prevent LC3 degradation and to allow accurate interpretation (Klionsky et al., 2008; Mizushima et al., 2010).

c. Role of Class III PI3K complex in initiating precursor autophagosomal membrane

Class III PI3K, Vps34 complex, plays an essential role for autophagosome formation, at a very early step. The involvement of PI3K and Vps34 in autophagy was discovered by using PI3K inhibitors and yeast genetic studies. Wortmannin or 3-methyladenine (3-MA) strongly inhibits autophagy (Petiot et al., 2000). In vitro delivery of Vps34 product PI(3)P stimulates autophagy (Petiot et al., 2000). In yeast, Vps34 mutant showed defective autophagy, and Vps34 was found to be in a complex with Vps15, Vps30, and Atg14 that regulates autophagy (Kihara et al., 2001b). A subsequent study showed that Beclin 1, a mammalian homolog of Vps30, associates with Vps34 (Kihara et al., 2001a). These pioneer studies suggested a critical role of Vps34 in autophagy, provoked the identification of new partners in the complex, and provided a convenient tool for pharmacological inhibition of autophagy.

A number of proteins have been identified in the Vps34-Vps15 complex that regulates autophagy, including Beclin 1(Kihara et al., 2001a) , UVRAG (Liang et al., 2006), Ambra (Fimia et al., 2007), Atg14L (Matsunaga et al., 2009; Sun et al., 2008; Zhong et al., 2009), Rubicon (Matsunaga et al., 2009; Zhong et al., 2009), and Rab5 (Ravikumar et al., 2008). The interaction of Vps34 with its associated proteins alters Vps34 catalytic activity and/or directs Vps34 to distinct subcellular compartments. The interaction of Atg14L diverts Vps34 to the pre-autophagosomal membrane (Fan et al., 2011; Matsunaga et al., 2010), whereas the interaction of UVRAG and Rubicon diverts it to the late endosome where it regulates autophagosome maturation (Liang et al., 2008; Matsunaga et al., 2009; Zhong et al., 2009). Vps34 interaction with Atg14L and UVRAG/Rubicon appeared to be mutually exclusive (Matsunaga et al., 2009). The mechanism of Vps34 targeting to the pre-autophagosomal membrane is not fully understood, but may involve the activity of Atg14L (Matsunaga et al., 2010). Atg14L possesses an ER-localization motif that is shown to be required for the nascent precursor autophagosome membrane formation (Matsunaga et al., 2010). Another report identified that Atg14L binds to membrane through a distinct motif, which may be dependent on PI(3)P binding (Fan et al., 2011). Despite distinct mechanisms of Atg14L membrane recruitment, hierarchy analysis revealed that Atg14L puncta formation is independent of PI3K activity, suggesting that Atg14L acts upstream of Vps34 (Itakura and Mizushima, 2010).

Vps34 complex produces PI(3)P at the localized precursor autophagosomal membrane, and recruits PI(3)P binding proteins to the nascent membrane structure which further facilitate autophagosome biogenesis. How PI(3)P regulates autophagosome formation is not well understood, and the PI(3)P effectors required for the precursor membrane have not been fully identified. Vps34 and PI(3)P are suggested to be required for Atg5-Atg12 puncta formation that directs LC3 lipidation, although through a largely unknown mechanism (Itakura and Mizushima, 2010; Mizushima et al., 2011). WIPI family proteins are PI(3)P binding proteins that localize to the precursor membrane. Disruption of WIPI2 inhibits Atg5-Atg12 puncta, LC3 lipidation and

autophagosome formation, suggesting that WIPI2 is downstream of Vps34 and PI(3)P, but upstream of Atg5-Atg12 complex that lipidates LC3 (Itakura and Mizushima, 2010; Polson et al., 2010). However, the detailed machinery how WIPI family proteins direct the Atg5-Atg12 complex is not well established. Identification of other PI(3)P binding proteins that target to the nascent precursor membranes will help the understanding of this issue.

Despite the largely unknown mechanisms of Vps34 complex action on autophagosome formation, studies using genetic knockout systems have determined an essential role of Vps34 complex in initiating autophagy. Inactivation of Vps34 in MEFs, liver and heart abrogated the autophagosome formation (Jaber et al., 2012). In line with this, DFCP1 puncta, a marker for PI(3)P enriched in precursor autophagosomal membrane, and the Atg12 puncta are severely impaired in the Vps34-deficient MEFs (Jaber et al., 2012). Similarly, Atg14L deficient cells showed reduced Atg16L puncta, LC3 lipidation, and autophagosome formation (Itakura et al., 2008; Matsunaga et al., 2009).

d. Role of Rab5 in autophagosome formation

Another component of the Vps34 complex is Rab5. Rab5 is a small GTPase that switches between an inactive GDP state and an active GTP state (Bucci et al., 1992). The GDP to GTP transition of Rab5 is driven by its guanine nucleotide exchange factors (GEFs), while the hydrolysis of Rab5-GTP to GDP state is stimulated by GTPase activating proteins (GAPs) (Zerial and McBride, 2001). Rab5 in its GTP form binds to and activates its effectors that regulate a variety of membrane trafficking processes, such as endocytosis and vesicle fusion (Barbieri et al., 1994; Stenmark et al., 1994; Zerial and McBride, 2001). One group of Rab5 effectors is PI3Ks (Christoforidis et al., 1999b). p110β, but not p110α, has been shown to directly bind to Rab5-GTP (Christoforidis et al., 1999b). Vps34 also associates with Rab5, through Vps15 (Christoforidis et al., 1999b). The association of Class II PI3Ks with Rab5 is not reported. The interaction of Rab5 enhances the catalytic activity of p110β and Vps34, and it is suggested that p110β produces 30% of PI(3)P, through a phosphatase complex that converts $PI(3,4,5)P_3$, and that Vps34 contributes to 70% of PI(3)P in the early endosomal environment (Shin et al., 2005). It should be noted that this observation is made using blocking antibodies to p110β and Vps34, but not through genetic inactivation of these two proteins, and that the contribution of endosomal PI(3)P from the two proteins is cell line dependent.

In addition to a role in endosomes, Rab5 has recently been reported to play a role in autophagy (Ravikumar et al., 2008). A constitute active mutant of Rab5 stimulates, whereas a dominant negative mutant inhibits, autophagosome formation. Rab5 is shown to be in a complex with Beclin 1, through Vps34, which is required for Atg5-Atg12 conjugation and the puncta formation. The role of Rab5 in autophagy is independent of its activities on endocytosis or mTOR, but is involved in the early step of precursor membrane formation, likely through positive regulation of Vps34 (Ravikumar et al., 2008). In line with this notion, gel filtration analysis showed that Rab5 appeared in the same fractions with Atg5-Atg12 (Takahashi et al., 2011). As Rab5 is a small protein that involved in growth factor signaling, membrane trafficking, endocytosis, and autophagy, its versatile functions are possibly regulated by association with different regulators and effectors. How Rab5 senses different cell stimuli and responds to distinct environmental clues are not well understood, but represents an important area for investigation.

(3) General aims of this dissertation

As mentioned above, PI3Ks and autophagy are both important topics in general biology and in medicine. At the molecular level, the involvement of PI3Ks in autophagy regulation has long been recognized. The general understanding is that Class I PI3Ks play an inhibitory role in autophagy by producing $PI(3,4,5)P_3$ that activates the Akt/TOR kinase pathway, whereas Class III PI3K plays a stimulatory role by producing PI(3)P that is essential for autophagosome formation. However, a direct function of the Class IA PI3Ks on autophagy remains undetermined. In the course of my dissertation study, I used conditional gene knockout mice deficient in the Class IA PI3K p110α or p110β catalytic subunit (Lu et al., 2009) to study their involvements and mechanisms in the regulation of autophagy.

II. Results

1) Generation and characterization of p110α and p110β knockout mouse embryonic fibroblasts.

To facilitate mechanistic studies, mouse embryonic fibroblasts (MEFs) were generated from *p110*$\alpha^{flox/flox}$ and *p110*$\beta^{flox/flox}$ mice , in which the exon 3 and 4 deletion of *p110β* creates a frame shift mutation and loss of the *p110β* fragment (Lu et al., 2009). The MEFs were then immortalized using SV40 large T antigen. Expression of the Cre recombinase in *p110*$\alpha^{flox/flox}$ or *p110*$\beta^{flox/flox}$ MEFs by adenovirus infection resulted in virtually complete loss of p110α or p110β protein, respectively (Fig. 1A), while the steady-state level of p85 was not affected in $\alpha^{-/-}$ or $\beta^{-/-}$ MEFs (Fig. 1A). I hereafter refer to the flox/flox MEFs without Cre recombination as $\alpha^{+/+}$ or $\beta^{+/+}$ MEFs, and the knockout cells as $\alpha^{-/-}$ or $\beta^{-/-}$ MEFs.

To test the functional consequence of p110 loss in these MEFs, phosphorylation of Akt in response to various trophic factor stimulations was examined. Although both producing PI(3,4,5)P_3, p110α and p110β isoforms have been shown to play divergent roles in response to different trophic factor receptors. p110α plays a major role in receptor tyrosine kinase (RTK)-mediated signaling, while p110β is preferentially activated by G protein coupled receptors (GPCR). Consistent with previous reports (Guillermet-Guibert et al., 2008; Jia et al., 2008; Zhao et al., 2006), $\alpha^{-/-}$ MEFs showed a significant decrease in Akt phosphorylation in response to RTK signaling such as that triggered by EGF, PDGF, and insulin (Fig. 1B), whereas $\beta^{-/-}$ MEFs were defective in GPCR signaling triggered by lysophosphatidic acid (LPA; Fig. 1, C and D).

2) Autophagy is impaired in $\beta^{-/-}$ but not $\alpha^{-/-}$ MEFs.

To determine the effect of *p110α* and *p110β* deletion on autophagy, I first observed the MEFs by transmission electron microscopy (TEM), which is one of the best characterized standards for autophagy. $\beta^{+/+}$ MEFs upon serum deprivation displayed an increase in double-layered membrane structures enclosing electron-dense material, characteristic of autophagosomes (Fig. 2A). In contrast, $\beta^{-/-}$ MEFs showed deficient autophagosome formation upon serum deprivation. In addition, deformed mitochondria and accumulation of ribosome aggregates were observed in $\beta^{-/-}$ MEFs (Fig. 2A), consistent with previous observations made in autophagy-deficient cells (Komatsu et al., 2005; Kraft et al., 2008; Kundu et al., 2008). Besides the ultra-structural analysis, I also examined the function of autophagy, namely the degradation of long-lived proteins that are considered as autophagy substrates. This revealed a significant defect in autophagic degradation in $\beta^{-/-}$ MEFs in both basal and starvation conditions (Fig. 2B). In addition, I examined the lysosomal activity that is associated with autophagy using the pH-dependent lysosomal dye LysoTracker red. $\beta^{+/+}$ MEFs showed a higher basal level of lysosomal activity than $\beta^{-/-}$ MEFs (Fig. 2C). Serum deprivation further enhanced the lysosomal activity in $\beta^{+/+}$ MEFs, but the enhancement was markedly impaired in $\beta^{-/-}$ MEFs (Fig. 2C).

To further determine the effect of *p110β* gene deletion on autophagy, I exposed the MEFs, in the absence or presence of lysosomal peptidase inhibitors E64D and pepstatin A (Klionsky et al., 2008; Mizushima et al., 2010), to a number of known autophagy-inducing conditions including glucose deprivation, serum deprivation, and the DNA-damaging agent etoposide. The

conversion of microtubule-associated protein 1 light chain 3 (LC3) from its cytosolic form (LC3-I) to a membrane-bound form (LC3-II) was examined as a molecular marker for autophagosomal formation. The intensity of LC3-II against that of β-tubulin was used to determine autophagy induction. All autophagy-inducing conditions resulted in accumulation of LC3-II in $\beta^{+/+}$ cells, whereas the accumulation of LC3-II was markedly lower in $\beta^{-/-}$ MEFs (Fig. 2D). Reconstitution of $\beta^{-/-}$ MEFs with p110β restored LC3 conversion (Fig. 2E). In addition to the LC3 immunoblot analysis, the ability of GFP-tagged LC3 to form autophagic puncta has been used to monitor autophagy (Kabeya et al., 2000). $\beta^{+/+}$ and p110β-reconstituted $\beta^{-/-}$MEFs expressing GFP-LC3 showed a change from a diffuse pattern to a punctate pattern upon autophagic stimuli, whereas both the size and number of GFP-LC3 puncta were markedly reduced in $\beta^{-/-}$ MEFs (Fig. 2F). Taken together, these data indicate that autophagy is deficient in $\beta^{-/-}$ MEFs.

To reassure a positive role of p110β in autophagy, p110β was disrupted by shRNA in other cell lines. Knockdown of p110β in HEK293 cells results in accumulation of the autophagy substrate p62/SQSTM1 (Fig. 3A) and deficient formation of LC3-II (Fig. 3B). Knockdown of p110β in MDA-MB-231 cells caused impaired level of LC3-II under both fed and starvation conditions (Fig. 3C). Similar effects were also seen in MCF10A, HEK293T, and HeLa cells.

Autophagy in $\alpha^{-/-}$ MEFs was also investigated. As revealed by TEM, $\alpha^{-/-}$ MEFs displayed similar induction of autophagosomes as compared to the wild-type control (Fig 4A). The LysoTracker red staining and LC3 immunoblotting showed similar or slightly elevated autophagic activities in $\alpha^{-/-}$ MEFs (Fig 4 B and C, respectively). GFP-LC3 puncta analysis indicates similar level of autophagic puncta formation. These data suggest that disruption of p110β, but not p110α, leads to impaired autophagy.

3) Ectopic expression of p110β stimulates autophagy.

To examine the opposite effect of *p110β* gene deletion, Flag-tagged p110β was ectopically expressed in HEK293 cells. With serum deprivation, the p110β-overexpressing cells maintained higher Akt phosphorylation than control cells (Fig. 5A). Despite the elevated Akt phosphorylation, the amount of LC3-II was significantly higher in cells expressing Flag-p110β, whereas the steady-state levels of the key autophagy regulators Beclin 1 and Vps34 remained unchanged (Fig. 5A). In another HEK293 line where GFP-LC3 was stably expressed, overexpression of p110β, but not p110α, enhanced the generation of GFP-LC3-II (Fig. 5B). In addition, an increased amount of the cleaved free-GFP was observed in Flag-p110β-expressing cells, suggesting an enhanced autophagy flux (Fig. 5B). Similarly, expression of Flag-p110β markedly increased the number and size of GFP-LC3 puncta both at the basal state and upon nutrient starvation in HeLa cells (Fig. 5C). These results support a stimulatory role of p110β in autophagy, and suggest that the autophagy-promoting role of p110β is dominant over the inhibitory effect imposed by elevated Akt activity.

4) p110β does not act through the Akt-TOR pathway to promote autophagy.

I next went on to dissect the possible mechanisms by which p110β stimulates autophagy. I first asked whether p110β promotes autophagy through modulation of the Akt-TOR pathway. The canonical PI3K-Akt-TOR pathway plays an inhibitory role in autophagy (Levine and

Kroemer, 2008; Lindmo and Stenmark, 2006). However, the observation above suggested that p110β positively regulates both Akt and autophagy (Fig. 5A). One explanation for this apparent paradox is that p110β has two distinct functions: one is to promote Akt activation, and the other to promote autophagy. I went on to examine whether inhibition of Akt and TOR can induce autophagy in the absence of p110β. $\beta^{+/+}$ and $\beta^{-/-}$MEFs were treated with pharmacological inhibitors of Akt (Akti) or TOR (rapamycin). In $\beta^{+/+}$ MEFs growing in complete medium, both inhibitors stimulated autophagy as indicated by LC3 conversion (Fig. 6A) and GFP-LC3 puncta formation (Fig. 6, B and C), and the induction of autophagy was further enhanced when cells were deprived of glucose or serum (Fig. 6A). In sharp contrast, autophagy induced by Akt and TOR inhibitors was dramatically reduced in $\beta^{-/-}$ MEFs under all of these conditions (Fig. 6, A-C). The failure of p110β kinase-specific inhibitor TGX-221 to inhibit autophagy (Fig. 6A) suggests that p110β kinase activity may not be required for regulating autophagy, a point I will discuss later. Together with my finding that overexpression of p110β could stimulate Akt phosphorylation and autophagy simultaneously (Fig. 5A), these data indicate that p110β-mediated autophagy is independent of Akt-TOR signaling.

5) p110β modulates the level of cellular PI(3)P and Vps34 catalytic activity.

I then determined other possible molecular mechanisms through which p110β regulates autophagy. I tested whether p110β affects the expression level of key autophagy proteins, and found that the steady-state levels of the key autophagy regulators Vps34, Beclin 1, Atg14L, and Rubicon appeared unaltered in $\beta^{-/-}$ MEFs (Fig. 7A), and the expression levels of Beclin 1, Vps34, and Rubicon remained unaltered in $\beta^{-/-}$ livers (Fig. 7B). The decreased lysosomal acidification in $\beta^{-/-}$ MEFs (Fig. 2C), however, indicated a possible deficiency in endosomal and lysosomal maturation in these cells. In fact, expression of a GFP-conjugated FYVE domain that specifically binds to PI(3)P on endosomes and indicates endo-lysosomal activities revealed decreased GFP puncta in $\beta^{-/-}$ MEFs compared with $\beta^{+/+}$ MEFs (Fig. 8A). This finding suggests that $\beta^{-/-}$ MEFs have decreased level of PI(3)P, a lipid that is required for autophagy. To test this, I used a protein-lipid overlay assay to measure the intracellular level of PI(3)P. The specificity of the assay was confirmed using a number of different PI species as negative controls, and by treating cells with 3-methyladenine (3-MA), a pharmacological inhibitor of Vps34 that resulted in a decreased level of intracellular PI(3)P (Fig. 8B). A decrease of ~30% in the steady-state level of PI(3)P was detected in $\beta^{-/-}$ MEFs as compared with $\beta^{+/+}$ cells (Fig. 8B). Reconstitution of p110β in $\beta^{-/-}$ MEFs restored PI(3)P levels (Fig. 11E). The decreased amount of PI(3)P in $\beta^{-/-}$ MEFs was also detected by flow cytometry using a PI(3)P-specific antibody, similar to the decreased level of PI(3,4,5)P_3 in the $\beta^{-/-}$ MEFs (Fig. 8C).

Vps34 is the predominant kinase that produces intracellular PI(3)P and promotes autophagy, as part of a complex with Vps15 and Beclin 1 (Simonsen and Tooze, 2009). I thus examined if p110β affects PI(3)P levels by modulating Vps34 activity. The bicistronic Myc-Vps34-V5-Vps15 expression construct (Yan et al., 2009) and the Beclin 1-GFP construct were co-transfected into HEK293T cells with or without Flag-p110β. Vps34 kinase activity was then assayed in anti-Myc or anti-GFP immunoprecipitates using PI as a substrate. In both assays, Vps34 kinase activity was enhanced in the presence of p110β (Fig. 8, D and E). The increased conversion of PI to PI(3)P in the assay was not due to phosphorylation of PI by p110β because p110β exhibits little kinase activity in the assay conditions used to measure Vps34 activity (Fig.

8F). Taken together, these results indicate that p110β promotes Vps34 kinase activity and PI(3)P production, a process prerequisite for autophagosome formation.

6) p110β is required for the early stage of autophagosome formation.

PI(3)P is known to regulate both endocytic and autophagic pathways (Burman and Ktistakis, 2010). As I observed that the PI(3)P level and autophagy are lower in $\beta^{-/-}$ cells, I went on to determine whether the autophagic pool of PI(3)P is affected by p110β. DFCP1 (double FYVE domain-containing protein 1) has been shown to relocalize from the ER/Golgi to omegasome, the precursor membrane structure of autophagosome, in a PI(3)P-dependent manner upon autophagy induction (Axe et al., 2008). To test if the formation of the omegasome structure is affected in the $\beta^{-/-}$MEFs, I expressed GFP-DFCP1 in $\beta^{+/+}$ and $\beta^{-/-}$ MEFs. Under fed state, $\beta^{+/+}$ MEFs displayed a diffuse pattern of GFP-DFCP1, which turned into a punctuate pattern upon serum starvation or Hank's buffer treatment (Fig. 9A), consistent with previous reports (Axe et al., 2008; Polson et al., 2010). In contrast, under fed condition, $\beta^{-/-}$ MEFs showed an accumulation of GFP-DFCP1 puncta, which appeared to form aggregates that differed from the starvation-induced puncta in $\beta^{+/+}$ MEFs (Fig. 9A). The accumulation of the abnormal GFP-DFCP1 puncta in $\beta^{-/-}$ cells is reminiscent of that observed in cells deficient in WIPI2, which is localized to omegasomes and promotes LC3 lipidation (Polson et al., 2010). Importantly, upon starvation, the amount of GFP-DFCP1 puncta in $\beta^{-/-}$ MEFs was significantly lower than that in $\beta^{+/+}$ MEFs (Fig. 9A), indicating a deficient autophagy pool of PI(3)P in $\beta^{-/-}$ MEFs. Consistent with this, another PI(3)P-dependent event during early autophagosome formation, Atg5-Atg12 conjugation (Ravikumar et al., 2008), was also compromised in $\beta^{-/-}$ MEFs (Fig. 9B).

To further confirm the early stage of autophagy influx is deficient in $\beta^{-/-}$ MEFs, I expressed the mCherry-GFP-LC3 construct in the MEFs. Owing to the more stable nature of mCherry than GFP in the acidified compartment, the relative amount of the yellow puncta (represent autophagosomes as a result of the merged green and red signals) and the red puncta (represent autolysosomes) can be used to indicate whether the early or late steps of the autophagic flux are affected (Mizushima et al., 2010). $\beta^{-/-}$ MEFs displayed significantly less yellow and red puncta than $\beta^{+/+}$ MEFs, in both basal state and under serum deprivation (Fig. 9C). These data indicate that the lower PI(3)P level in $\beta^{-/-}$ MEFs has a major impact on the early stage of autophagosome formation.

7) p110β is a component of the autophagy-promoting Rab5-Vps34-Vps15-Beclin 1-Atg14L complex.

I subsequently studied the mechanisms by which p110β stimulates PI(3)P production. In mammalian cells, the autophagy-essential PI(3)P is known to be produced by the Vps34 complex. It has been reported that Rab5 can also participate in the autophagosome formation through its interaction with the Vps34-Beclin 1 complex (Ravikumar et al., 2008). p110β, but not p110α, has been reported to directly associate with Rab5 (Christoforidis et al., 1999b). These studies suggested to me that p110β may participate in autophagy induction as part of the Rab5-Vps34-Beclin1 complex. Indeed, in the Vps34 assays, p110β was observed to coprecipitate with Vps34

(Fig. 8D) and Beclin 1 (Fig. 8E). I confirmed that Rab5 immunoprecipitation was able to bring down overexpressed Vps15 and Vps34, as well as Flag-p110β (Fig. 10A). Furthermore, Rab5 pulled down endogenous p110β, but not p110α (Fig. 10B). I then went on to test whether p110β associates with the Vps34-Vps15-Beclin 1 complex. I found that Vps34 immunoprecipitation pulled down Vps15 and p110β (Fig. 10C), and likewise, p110β immunoprecipitation pulled down Vps15 and Vps34 (Fig. 10D). Vps15 immunoprecipitation pulled down Vps34 and p110β, but not p110α (Fig. 10E). The presence of p110β in the Vps34-Vps15 complex appeared unchanged or slightly enhanced upon serum deprivation (Fig. 10, C and D). I also detected interaction between endogenous p110β and Beclin 1 by immunoprecipitation (Fig. 10, F and G).

The Vps34-Vps15-Beclin 1 complex has been shown to interact with different partners and act at distinct stages of the autophagy pathway. The complex with Atg14L is known to promote autophagosome initiation, whereas the complex with UVRAG and Rubicon mainly regulates autophagosome maturation (Matsunaga et al., 2009; Sun et al., 2008; Zhong et al., 2009). I thus asked whether p110β interacts with the Atg14L, or UVRAG and Rubicon-containing complexes. I used the human p110β-reconstituted $\beta^{-/-}$ MEFs to perform immunoprecipitation because our Atg14L and Rubicon antibodies preferentially recognize mouse antigens, whereas our p110β antibody preferentially recognizes human p110β. I found that p110β immunoprecipitation pulled down Atg14L, but not UVRAG or Rubicon (Fig. 10H). Likewise, Atg14L, but not Rubicon immunoprecipitation was able to bring down p110β (Fig. 10I). Immunofluorescence analysis confirmed that p110β colocalized at least partially with Atg14L, both at fed and starved conditions (Fig. 10J). Taken together, these data demonstrate that p110β associates and colocalizes with the autophagy-promoting Rab5-Vps34-Vps15-Beclin 1-Atg14L complex that generates PI(3)P and is required for autophagosome initiation.

8) p110β promotes autophagy and PI(3)P production independently of its kinase activity.

I next determined whether the kinase activity of p110β is required for the PI(3)P production, since it has been reported that p110β associates with a protein complex containing PI 4- and 5-phosphatases that dephosphorylate PI(3,4,5)P_3 generated by p110β to produce PI(3)P in the endosomal compartment (Shin et al., 2005). This mechanism would provide an alternate route for PI(3)P production within the Vps34-Vps15-Beclin 1 complex that would require p110β kinase activity. To test if p110β kinase activity is required for autophagy, $\beta^{+/+}$ MEFs were treated with TGX-221, a selective p110β kinase inhibitor. TGX-221 did not inhibit LC3 conversion in basal state or under glucose or serum deprivation conditions (Fig. 6A), suggesting that p110β promotes autophagy independently of its kinase activity. To further address the kinase dependency issue, I reconstituted $\beta^{-/-}$ MEFs with either wild-type p110β or the kinase-dead p110βK805R mutant. The p110βK805R mutant showed similar capabilities in restoring GFP-LC3 puncta formation as that of p110βWT (Fig. 11, A and B). In addition, both p110βWT and p110βK805R restored LC3 conversion to a similar extent (Fig. 11C). Another kinase-dead mutant, p110βN924K (Ballou et al., 2007) (Fig. 11D), also restored LC3 conversion in $\beta^{-/-}$ MEFs (Fig. 11D). Expression of p110βK805R also enhanced PI(3)P production, as indicated by the lipid-protein overlay assay (Fig. 11E), GFP-FYVE puncta formation (Fig. 11F), and increased Vps34 kinase activity (Fig. 11, G and H). Similar to wild-type p110β, both p110βK805R and p110βN924K were able to interact with Vps34 and Beclin 1 (Fig. 11, I and J). Taken together, these results strongly suggest that p110β functions as a scaffold, within the

Vps34-Vps15-Beclin 1 complex, to positively regulate Vps34 activity, PI(3)P production, and autophagy.

9) Active Rab5 rescues the autophagy deficiency in p110β$^{-/-}$ cells.

The above results indicate that p110β associates with the Vps34-Vps15-Beclin 1-Atg14L complex and stimulates Vps34 kinase activity to promote PI(3)P production via a scaffold activity. To further study the role of p110β within the Vps34 complex, I performed pull-down or immunoprecipitations using purified or in vitro-translated proteins, and revealed a lack of direct interaction of p110β with Vps34, Vps15, or Beclin 1, raising the possibility that p110β interacts with other proteins to modulate Vps34 catalytic activity. One candidate is the small GTPase Rab5. If p110β promotes autophagy by activating Rab5, I predict that a constitutively active form of Rab5 will restore autophagy in p110β-deficient cells. To test this hypothesis, I expressed wild-type Rab5 (Rab5-WT), the Rab5-Q79L constitutively active mutant (Rab5-CA), Vps34-Vps15, or Atg14L in β$^{+/+}$ and β$^{-/-}$ MEFs (Fig. 12A) and measured autophagy. As expected, expression of Vps34-Vps15 or Atg14L induced autophagy in β$^{+/+}$ cells, as indicated by an increase in autophagic GFP-LC3 puncta (Fig. 12, B and C). However, in β$^{-/-}$ cells, Vps34-Vps15 or Atg14L failed to induce autophagy under basal conditions (Fig. 12, B and C) or in cells treated with the mTOR inhibitor rapamycin (Fig. 12E). This result is consistent with the above conclusion that p110β induces autophagy via the regulation of Vps34-Vps15-Beclin 1-Atg14L complex activity. Interestingly, while both Rab5-WT and Rab5-CA promoted the formation of GFP-LC3 puncta in β$^{+/+}$ cells as previously reported (Ravikumar et al., 2008), only Rab5-CA induced autophagy in β$^{-/-}$ cells (Fig. 12, B and C). Moreover, Rab5-CA but not Rab5-WT enhanced the accumulation of LC3-II in cells treated with the lysosomal inhibitor bafilomycin A1 (Fig. 12D). Taken together, these data suggest that Rab5-CA can bypass the requirement for p110β in autophagy induction, and that Rab5-WT can be activated in a p110β-dependent manner.

10) p110β is required for Rab5 activity.

The differential effects of Rab5-WT and Rab5-CA in β$^{-/-}$ MEFs suggest that p110β may act upstream of Rab5 to increase its autophagy-promoting activity. Like other G proteins, Rab5 cycles between an inactive GDP-bound state and an active GTP-bound form that binds and activates its effectors (Christoforidis et al., 1999a; Zerial and McBride, 2001). To determine whether p110β can promote Rab5 activation, I performed pull-down assays using the GST-tagged Rab5-binding domain of Rabaptin5 (residues 739-862, R5BD), which specifically binds to Rab5-GTP (Liu et al., 2007). The specificity of GST-R5BD binding to active Rab5 was verified by its more efficient binding to Rab5-CA compared to Rab5-WT and lack of binding to Rab5-DN (Fig. 13A). Importantly, GST-R5BD pulled down less active Rab5 from β$^{-/-}$ cells than from β$^{+/+}$ cells, while no difference was detected between α$^{+/+}$ and α$^{-/-}$ MEFs (Fig. 13B). Stable (Fig. 13C) or transient (Fig. 13D) expression of either p110β-WT or the kinase-dead mutant p110β K805R in β$^{-/-}$ cells increased the amount of Rab5-GTP. Consistent with the lower amount of activated Rab5 in β$^{-/-}$ versus β$^{+/+}$ MEFs, coimmunoprecipitation of Rab5 with two of its effectors related to autophagy and endocytosis, Vps34 and EEA1, was reduced in β$^{-/-}$ cells (Fig. 13E). Re-expression of p110β restored Rab5 binding to Vps34 and EEA1 (Fig. 13E). Consistent with the effect seen in MEFs, shRNA silencing of p110β in HEK293T cells resulted

in a large decrease in Rab5-GTP (Fig. 13F). Taken together, these data suggest that p110β plays a critical role in promoting the activation of Rab5.

11) p110β antagonizes the Rab5 GAP activity of p85α.

I next explored the mechanisms by which p110β regulates Rab5 activity. Sequence and structure analysis of p110β did not indicate it as a putative guanine nucleotide exchange factor (GEF) that activates monomeric GTPase by stimulating the release of GDP to allow binding of GTP. In addition, as p110β binds specifically to Rab5-GTP (Christoforidis et al., 1999b), it is unlikely that p110β acts as a Rab5 GEF or guanine nucleotide dissociation inhibitor (GDI) because these functions require binding to Rab5-GDP. Interestingly, the Class IA PI3K regulatory subunit p85α has been reported to bind directly to Rab5 and to function as a Rab5 GAP (Chamberlain et al., 2004). The Bcr homology (BH) domain of p85α possesses Rab5 GAP activity, and disruption of this activity was reported to affect receptor trafficking (Chamberlain et al., 2004; Chamberlain et al., 2010). A working model can be postulated that while p110-free p85α can function as a Rab5 GAP, the presence of p110β in the Rab5 complex can sequester Rab5 from the p85α GAP function. This hypothesis would suggest that loss of p85α will lead to an increase in Rab5-GTP levels and enhanced autophagy. Indeed, stable silencing of p85α (Fig. 14A) led to increased amounts of Rab5-GTP (Fig. 14B) and increased GFP-LC3 puncta formation (Fig. 14C) in both $\beta^{+/+}$ and $\beta^{-/-}$ cells. The lower level of Rab5-GTP in $\beta^{-/-}$ versus $\beta^{+/+}$ cells upon p85α silencing could be due to the incomplete knockdown of p85α (Fig. 14, A and B). To test the effect of p85α silencing on autophagosome maturation, LC3 with the tandem conjugation of mCherry and GFP was expressed in MEFs. While the number of both red and yellow puncta was higher in $\beta^{+/+}$ than in $\beta^{-/-}$ cells, consistent with defective autophagy in $\beta^{-/-}$ cells, silencing of p85α led to a marked increase in the number of autophagosomes and autolysosomes in both cell lines (Fig. 14D). These results indicate that downregulation of p85α relieves the inhibition of Rab5 and thus bypasses the requirement of p110β for autophagy induction.

To test the effect of p85α and p110β on Rab5 activation in a more direct fashion, I assayed Rab5 GAP activity *in vitro* using purified Rab5, p85α, and the p110β/p85α and p110α/p85α PI3K complexes. Free p110 proteins were not tested because they are thermally unstable and always form heterodimers with p85 *in vivo* (Geering et al., 2007; Yu et al., 1998). Control experiments showed that GST-R5BD specifically pulled down Rab5 loaded with GTP but not GDP under these *in vitro* assay conditions (Fig. 14E). Incubation of Rab5-GTP with free p85α led to a decrease in the amount of Rab5-GTP in a dose-dependent manner (Fig. 14F), consistent with the ability of p85α to act as a Rab5 GAP *in vitro* (Chamberlain et al., 2004). p85α complexed with p110β showed no Rab5 GAP activity, whereas p85α complexed with p110α still possessed GAP activity toward Rab5 (Fig. 14F). These results strongly indicate that p110β, but not p110α, has a negative effect on the Rab5 GAP activity of p85α. It was speculated that the binding affinity of Rab5 is higher for p110β than for p85α (Chamberlain et al., 2004; Christoforidis et al., 1999b). Addition of the p110β/p85α complex antagonized the Rab5 GAP activity of free p85α, whereas the p110α/p85α complex failed to do so (Fig. 14G). Since p110β/p85α dimers are unlikely to interact with free p85, the ability of p110β/p85α to reduce the GAP activity of p85 in trans suggests that it acts by sequestering Rab5 from the p85 GAP.

12) Generation and characterization of Rab5 binding deficient p110β mutants.

I next went on to determine whether the association between p110β and Rab5 is necessary for the activation of Rab5 and autophagy. Despite high sequence homology with other p110 isoforms, p110β is the only Class IA isoform known to date to associate Rab5 (Christoforidis et al., 1999b; Vanhaesebroeck et al., 2012). A previous study done in yeast two-hybrid system, where a series of p110β truncations were used, suggested that part of the Ras-binding domain and the N-terminus of the kinase domain of p110β may be involved in Rab5 binding (Kurosu and Katada, 2001). However, large truncations of a protein in general are likely to result in a misfolded protein, especially for p110 that has a compact 3-D structure and whose domains have close contacts with each other. Indeed, I have designed a number of point mutations of the critical residues within the two domains previous suggested, but were unable to prove an important role for Rab5 binding. For an alternative strategy, I used a swapping mutant that replaced the N-terminal p85 binding domain and Ras binding domain with that of p110α (Fig. 15A). This chimera has been shown to possess intact kinase activity (Dbouk et al., 2010). Importantly, pull-down of GST-Rab5 loaded with GTPγS revealed a positive binding of the chimera to Rab5 (Fig. 15B), arguing against a role of the Ras-binding domain for Rab5 binding.

Using a structure based scanning mutagenesis strategy for the rest domains of p110β, a series of point mutations were generated (Fig. 15C), harboring intact kinase activity, for the GST-Rab5-GTPγS pull-down analysis. Two mutants, namely Q596C and the I597S, consistently showed abrogated association with Rab5 (Fig. 15C). These two mutants possess intact kinase activity (Fig. 15D) and the ability to associate p85α (Fig. 15E).

The Q596 and I597 are evolutionarily conserved residues within the helical domain of p110β (Fig. 16, A and B). Investigation of the crystal structure of p110β (Zhang et al., 2011) revealed that these two residues are exposed on the outer surface of the helical domain of p110β (Fig. 16, C and D). In summary, I concluded that the Q596 and I597 residues of p110β are necessary for Rab5 association.

13) The p110β-Rab5 interaction plays an essential role in Rab5 activation and autophagy.

To test the ability of these mutants to activate Rab5 and autophagy, p110β-Q596C and p110β- I597S were stably expressed in $\beta^{-/-}$ MEFs to levels similar to those seen in cells reconstituted with p110β-WT (Fig. 17A). GST-R5BD pull-down assays revealed that p110β-WT, but not the Q596C or I597S mutants, increased the level of Rab5-GTP (Fig. 17B). Consistent with the autophagy-promoting role of p110β-mediated Rab5 activation, the two mutants failed to rescue autophagy in $\beta^{-/-}$ MEFs, as indicated by reduced accumulation of LC3-II (Fig. 17C) and decreased GFP-LC3 autophagic puncta formation (Fig. 17D) in both untreated and serum-deprived conditions. Taken together, these results demonstrate that the physical interaction of p110β with Rab5 is required for Rab5 activity and its autophagy-promoting function.

14) p110β-mediated Rab5 activation is selectively regulated by trophic factor availability, but not by nutrient signaling.

My results indicate that p110β can function to activate Rab5 that in turn stimulate autophagy in the cytosolic membrane environment. On the other hand, Class IA PI3Ks are well known to be recruited to trophic factor receptor signaling complexes where it produces

$PI(3,4,5)P_3$ to stimulate downstream signaling cascades, such as the Akt/mTOR pathway (Cantley, 2002; Engelman et al., 2006; Vanhaesebroeck et al., 2010). These two distinct activities of p110β suggest that metazoan cells may be able to respond to trophic factor limitation to activate Rab5 in a manner that can be directly transduced from the trophic factor receptors. To examine this hypothesis, I performed Rab5 immunoprecipitations under various conditions in the genetically modified MEFs. The appropriate effect of these treatments on cell signaling pathways was verified by monitoring the phosphorylation of Akt, S6 (a downstream effector of mTOR), and AMPK (Fig. 18A). Coimmunoprecipitation experiments showed that only serum deprivation enhanced the p110β-Rab5 association (Fig. 18B). Vps34 binding to Rab5, which has been reported to promote Vps34 activity and autophagy (Ravikumar et al., 2008; Shin et al., 2005), was also selectively enhanced by serum deprivation (Fig. 18B).

To test whether Rab5 activation induced by serum deprivation is dependent on p110β, I performed GST-R5BD pull-down assays on lysates of $\beta^{+/+}$ and $\beta^{-/-}$ MEFs. Indeed, serum withdrawal increased the level of Rab5-GTP in $\beta^{+/+}$ but not in $\beta^{-/-}$ cells (Fig. 18C). Similar effect was also seen in HEK293T cells with shRNA silencing of p110β (Fig. 13F). As a correlative measure of Rab5 activation, I observed enhanced coimmunoprecipitation of Rab5 with its effectors Vps34 and EEA1 in response to serum deprivation only in $\beta^{+/+}$ MEFs (Fig. 18D). Reconstitution of $\beta^{-/-}$ MEFs with p110β restored Rab5 activation induced by serum deprivation (Fig. 18D).

To establish a role of Rab5 in serum deprivation-induced autophagy, I expressed Rab5-DN construct, and observed impaired LC3-II (Fig. 18E) and GFP-LC3 puncta formation (Fig. 18F). Taken together, these results indicate that trophic factor limitation selectively enhances the p110β-Rab5 interaction, which plays an essential role in Rab5 activation and autophagy induction.

15) p110β dissociates from trophic factor signaling complexes and increases its interaction with Rab5 upon trophic factor limitation.

The above results show that serum deprivation selectively induces p110β-mediated Rab5 activation, which may be responsible for autophagy induction under these conditions. However, although serum is well regarded as a source of trophic factors, it is a less defined system that modulates complex signalings and contains various nutrients. Therefore, to further pursue the possible selective role of p110β in Rab5 activation and autophagy in response to trophic factor limitation, I used the immortalized breast epithelial MCF10A cell line, whose growth is dependent on the presence of defined trophic factors (insulin, EGF, cholera toxin, and hydrocortisone). Removal of the trophic factors has been shown to induce autophagy in MCF10A cells (Fung et al., 2008). To detect changes in p110β partitioning between subcellular pools, I immunoprecipitated insulin receptor signaling complexes and found that the association of p110β with insulin receptor substrate (IRS)-1 and IRS-2 was diminished upon deprivation of the trophic factors (Fig. 19A, left panel). Similarly, pull-down with phosphotyrosine antibodies showed reduced binding of p110β (Fig. 19A, left panel). By contrast, p110β and Rab5 coprecipitation increased upon withdrawal of the trophic factors (Fig. 19A, middle panel). To visualize the change in subcellular localization of p110β, I performed immunofluorescence microscopy imaging of MCF10A cells. The specificity of the p110β antibody used for

immunofluorescence was verified using cells treated with shRNA to knock down p110β (data not shown). Staining of endogenous p110β and Rab5 in cells cultured in complete medium showed a portion of p110β on the plasma membrane and Rab5 mostly in the cytoplasm (Fig. 19B). In the absence of the hormonal factors, the plasma membrane p110β signal was greatly reduced, and enhanced colocalization of p110β and Rab5 was observed (Fig. 19B). These data indicate that trophic factor limitation leads to p110β dissociation from trophic factor receptor signaling complexes and increased p110β-Rab5 interaction.

To study the requirement for p110β in trophic factor limitation-induced Rab5 activation and autophagy, I stably expressed an shRNA against p110β or a non-targeting control shRNA under the control of a tetracycline-inducible system in MCF10A cells. Addition of doxycycline led to a progressive reduction in p110β protein levels (Fig. 19C). Similar to what I observed in serum-deprived MEFs (Fig. 18C) and HEK293T cells (Fig. 13F), trophic factor deprivation led to an increased amount of Rab5-GTP in the control but not in p110β knock-down MCF10A cells with endogenous Rab5 (Fig. 19D). Upon removal of the trophic factors, there was a marked increase in GFP-LC3 puncta in control MCF10A cells, whereas this response was greatly impaired in the p110β knock-down cells (Fig. 19E). These data suggest that p110β is critical for promoting Rab5 activation and autophagy upon trophic factor limitation.

16) p110β selectively regulates trophic factor limitation-induced autophagy.

To further examine a specific role of p110β in mediating trophic factor limitation-induced autophagy, I performed LC3 immunoblotting, which allows convenient quantitative measurement of autophagy. In MCF10A cells, LC3 signal was not readily detectable by immunoblotting (Fig. 20), suggesting a rapid basal level autophagy flux. In the presence of the lysosomal inhibitor bafilomycin A1, a significant increase of LC3 was observed. p110β knock-down cells displayed a lower level of LC3-II than the control cells (Fig. 20), consistent with the positive role of p110β in basal level Rab5 activity and autophagy. Noticeably, the amount of LC3-II induced by trophic factor withdrawal was greatly reduced in p110β knock-down cells (Fig. 20A). By contrast, when treated by other autophagic stimuli including rapamycin (Fig. 20B), the ER stressor tunicamycin (Fig. 20C), or the proteasome inhibitor MG132 (Fig. 20D), the inducibility of LC3-II remained at similar levels in the p110β knock-down cells (Fig. 20). It is noteworthy that the levels of autophagy were lower in p110β-deficient cells similar to what was observed in $\beta^{-/-}$ MEFs, indicating a general role of p110β in regulating autophagy. Nevertheless, the data here indicate that p110β plays an indispensable and selective role in trophic factor limitation-induced autophagy.

17) Plasma membrane targeted p110β does not activate autophagy upon trophic factor limitation.

To validate the role of p110β translocation in mediating trophic factor limitation-induced autophagy, I investigated a loss-of-function p110β mutant that cannot translocate to interact with cytosolic Rab5. Here, I ectopically targeted p110β to the plasma membrane by tagging it with the carboxy-terminal CAAX sequence of K-Ras, which has been shown to effectively target proteins to the plasma membrane (Hancock et al., 1991). Immunofluorescence imaging of the Flag-p110β-CAAX mutant expressed in Hs578T cells confirmed that it did not dissociate from

the plasma membrane upon serum deprivation (Fig. 21A). Coimmunoprecipitation experiments showed a reduced interaction between Rab5 and the p110β-CAAX mutant under basal conditions and a lack of enhanced binding upon serum starvation (Fig. 21B). Importantly, while reconstitution of wild-type p110β in $\beta^{-/-}$ MEFs restored the serum deprivation-induced increases in LC3-II level (Fig. 21C) and GFP-LC3 puncta accumulation (Fig. 21, D and E), expression of the p110β-CAAX mutant failed to do so. The failure of p110β-CAAX to restore autophagy is not due to its possible elevated kinase activity because the p110β-specific kinase inhibitor TGX-221 did not induce GFP-LC3 puncta in the $\beta^{-/-}$ cells expressing p110β-CAAX (Fig. 21F). The same concentration of TGX-221 inhibited lysophosphatidic acid (LPA)-stimulated Akt phosphorylation (Fig. 21F). Therefore, these results strongly support the theory that cytosolic p110β, through its interaction with Rab5, plays a critical role in promoting autophagy induced by trophic factor limitation.

18) Deficiency of p110β results in impaired autophagy in mouse liver.

To investigate the role of p110β in regulating autophagy in vivo, I tested autophagy response in the liver and the heart. The liver is one of the best characterized organs where autophagy plays an important physiological role (Komatsu et al., 2005). Here, $p110\beta^{flox/flox}$ mice were bred with albumin-*Cre* mice, in which expression of the Cre recombinase is under the control of the liver-specific albumin promoter resulting in deletion of floxed genes by 6 wk after birth (Postic and Magnuson, 2000). Successful deletion of p110β was confirmed in 8-wk-old mice (Chattopadhyay et al., 2011). Littermates with either $p110\beta^{flox/flox}$; albumin-Cre^{-} or $p110\beta^{wt/wt}$; albumin-Cre^{+} genotypes were used as controls for the possible effect of either floxed *p110β* or Cre. Because no obvious differences between these two groups were observed, I refer to both control lines as $\beta^{+/+}$ and hereafter do not distinguish between them. Upon 24 h of fasting, protein content significantly decreased in $\beta^{+/+}$ livers, but fasting-induced liver protein degradation was suppressed in $\beta^{-/-}$ livers (Fig. 22A). Compared with the $\beta^{+/+}$liver, EM analysis revealed deformed mitochondria and deficient formation of hyaloplasmic glycogen areas in $\beta^{-/-}$ livers (Fig. 22B), reminiscent of the autophagy-deficient $Atg7^{-/-}$ liver (Komatsu et al., 2005). After 24 h fasting, the $\beta^{+/+}$ liver showed accumulation of autophagosomes, whereas the $\beta^{-/-}$ liver did not (Fig. 22B). Western blotting of liver lysates showed elevated levels of polyubiquitinated proteins and p62 in the $\beta^{-/-}$ liver (Fig. 22, C and D). To further study the involvement of p110β in liver autophagy, $p110\beta^{flox/flox}$ mice were bred with GFP-LC3 transgenic mice (Mizushima et al., 2004), then with the albumin-*Cre* mice. A 24-h fasting resulted in the accumulation of GFP-LC3 puncta in the $\beta^{+/+}$ liver, whereas this response was markedly decreased in the $\beta^{-/-}$ liver (Fig. 22E). Similarly, Beclin 1-GFP mice (Zhong et al., 2009) were bred with $p110\beta^{flox/flox}$; albumin-*Cre* mice. Although a 24-h fasting resulted in accumulation of Beclin 1-GFP puncta in the $\beta^{+/+}$ liver, this response was markedly impaired in the $\beta^{-/-}$ liver (Fig. 22F), suggesting a defect in the early stage of autophagy.

19) Genetic deletion of p110β leads to defective autophagy in mouse heart.

In addition to the liver, I investigated fasting-induced autophagy in the $p110\beta^{-/-}$ heart. $p110\beta^{flox/flox}$ mice were bred with MCK-*Cre* mice (Bruning et al., 1998) to delete p110β in cardiac and skeletal muscles (Wu et al., 2011), then with GFP-LC3 mice. 48 h of

fasting dramatically induced GFP-LC3 puncta in the $\beta^{+/+}$ heart, whereas it failed to do so in the $\beta^{-/-}$ heart (Fig. 23 A).

Besides starvation-induced autophagy, I also tested autophagy induced by pressure overload in the heart by transverse aortic constriction (TAC) (Zhu et al., 2007). In this study, p110β is deleted in the heart of adult MerCreMer; *p110β*$^{flox/flox}$ mice by tamoxifen injection (Lu et al., 2009). As compared with the tamoxifen-injected littermate controls (do not express MerCreMer), the *p110β*-deleted hearts displayed deficiency in autophagosome formation upon TAC (Fig. 23 B). In agreement with this observation, the MCK-*Cre*; GFP-LC3; *p110β*$^{flox/flox}$ and their littermate control mice were also subjected to TAC. The procedure induced a marked increase in the number of GFP-LC3 puncta in $\beta^{+/+}$ hearts, whereas very few GFP-LC3 puncta were observed in $\beta^{-/-}$ hearts after TAC (Fig. 23 C). Taken together, these results indicate that p110β is a positive regulator of autophagy in vivo.

20) Schematic representation of the role of p110β in regulating autophagy.

In summary, this dissertation demonstrates a positive role of p110β in autophagy. In the presence of trophic factors, Class IA PI3Ks are activated by trophic factor receptors and activate signaling pathways such as Akt/mTOR, which maintains basal autophagy at a low level. A fraction of intracellular p110β functions to mediate basal autophagy. The small GTPase Rab5 is kept inactive by the GAP activity of p85 (Fig. 24, left). Upon trophic factor limitation, p110β dissociates from the trophic factor receptor complexes and increases its interaction with Rab5. This p110β-Rab5 interaction alleviates the suppression of Rab5 activity by p85 and increases the interaction of Rab5 with its effectors such as Vps34 that in turn activate autophagy (Fig. 24, right).

III. Discussions

In this dissertation, I showed that p110β is unexpectedly a positive regulator of autophagy. Genetic deletion of p110β results in impaired autophagy in MEFs, liver and heart. shRNA silencing of p110β inhibits autophagy in multiple cell lines. By contrast, overexpression of p110β stimulates autophagy. Mechanistically, p110β does not promote autophagy through the canonical Akt/mTOR pathway or through its kinase activity. Rather, it acts as a scaffold, within the Rab5-Vps34 macro-complex, and stimulates Rab5-GTP that in turn activates Vps34 and autophagy. Upon growth factor limitation, p110β switches from the growth factor receptor complex to the Rab5 complex which enhances Rab5-Vps34 association that promotes autophagy. As supporting evidence of this mechanism, forced expression of Rab5-CA mutant rescued the autophagy deficiency in $\beta^{-/-}$ cells, whereas ectopic targeting of p110β to plasma membrane inhibits autophagy. These findings uncovered a novel role of Class IA PI3K, and suggest a new mechanism of autophagy induction in metazoans.

1) mTOR independent mechanisms of autophagy induction

My data indicate that p110β does not promote autophagy through the Akt/mTOR pathway. Overexpression of p110β stimulates Akt activity yet enhances autophagy (Fig. 5A). Pharmacological inhibition of Akt or mTOR failed to rescue the autophagy deficiency in the $\beta^{-/-}$ MEFs (Fig. 6). I found that p110β-induced autophagy is instead dependent on Rab5 and Vps34. It is noteworthy that the activity of Rab5 is not regulated by mTOR. Inhibition of Akt or mTOR does not affect Rab5 interaction with p110β or Vps34 (Fig. 18 A and B), suggesting that Rab5 activation for autophagy shared distinct mechanism from mTOR inhibition. In line with this notion, expression of Rab5-DN mutant inhibits autophagy both in the basal and in the serum-deprivation conditions (Fig. 18E). Because Rab5-DN inhibits endosomal maturation and thus inhibits mTOR (Flinn et al., 2010), it is unlikely that the lower autophagy is due to elevated mTOR in the Rab5-DN expressing cells. Rather, it points to a direct involvement of Rab5 activity in autophagy that is regulated by p110β and trophic factors.

Consistent with this theory, Vps34 has been shown to integrate growth factor signals and alter its catalytic activity for autophagy (Lipinski et al., 2010). Using an automatic quantification of FYVE-GFP puncta, a probe for PI(3)P that suggests Vps34 activity, Lipinski et al discovered that serum deprivation, but not mTOR inhibition, leads to elevated Vps34 activity (Lipinski et al., 2010). Furthermore, Vps34 activity is inhibited by multiple trophic factors that also suppress autophagy, suggesting that trophic factors go through a mechanism that involved in Vps34 (Lipinski et al., 2010). My findings that Rab5-Vps34 showed enhanced association support this theory, and provide a first direct molecular connection between growth factor receptors and the Vps34 complex that is mediated by p110β and Rab5. It should be noted that the total cellular Vps34 catalytic activity is down-regulated upon serum or nutrient limitation (Backer, 2008). This observation does not contradict my model that showed enhanced Rab5-associated Vps34 activity specifically to serum deprivation. My model suggests that the localized Vps34 activity and PI(3)P production, but not the total cellular Vps34 activity, is required for trophic factor limitation-induced autophagy.

My finding does not challenge an important role of mTOR in mediating autophagy. Rather, it suggests an alternative route for autophagy induction that is independent or in parallel with mTOR inhibition that activates ULK1 complex activity (Fig. 24). It is interesting to note that the ULK1 deficient cells are generally lower in autophagy; however, serum-deprivation is still able to induce LC3-II (Lin et al., 2012), suggesting another pathway that is responsible for

the autophagy induction. It is therefore possible that ULK1-mediated pathway and Rab5-Vps34 mediated pathway function parallelly or synergistically to induce autophagy in response to trophic factor limitation, as depicted in Figure 24.

2) Physiological relevance of p110β in mediating trophic factor limitation-induced autophagy

My findings help to broaden the mechanisms for mammalian autophagy. Bioenergetics in yeasts and other unicellular eukaryotes are largely dependent on the abundance of extracellular nutrients. Upon nutrient or energy shortage, they trigger autophagy in order to increase energy supply and survival (Inoue and Klionsky, 2010), mostly through TOR inhibition and AMPK activation that target the Atg1 complex. While autophagy induction from yeasts to mammals shares many common features and is believed to be induced largely by intracellular nutrient shortage, mammalian cells have evolved trophic factor signaling machineries that responds to environmental clues. One major machinery that transduces trophic factor signalings is the Class I PI3Ks that associate with the trophic factor receptors and produces $PI(3,4,5)P_3$ that serves as a second messenger for cell activation (Lum et al., 2005). Unlike yeasts, mammalian cells have lost the capability to take up nutrients autonomously. Even surround by ample nutrient supplies, mammalian cells are directed by extrinsic growth factor signals for their nutrient uptake and metabolism (Lum et al., 2005). One well established example is insulin-mediated glucose uptake that is executed by the Class I PI3K/Akt pathway that activates the glucose transporter. In the pathology of diabetes, patients typically show hyperglycemia, resulted from impaired insulin/Class I PI3K/Akt signaling (Cantley, 2002; Engelman et al., 2006; Vanhaesebroeck et al., 2010).

Limitation of trophic factors induces autophagy, which is a unique mechanism in multicellular organisms. While current understanding of this autophagy induction mainly focuses on mTOR inhibition, my results here expand the complexity of the autophagy mechanisms. The model implicated that Class I PI3Ks are not only responsible for growth factor-induced cell activation, but are also mediators of cell homeostasis by promoting autophagy upon growth factor limitation. p110β exerts these two distinct activities (cell activation vs. autophagy) by switching its subcellular localization. In response to growth factor stimulation, p110β transduces the signals by producing $PI(3,4,5)P_3$ through its kinase activity, whereas upon growth factor limitation, p110β shifts to the intracellular Rab5 compartment and acts as a scaffold to modulate Rab5 and Vps34 activity to induce autophagy. This study hence helps to advance our understanding of the molecular evolution of Class I PI3K function in metazoans and provides new insight into the regulation of autophagic responses in mammalian cells, which exist in a complex and context-dependent environment.

3) Mechanisms of Rab5-mediated autophagy initiation

Rab5 has been shown to promote autophagy at an early stage that aids the formation of nascent precursor autophagosomal membrane (Ravikumar et al., 2008). My data support this conclusion, and showed Rab5 dependency for autophagy induction by the Vps34 complex (Fig. 12). While Vps34 is an important regulator of autophagy and certainly a critical effector of Rab5 (Christoforidis et al., 1999b; Kihara et al., 2001b), I cannot attribute the effect of p110β-Rab5 on autophagy exclusively to modulation of Vps34 kinase activity. The inhibitory effect on autophagy caused by genetic deletion of p110β or Rab5 inhibition does not perfectly resemble

that of Vps34 inactivation. For example, while genetic deletion of Vps34 did not abolish LC3-II production (Jaber et al., 2012), p110β deficiency and the Rab5-DN mutant caused a reduction in LC3-II levels (Dou et al., 2010; Ravikumar et al., 2008). These results suggest that other Rab5 effectors in addition to Vps34 may also contribute to autophagy. Such effectors may include SNARE proteins, which are well known for regulating membrane fusion events. In particular, SNARE proteins were recently reported to be essential for homotypic fusion of autophagosome precursor membranes (Moreau et al., 2011; Nair et al., 2011). Interestingly, Rab5 and SNARE proteins function synergistically in regulating membrane tethering and fusion (Ohya et al., 2009). Further investigation of SNAREs and other Rab5 effectors will help understand the biogenesis of early precursor autophagosomes.

Moreover, my results imply that Rab5-GTP complexed with p110β is able to bind other effectors. The ability of Rab5, a rather small protein, to simultaneously bind multiple factors may be facilitated by its oligomerization (Daitoku et al., 2001). It remained to be determined whether Rab5 oligomerization regulates Rab5 activity and autophagy.

4) p85 as a versatile factor for PI3K and autophagy

p85 was originally found as a regulatory subunit of Class I PI3K. The strong interaction with p110 stabilizes p110 and keeps p110 in its dormant activity until activated by growth factor receptors. p85 was yet discovered to have more diverse functions besides regulating p110, such as its modulation of PTEN activity (Chagpar et al., 2010), and the control of Rabs as a GAP (Chamberlain et al., 2004). Although p85α was noticed as a weak Rab5 GAP from the in vitro assay, one single mutation that disrupted its GAP activity results in profound cellular phenotype and is tumorigenic (Chamberlain et al., 2004; Chamberlain et al., 2008; Chamberlain et al., 2010). I have found that, using eukaryotic expressed p85α, the Rab5 GAP activity appeared to be more potent than previously described, since Rab5-GTP hydrolysis could be greatly stimulated at a much lower dose (Fig. 14F and our unpublished results), and that knockdown of p85α results in apparent increase in cellular Rab5-GTP (Fig. 14B). The difference in prokaryotic and eukaryotic expressed p85α might account for the different activities.

When PI3Ks was first identified as a Rab5 effector, p85 was found to associate with Rab5 only in the presence of p110β (Christoforidis et al., 1999b), suggesting a stronger affinity of p110β than p85 with Rab5. Together with my results that p110β inhibits the Rab5 GAP function of p85 in vitro (Fig. 14), these evidence collectively suggest that p110β association with Rab5 displaces p85 GAP from Rab5 interaction. The crystal structure of p110β (Zhang et al., 2011) reveals that the Q596 and I597 residues within the helical domain of p110β folds distal and opposing to the iSH2 domain of p85 (Fig. 16). However, as the BH domain of p85 was not present in the co-crystals, the detailed molecular mechanisms remained to be clarified. The co-structures with Rab5 and p110β/p85 complex would greatly facilitate the interpretation. Although I provided evidence showing that p110β antagonizes p85α for Rab5 activity, I am still open to other possible mechanisms how p110β may regulate Rab5. The fact that p85α knockdown in the $\beta^{-/-}$ MEFs largely rescued Rab5 activity and autophagosome formation (Fig. 14, B-D) strongly argues that p85α inhibition on Rab5 is one of the major mechanisms contributing to autophagy defects in the $\beta^{-/-}$ cells.

5) Phenotypes of p110β-deficient liver

The $\beta^{-/-}$ liver displayed impaired fasting-induced protein turnover, GFP-LC3 and Beclin 1 puncta formation, and showed accumulation of autophagy substrate p62 and poly-ubiquitinated proteins (Fig. 22). Ultra-structural analysis revealed a lack of starvation-induced autophagosome formation, accumulation of mitochondria and lack of typical glycogen areas (Fig. 22B). While these data strongly supports a deficiency in autophagy in the $\beta^{-/-}$ liver, similar as those reported in the Atg5/7 deficient livers, it is noted that the $\beta^{-/-}$ liver do not show hepatomegaly or accumulation of lipid droplets as that of Atg5/7 liver or the Vps34 deficient liver (Jaber et al., 2012; Komatsu et al., 2005). One explanation for the discrepancy is that p110β plays a positive role for growth and lipid synthesis. Indeed, the kinase-dead knockin p110β mice showed severe growth retardation. In addition, the mutant mice displayed dyslipidemia, as serum triglyceride and cholesterol levels are significantly reduced, as well as decreased expression of transcription factor sterol regulatory element-binding protein factor 1c (SREBF1C) that is required for the lipogenic program (Ciraolo et al., 2008).

In addition to a deficiency in autophagy, mice with the $\beta^{-/-}$ liver showed hyperglycemia and insulin resistance (Chattopadhyay et al., 2011; Jia et al., 2008). The kinase activity of p110β may or may not be involved in this phenotype. Insulin-stimulated Akt phosphorylation appeared to be intact or slightly impaired in the $\beta^{-/-}$ liver (Chattopadhyay et al., 2011; Jia et al., 2008). Ex vivo experiments using isolated hepatocytes uncovered that the glucose uptake program is not impaired in the $\beta^{-/-}$ cells, however, the $\beta^{-/-}$ cells showed elevated glycogenolysis that may be responsible for the elevated blood glucose levels (Chattopadhyay et al., 2011). One explanation for the elevated glycogenolysis is that the mutant cells switched from protein metabolism to glycogen breakdown as a source for energy supply, due to deficiency in autophagy. In support of this theory, the Vps34-deficient liver showed lack of glycogen deposit, as measured by the PAS staining and EM analysis (Jaber et al., 2012). The role of p110β and autophagy in liver glycogen metabolism remain to be determined. It is also of great interest to investigate the role of the kinase-dead p110β and Rab5 binding deficient p110β mutants in liver autophagy and metabolism.

6) Divergent roles of Class IA PI3K p110α and p110β isoforms

Among Class I PI3Ks, p110β shared similar yet unique features. While all p110s produce PI(3,4,5)P_3, the kinase activity of p110β is more tightly controlled from phospho-tyrosine-peptide activation (Zhang et al., 2011) and showed a preference towards Gβγ in response to GPCRs (Maier et al., 1999). Activating mutations of p110α, but not p110β, are frequently observed in human cancers. Unlike p110α and γ, whose activity is regulated by Ras (Castellano and Downward, 2011), p110β does not seem to be modulated by Ras but by Rab5 (Kurosu and Katada, 2001). The association with Rab5 is a unique nature of p110β. My results identified the evolutionarily conserved 596 and 597 residues, within the helical domain, are critical for the interaction (Fig. 15C). Sequence alignment revealed a diverse homology between p110α and p110β surround the region (Fig. 16B), highlighting the specificity of p110β in Rab5 interaction. The association of Rab5 enhances p110β kinase activity, and that p110β was found to be in a complex containing PI 4- and 5-phosphatases that contributes to endosomal PI(3)P (Shin et al., 2005). While this mechanism suggests a route of PI(3)P production that may contribute to autophagy, the finding that the kinase-dead mutant of p110β is able to rescue PI(3)P production,Vps34 activity, and autophagy strongly suggests a scaffold activity of p110β to

regulate membrane trafficking events, independently of its kinase activity. Indeed, the scaffold function of p110β has been noted by other groups as well. The kinase deficient K805R mutant is able to correct the defects of p110β deficiency in embryonic development, endocytosis, EEA1 endosomal recruitment, and mTOR activation (Ciraolo et al., 2008; Jia et al., 2008), through an unknown mechanism. My finding that p110β activates Rab5 independently of its catalytic activity provides a plausible mechanism for p110β scaffold function, given an essential role of Rab5 in mediating membrane trafficking events.

While my findings point to the importance of the scaffold function of p110β, I cannot exclusively rule out the possibility that its kinase activity also contribute to membrane traffickings, considering its known role in producing endosomal PI(3)P. Although Vps34 deletion leads to defective autophagy in MEFs, liver and heart (Jaber et al., 2012), the Vps34-deficient sensory neurons are capable of autophagosome formation (Zhou et al., 2010). In addition, the Vps34-deficient cells showed intact early endosomal staining of Rab5 and EEA1 (Jaber et al., 2012; Johnson et al., 2006), an event dependent on PI(3)P (Christoforidis et al., 1999a). These facts suggest an alternative route of PI(3)P production for autophagy and endosomes, likely mediated by p110β kinase activity. Further studies with cells and animals doubly deficient in Vps34 and p110β will help to clarify this issue.

7) Rab5-p110β as a pharmacological target of modulating autophagy

My data indicate that p110β and Rab5 play stimulatory role for autophagy. Overexpression of p110β, or enhancing Rab5-GTP level, promotes autophagy. In contrast, downregulation of p110β or Rab5-GTP, or disrupting their interaction, inhibits autophagy. As described in the introduction session, boosting autophagy will be of great potentials for the cure of human diseases, such as obesity, diabetes, and neurodegeneration. Rab5 stimulates autophagy both at the early step of autophagosome formation and the later step of autophagosome maturation, unlike Atg14L or UVRAG, whose actions on autophagy are specific to the early step or later step of autophagy, respectively (Itakura et al., 2008). Therefore, enhancing Rab5 activity represents a promising target for autophagy induction.

Pharmacological targeting of the catalytic pocket of small GTPase, however, is technically difficult. So far, the attempt to inhibit Ras has been unsuccessful. As for p110β-Rab5, p110β activates Rab5 through interaction with Rab5 and thus sequestration of GAP interaction with Rab5, thereby protecting Rab5-GTP from hydrolysis. It is therefore reasonable that short peptide derived from p110β that binds to Rab5 will behave similarly in sequestrating GAP binding and enhancing cellular Rab5-GTP. The region surrounding the 596 and 597 residues represents a likely candidate for such short peptide design. The co-structure of p110β complexed with Rab5 will facilitate the design of peptide, and possibly small molecule inhibitors as well. In fact, the enhancement of autophagy by cell-permeable short peptide has been shown to be promising in preclinical evaluations. Peptide derived from Beclin 1 was reported to activate autophagy (http://www.utmb.edu/wrce/CAP.html).

8) Future directions and perspectives

My demonstration of an autophagy-promoting function of p110β-Rab5 suggests a novel perspective for understanding the physiological and pathological roles of PI3Ks in metabolism, tissue homeostasis, and cancer biology. This dissertation research also leads to several questions that may be worth addressing.

First, the mechanisms of p110β scaffold activity have not been fully addressed. While its interaction with Rab5 clearly plays an important role in autophagy, it remained unclear whether this interaction is also necessary for other events regulated by p110β, such as endocytosis, mTOR activation, and cell proliferation.

Second, as for p110β and Rab5 interaction, it remains to be addressed whether p110β specifically sequesters certain Rab5 GAPs, or it sequesters all Rab5 GAPs in general. In addition, my observation suggests that p110β dissociates from the trophic factor receptors and translocates to the Rab5 compartment upon trophic factor limitation. What is the mechanism for this translocation? How does p110β efficiently and accurately travel to Rab5? Is cytoskeleton mechanism involved in this translocation? Moreover, the GPCR subunit Gβγ is recently known to interact with the linker of C2-helical domain of p110β, in close proximity to where Rab5 binds. It will be interesting to investigate the crosstalk between Gβγ and Rab5, e.g., whether they associate with p110β in a competitive manner in response to distinct environmental clues.

Third, the physiological role of p110β in regulating metabolism needs further investigation. My preliminary results suggest that p110β may be involved in cell death and nutrient metabolism, such as glucose uptake and glycolysis. In addition, while p110β clearly regulates liver glycogen metabolism and the level of blood glucose, the underlying mechanisms are not understood. It is unclear whether the kinase activity or Rab5 binding is involved in these events.

Fourth, the involvement of p110β in pathological conditions is poorly understood. Although the oncogenic activity of p110β has been discovered in cell culture, the in vivo relevance of this finding is not clear. Because autophagy and Rab5 are both involved in multiple steps of tumorigenesis, it will be interesting to determine p110β mutations, gene amplifications or deletions in human cancers, and potentially other diseases as well. Pharmacological manipulations of p110β and Rab5 interaction may hold promising in the prevention or treatment of some diseases. Further studies of these open questions may help broaden our understanding of biological mechanisms and may lead to discovery of new drug targets.

IV. Figures

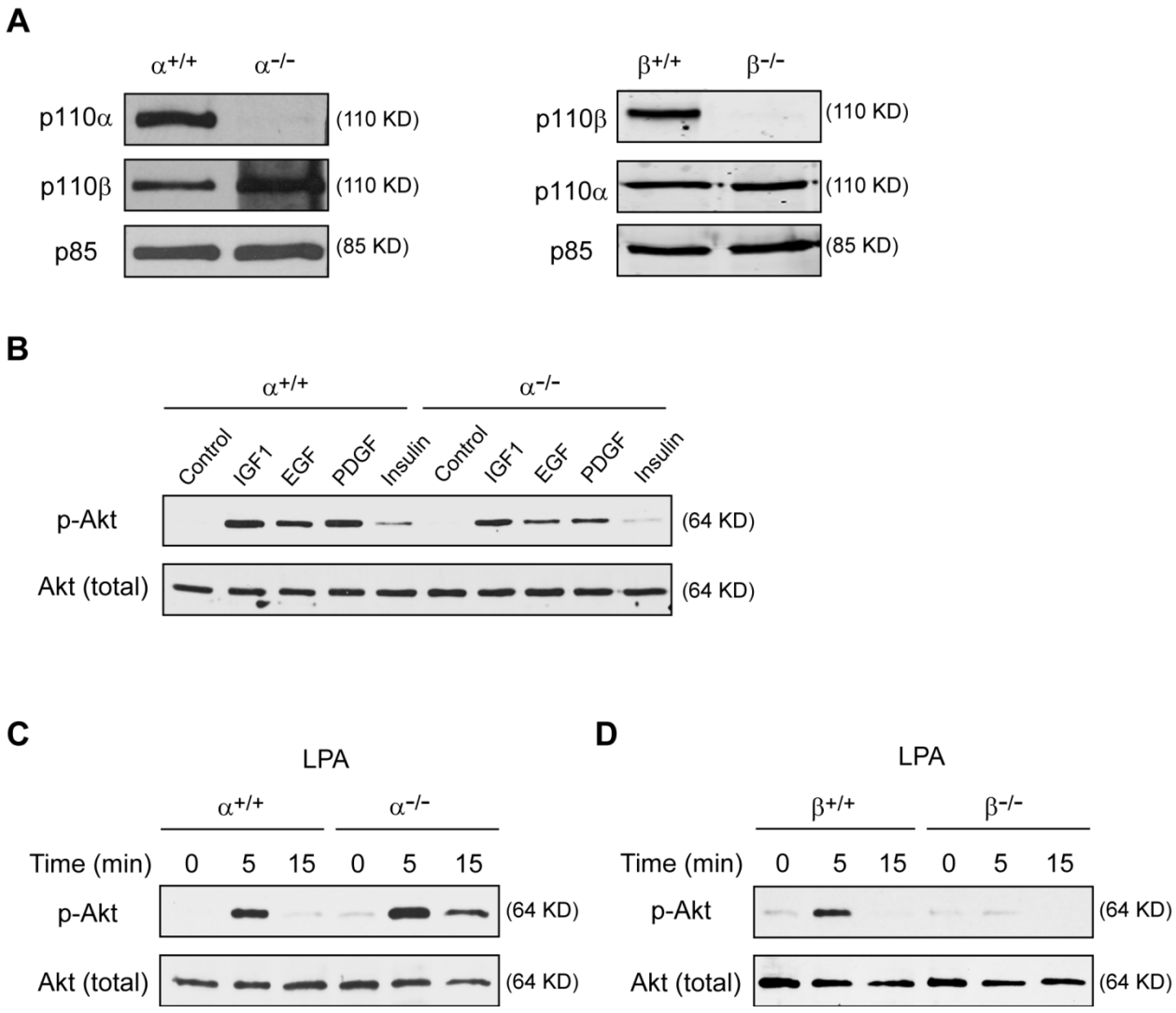

Figure 1. Validation of $\alpha^{-/-}$ and $\beta^{-/-}$ MEFs.

(A) MEFs with indicated genotypes were subjected to immunoprecipitation using phosphotyrosine peptide-conjugated agarose. The precipitates were analyzed with p110α, p110β, and p85 antibodies. (B) $\alpha^{+/+}$ and $\alpha^{-/-}$ MEFs were cultured in serum-free medium overnight, then stimulated with IGF1 (100 ng/ml), EGF (100 ng/ml), PDGF (50 ng/ml), or insulin (10 nM) for 10 min. Cell extracts were probed for p-Akt 308 and total Akt. (C and D) p110α (C) and p110β (D) MEFs with indicated genotypes were cultured in serum-free medium overnight, then stimulated with LPA(10 μM) for indicated time points. Cell lysates were probed for p-Akt 473 and total Akt. This figure was published in Journal of Cell Biology (Dou et al., 2010).

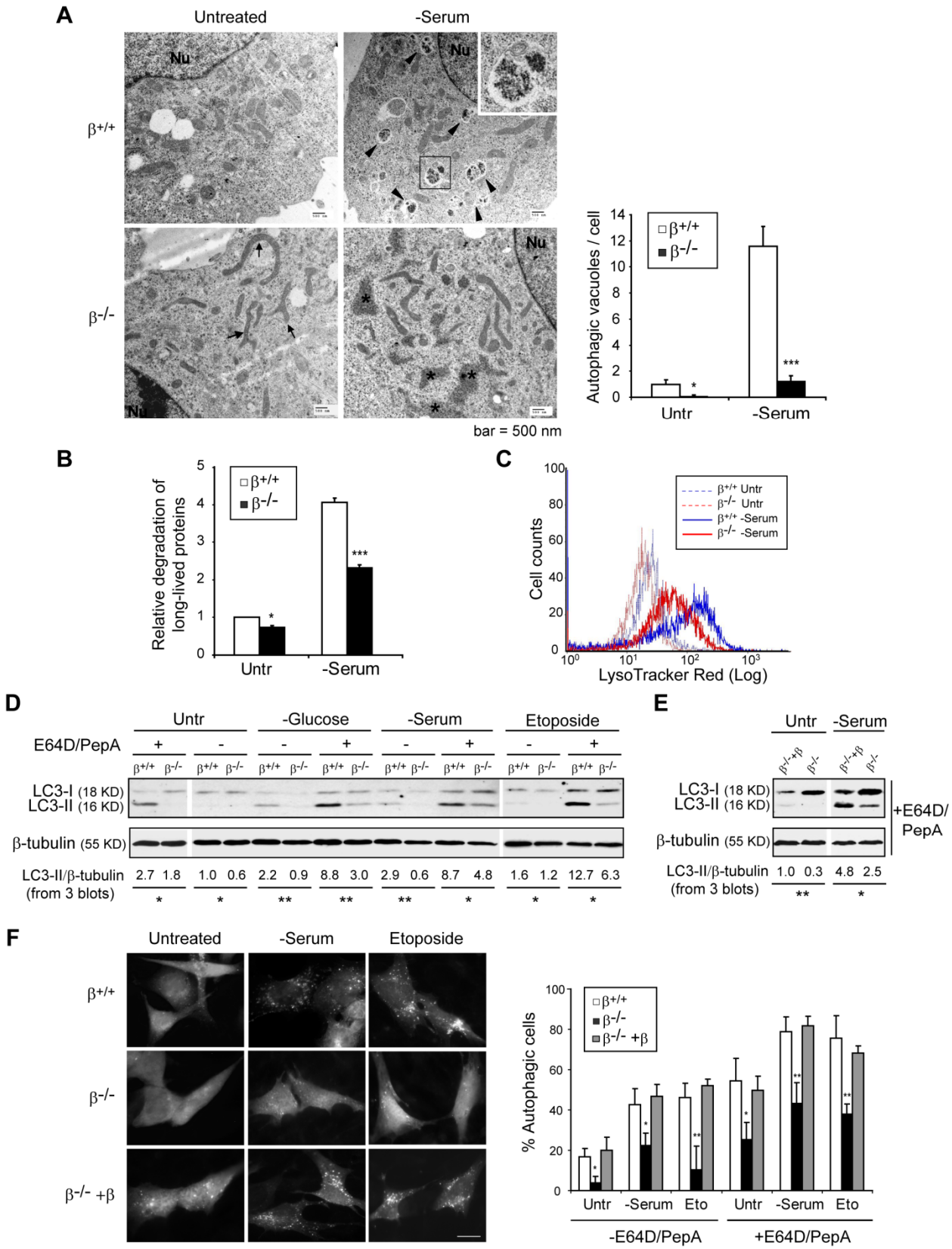

Figure 2. Autophagy is impaired in $\beta^{-/-}$ MEFs.

(A) $\beta^{+/+}$ and $\beta^{-/-}$ MEFs were cultured in complete (untreated) or serum-free medium for 6 h, then observed under an electron microscope. Note the appearance of autophagosomes in serum-deprived $\beta^{+/+}$ MEFs, indicated by arrowheads. A higher magnification view of an autophagosome is shown in the inset. In $\beta^{-/-}$ MEFs, deformed mitochondria are indicated by arrows. In serum-deprived $\beta^{-/-}$ MEFs, aggregated ribosomes are indicated by asterisks. Nu: nucleus. (Right) Quantification of autophagic vacuoles per cell. Error bars: S.E.M.; n=10; * $p<0.05$, *** $p<0.0001$. (B) MEFs were labeled with ^{14}C-valine for 24 h, and cultured in complete or serum-free medium for 6 h. Degradation of long-lived proteins was measured and normalized. Data presented are averages of three independent experiments + S.E.M.; * $p<0.05$, *** $p<0.0001$. (C) MEFs were cultured in complete or serum-free medium for 6 h. Cells were stained with LysoTracker Red, and subjected to flow cytometry analysis. Data shown are representative of three independent experiments. (D) MEFs were cultured in glucose-free medium for 12 h, serum-free medium for 6 h, or treated with 25 μM etoposide for 6 h, in the presence or absence of lysosomal inhibitors E64D and PepA. Cell lysates were probed for LC3 and β-tubulin. Quantification of LC3-II/ β-tubulin from three independent immunoblots is shown. Data presented are the mean values normalized to $\beta^{+/+}$ untreated condition. * $p<0.05$, ** $p<0.005$. (E) $\beta^{-/-}$ and p110β-reconstituted $\beta^{-/-}$ MEFs were left untreated or serum-starved for 6 h, in the presence of E64D and PepA. Cell lysates were subjected to LC3 and β-tubulin immunoblotting. Quantification of LC3-II/ β-tubulin from three independent experiments is shown. * $p<0.05$, ** $p<0.005$. (F) MEFs with indicated genotypes expressing GFP-LC3 were treated as indicated. Cells were observed under a deconvolution fluorescence microscope. Representative images are shown. Quantification of autophagic cells was determined as described in Materials and Methods. Data shown are averages of at least five blind countings + S.D.; * $p<0.05$, ** $p<0.005$. Scale bar: 20 μm. This figure was published in Journal of Cell Biology (Dou et al., 2010).

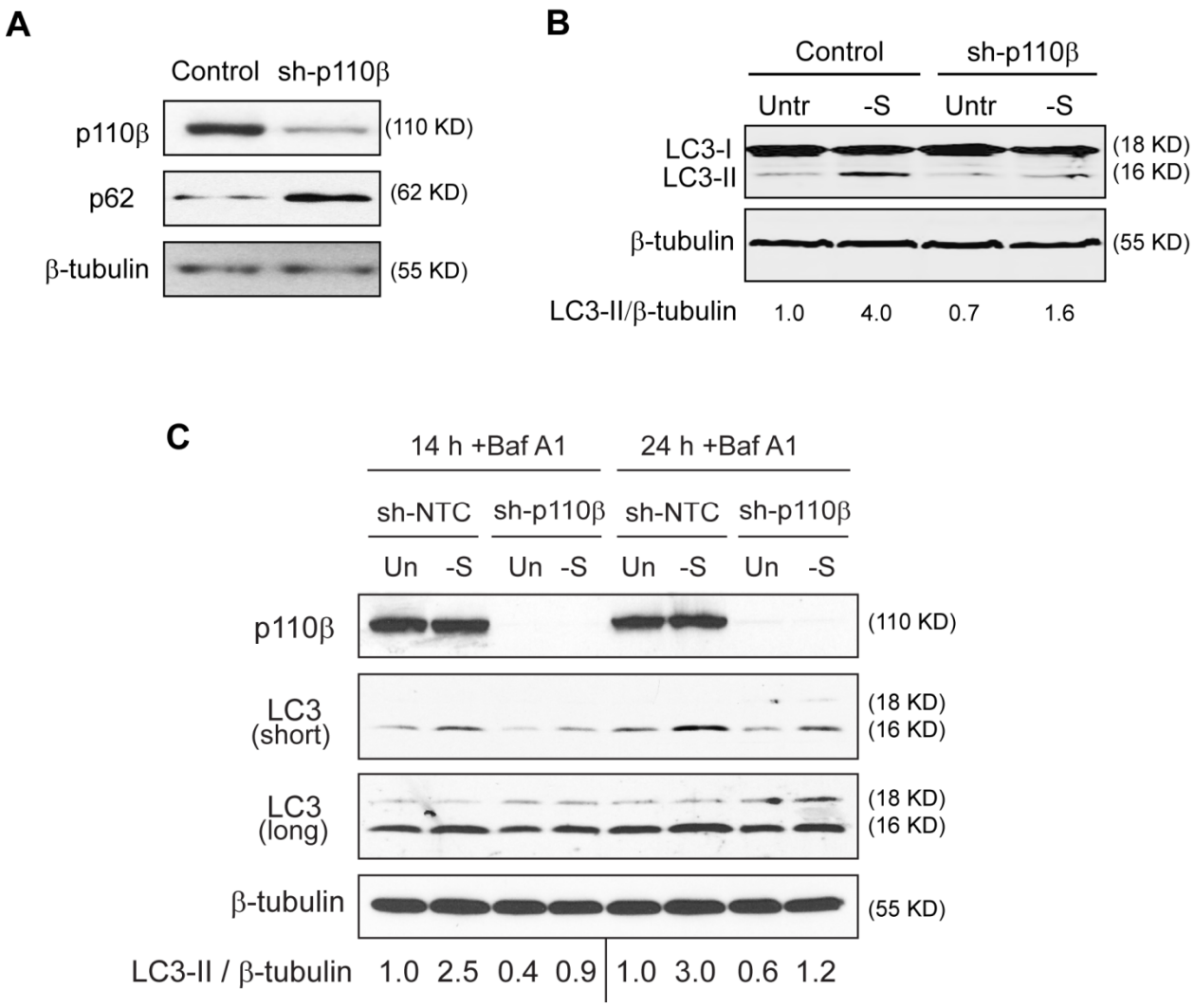

Figure 3. Knockdown of p110β disrupts autophagy

(A and B) HEK293 cells were infected with control lentivirus or lentivirus encoding p110β shRNA, and analyzed 4 days post infection. (A) Cell lysates were made and probed for indicated antibodies. (B) Cells were cultured in complete medium or in serum-free medium for 12 h, in the presence of E64D/PepA. Cell extracts were immunoblotted with LC3 and β-tubulin antibodies, and the ratio of LC3-II/ β-tubulin is shown at bottom. (C) MDA-MB-231 cells were stably infected with lentivirus encoding a tet-inducible non-targeting control or an shRNA against p110β. Cells were cultured in the presence of Doxycycline for 72 h, then left untreated or in serum-free medium, in the presence of 50 nM bafilomycin A1. The cell lysates were probed for indicated antibodies. The ratio of LC3-II against β-tubulin is shown. Panel A and B of this figure was published in Journal of Cell Biology (Dou et al., 2010).

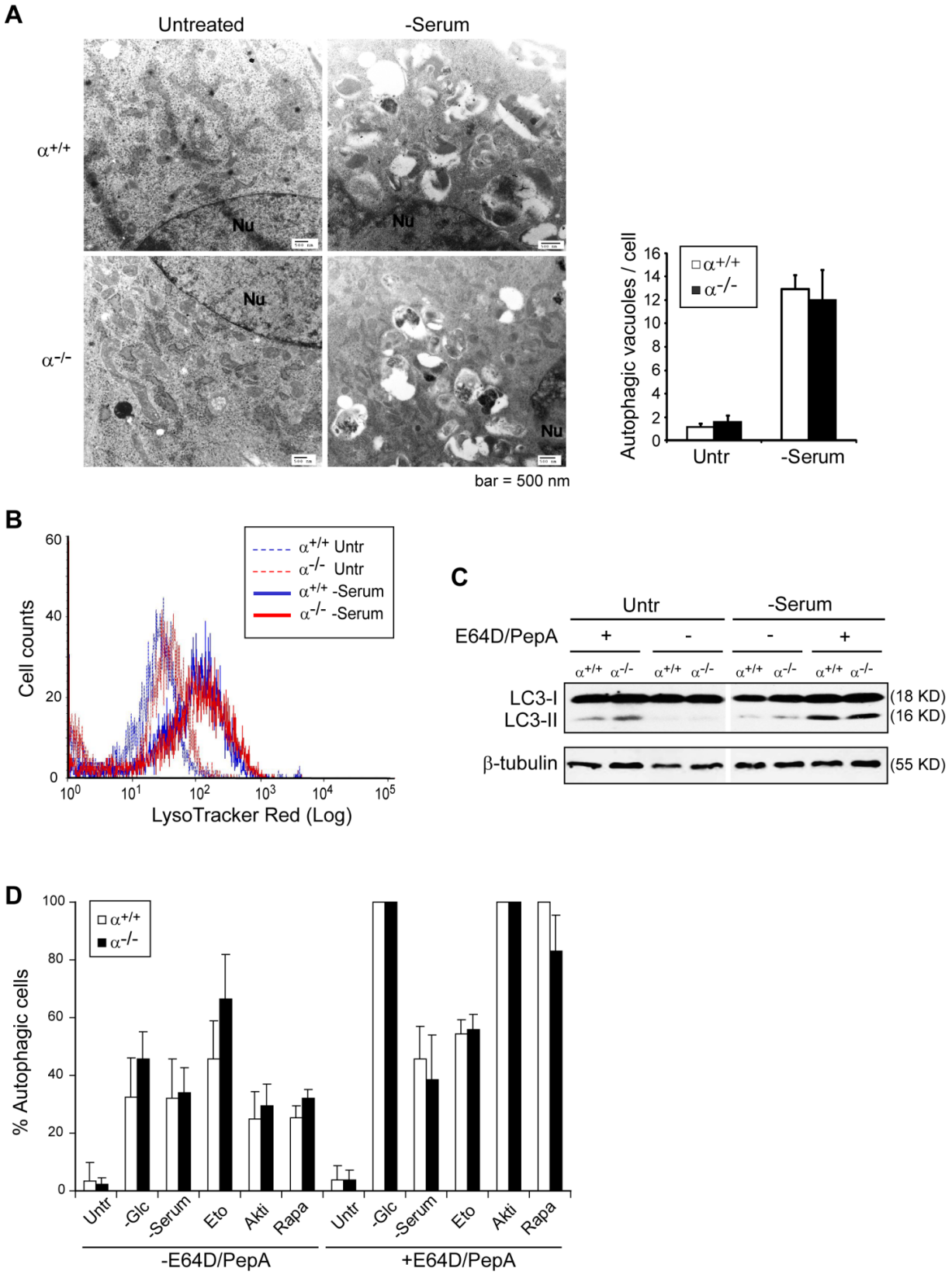

Figure 4. Autophagy is not impaired in $\alpha^{-/-}$ MEFs.

(A) $\alpha^{+/+}$ and $\alpha^{-/-}$ MEFs were cultured in complete (untreated) or serum-free medium for 6 h, then observed under an electron microscope. Note the induction of autophagosome in both $\alpha^{+/+}$ and $\alpha^{-/-}$ MEFs upon starvation. Nu: nucleus. (Right) Quantification of autophagic vacuoles per cell. The comparison between $\alpha^{+/+}$ and $\alpha^{-/-}$ MEFs is not significant, by Student's t-test. (B) MEFs were cultured in complete medium or in serum-free medium for 6 h, stained with LysoTracker Red, and subjected to flow cytometry analysis. (C) $\alpha^{+/+}$ and $\alpha^{-/-}$ MEFs were cultured in complete medium or serum-free medium for 6 h, in the presence or absence of lysosomal inhibitors E64D and PepA. Cell extracts were probed for LC3 and β-tubulin. (D) $\alpha^{+/+}$ and $\alpha^{-/-}$ MEFs stably expressing GFP-LC3 were cultured in complete medium, or treated with glucose withdrawal (12 h), serum withdrawal (6 h), 25 μM etoposide (6 h), 5 μM Akt inhibitor (Akti, 12 h), or 20 nM Rapamycin (Rapa, 12 h), in the presence or absence of E64D and PepA. The percentage of autophagic cells was quantified. Data shown are averages of at least three blind countings + S.D. The comparison between $\alpha^{+/+}$ and $\alpha^{-/-}$ MEFs in each individual treatment is not significant, as determined by Student's t-test. This figure was published in Journal of Cell Biology (Dou et al., 2010).

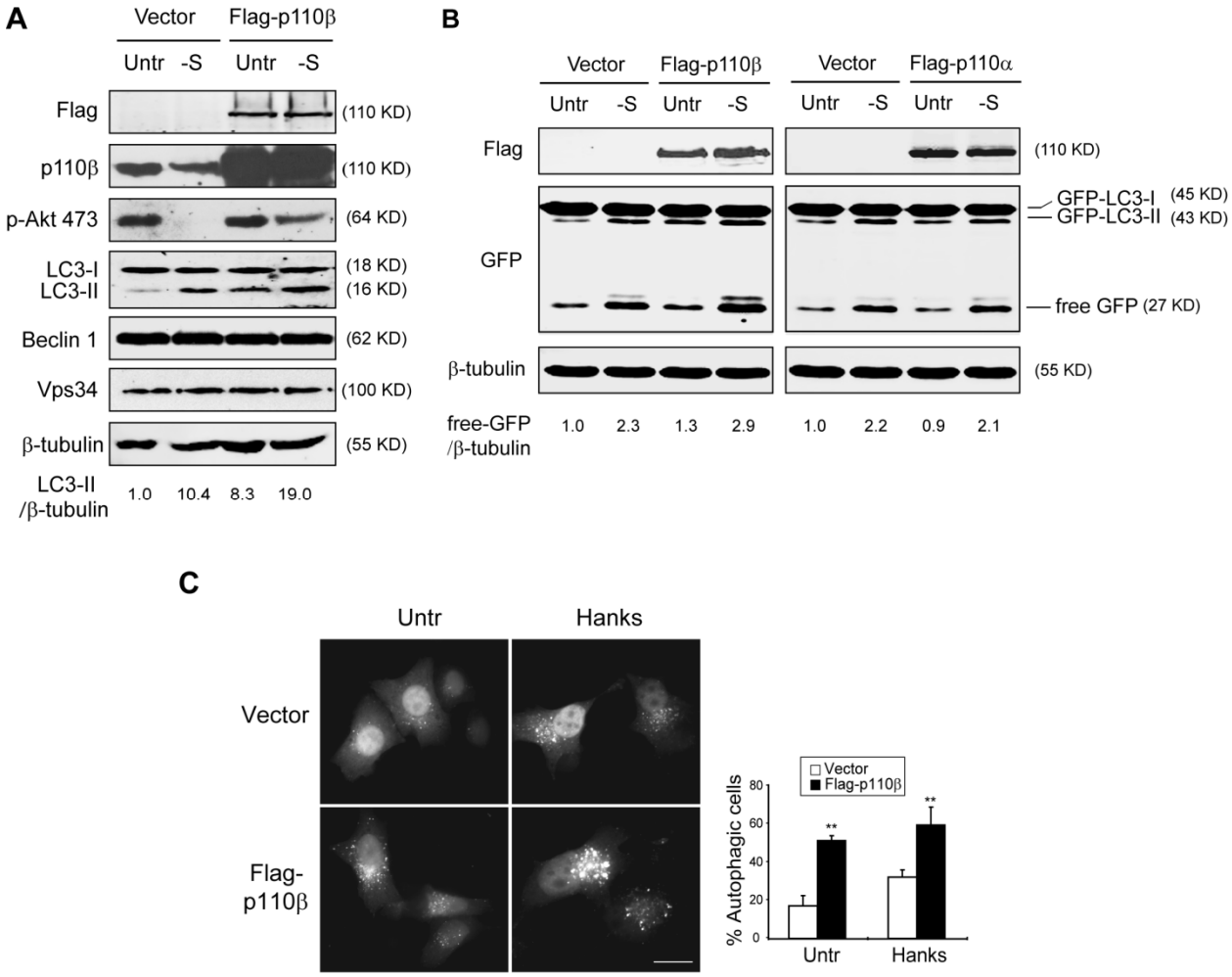

Figure 5. Overexpression of p110β stimulates autophagy.

(A) HEK293 cells were transfected with vector or Flag-p110β expression construct. 48 h post transfection, cells were left untreated or serum-starved for 12 h. Cell lysates were immunoblotted with indicated antibodies. Quantification of the relative LC3-II/ β-tubulin ratio is shown. (B) HEK293 cells stably expressing GFP-LC3 were transfected with vector control, Flag-p110β, or Flag-p110α construct. 48 h post transfection, cells were left untreated or serum-starved for 12 h. Cell extracts were probed for indicated antibodies. Free GFP indicates the lysosomal cleavage of GFP-LC3. The normalized ratio of free GFP/ β-tubulin is shown at bottom. (C) HeLa cells were transfected with GFP-LC3 construct, together with empty vector or Flag-p110β expression construct. 48 h post transfection, cells were cultured in complete medium or in Hanks buffer for 4.5 h. Cells were fixed and observed under fluorescence microscope. Representative images were taken, and quantification of autophagic cells is shown. Data presented are average of four blind countings + S.D.; ** $p<0.005$. Scale bar: 20 μm. This figure was published in Journal of Cell Biology (Dou et al., 2010).

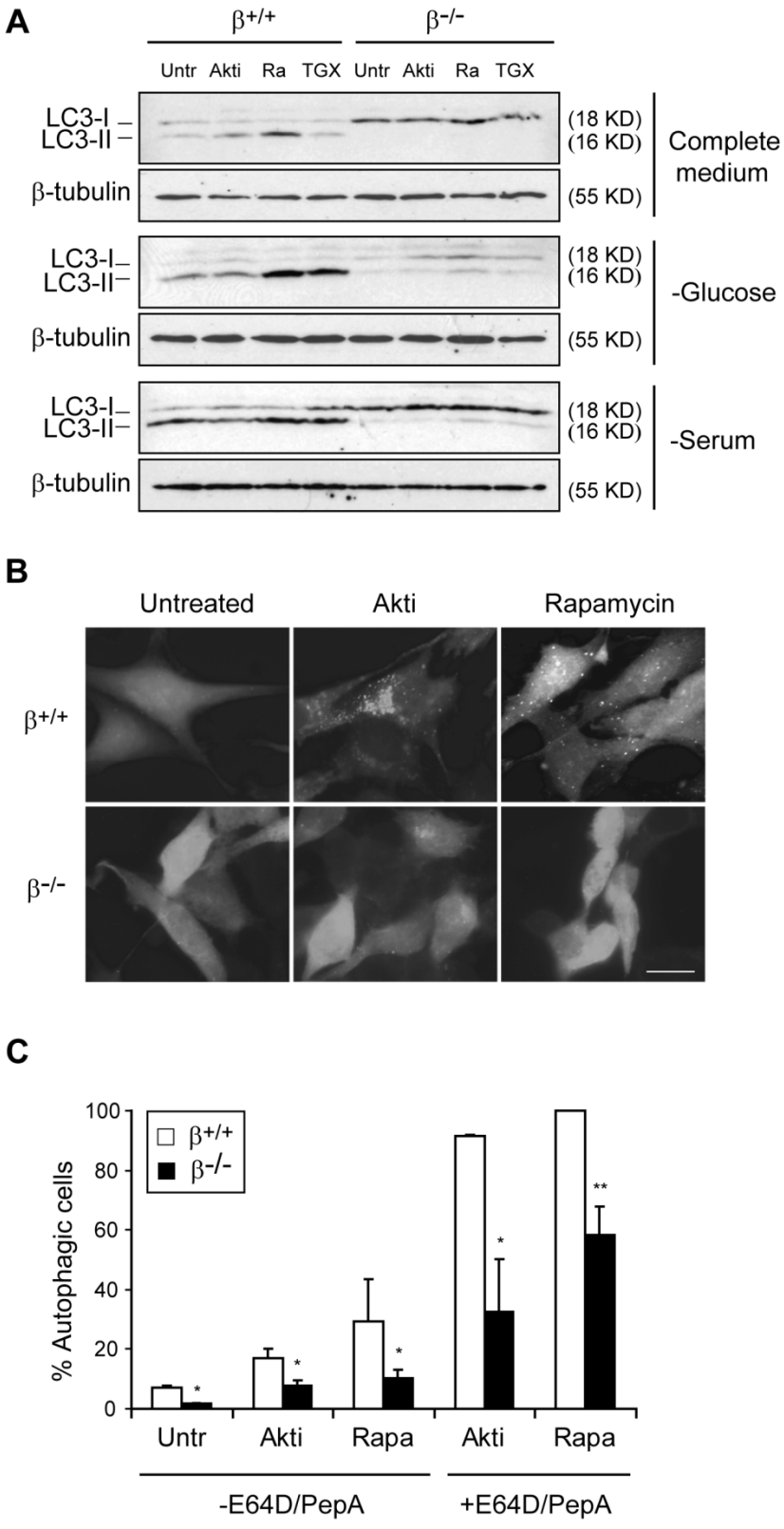

Figure 6. p110β promotes autophagy independently of Akt/TOR pathway.

(A) $\beta^{+/+}$ and $\beta^{-/-}$ MEFs were left untreated or treated with 5 μM Akt inhibitor (Akti), 20 nM rapamycin (Rapa), or 500 nM TGX-221 (TGX, pretreated overnight), in complete medium or in combination with glucose deprivation (12 h), or serum deprivation (6 h), all in the presence of lysosomal inhibitors E64D and PepA. Cell lysates were immunoblotted for LC3 and β-tubulin. (B) $\beta^{+/+}$ and $\beta^{-/-}$ MEFs stably expressing GFP-LC3 were treated with 5 μM Akti or 20 nM rapamycin for 12 h. Cells were observed under a deconvolution fluorescence microscope. Representative images are shown. Scale bar: 20 μm. (C) Quantification of autophagic cells in MEFs stably expressing GFP-LC3 in response to indicated treatments. Data shown are averages of at least three blind countings + S.D.; * $p<0.05$, ** $p<0.005$. This figure was published in Journal of Cell Biology (Dou et al., 2010).

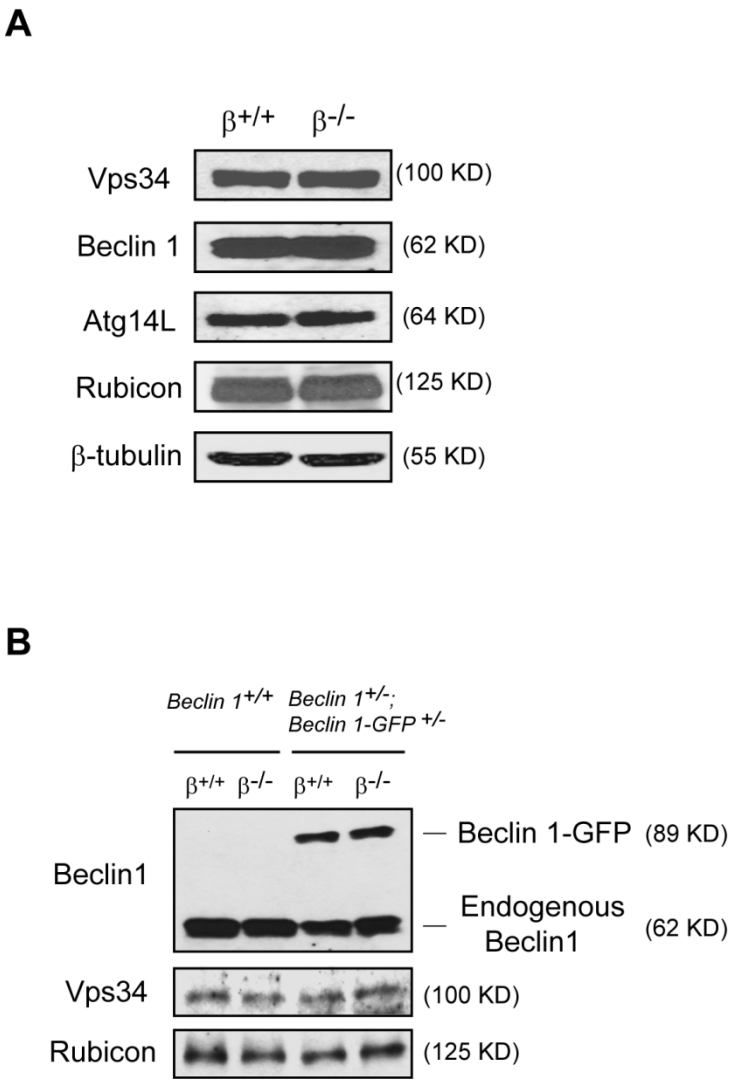

Figure 7. p110β does not affect the steady-state levels of key autophagy proteins.

(A) Protein extracts from $\beta^{+/+}$ or $\beta^{-/-}$ MEFs were immunoblotted with indicated antibodies. (B) Liver extracts from Beclin 1-GFP mice with indicated genotypes were analyzed for Beclin 1, Vps34, and Rubicon expression levels. This figure was published in Journal of Cell Biology (Dou et al., 2010).

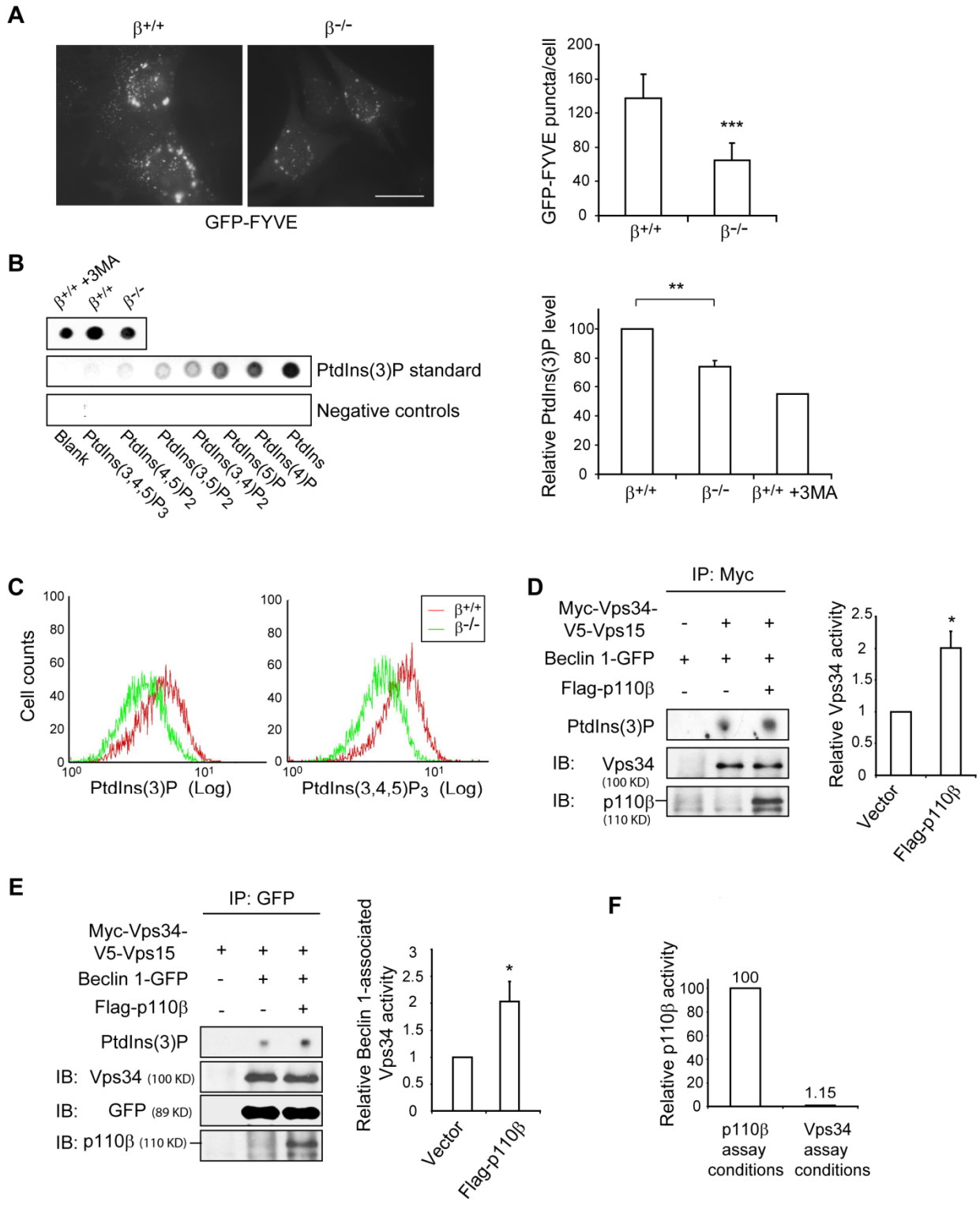

Figure 8. p110β positively regulates PI(3)P level and Vps34 catalytic activity.

(A) $\beta^{+/+}$ and $\beta^{-/-}$ MEFs stably expressing GFP-FYVE were observed under a deconvolution fluorescence microscope. Representative images (left) and quantification of GFP-FYVE puncta per cell (right) are shown. Scale bar: 20 μm; *** $p<0.0001$; $n>20$; error bars: S.E.M. (B) Total cellular lipids were extracted from $\beta^{+/+}$, $\beta^{-/-}$, and $\beta^{+/+}$ MEFs treated with 1 mM 3MA for 12 h. The lipid extracts were subjected to protein-lipid overlay analysis for PI(3)P content. PI(3)P standard and other PI species were used as controls. Data shown are representative of three independent experiments. Quantification of total cellular PI(3)P normalized against total protein is shown on the right. (n=3 for $\beta^{+/+}$ and $\beta^{-/-}$, n=2 for $\beta^{+/+}$ +3MA, ** $p<0.005$, error bars: S.E.M.). (C) $\beta^{+/+}$ and $\beta^{-/-}$ MEFs were stained with antibodies against PI(3)P or PI(3,4,5)P_3, and subjected to flow cytometry analysis. (D and E) HEK293T cells were transfected with indicated plasmids. 48 h post transfection, cell lysates were subjected to immunoprecipitation using Myc antibody-conjugated agarose (D) or GFP antibody and Protein A-conjugated agarose (E). 75% of the precipitates were assayed for Vps34 catalytic activity, and 25% of the precipitates were immunoblotted with indicated antibodies. Vps34 activity is calculated as the amount of PI(3)P generated normalized against the amount of Vps34 present in the precipitates. IP reaction using IgG isotype control showed no activity over the background scintillation readings. Representative autoradiographs of the in vitro Vps34 assay results and the corresponding immunoblots are shown on the left. Quantification of Vps34 activity and Beclin 1-associated Vps34 activity are shown on the right. Data shown are average of three independent experiments + S.E.M.; * $p<0.05$. (F) Purified p110β/p85α was assayed under p110β or Vps34 assay conditions. Results shown are the average of duplicate experiments. This figure was published in Journal of Cell Biology (Dou et al., 2010).

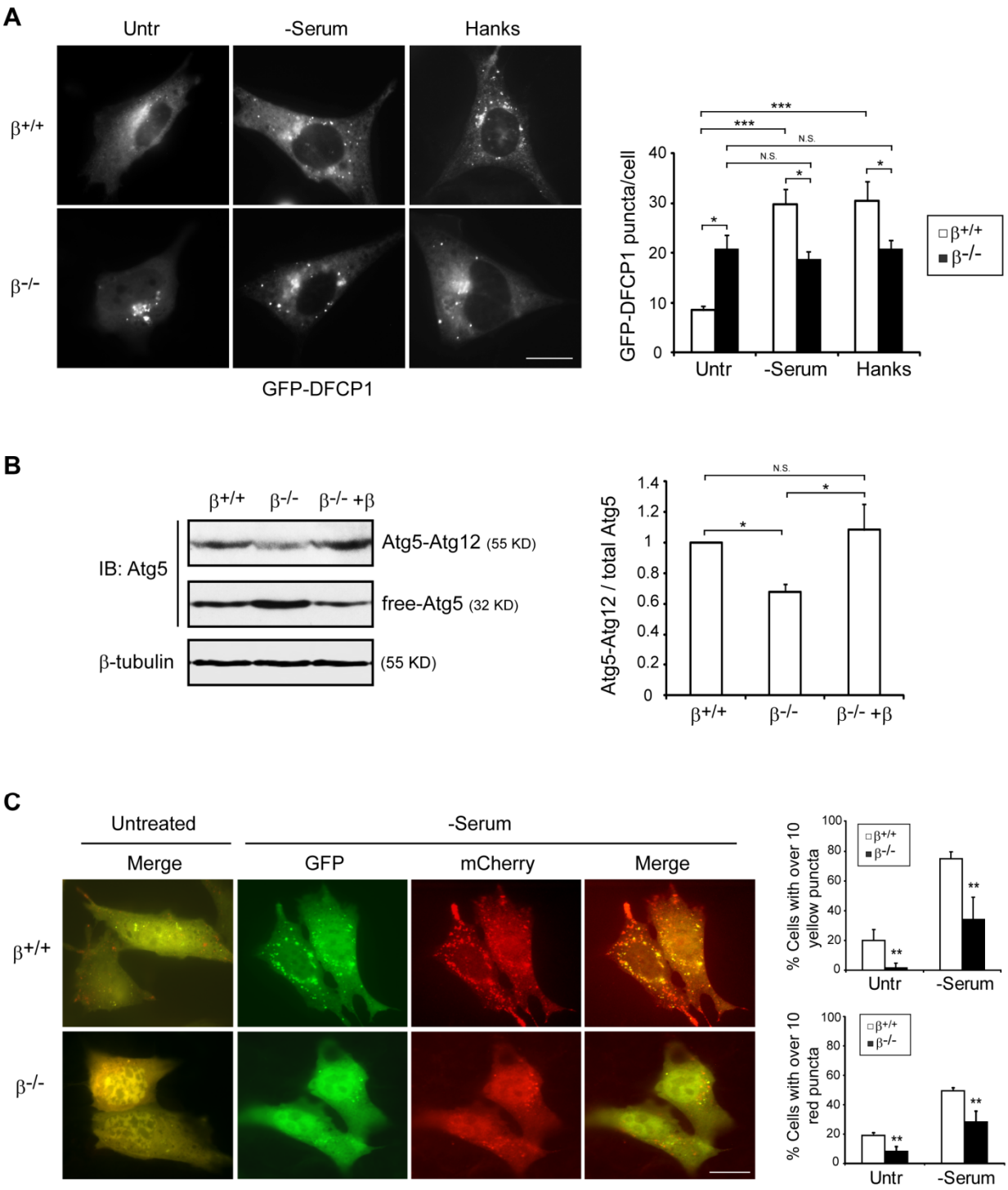

Figure 9. Early stage of autophagosome formation is suppressed in $\beta^{-/-}$ MEFs.

(A) $\beta^{+/+}$ and $\beta^{-/-}$ MEFs were transfected with GFP-DFCP1 expression construct. 24 h post transfection, cells were cultured in complete medium, serum-free medium (6 h), or Hanks buffer (2 h). Cells were fixed, observed, and imaged under a deconvolution fluorescence microscope. Only cells with moderate levels of GFP signal were quantified and imaged. Representative images are shown. Scale bar: 20 μm. Quantification of GFP puncta per cell is shown on right. Error bars: S.E.M.; n=10; * $p<0.05$, *** $p<0.001$; N.S.: non-significant. (B) $\beta^{+/+}$,$\beta^{-/-}$, and p110β reconstituted $\beta^{-/-}$ MEFs lysates were probed for Atg5 and β-tubulin antibodies. The quantification of relative Atg5-Atg12 conjugation is shown on right. Data shown are the mean values from three independent experiments. (* $p<0.05$, N.S., non-significant. Error bars: S.E.M.) (C) MEFs expressing mCherry-GFP-LC3 were cultured in complete medium or serum-free medium for 6 h, and observed under a deconvolution fluorescence microscope. Representative images with GFP, mCherry, or merged channels are shown. Scale bar: 20 μm. Quantification of cells with yellow or red puncta is shown on the right. Data shown are averages of five independent countings + S.D.; ** $p<0.005$. This figure was published in Journal of Cell Biology (Dou et al., 2010).

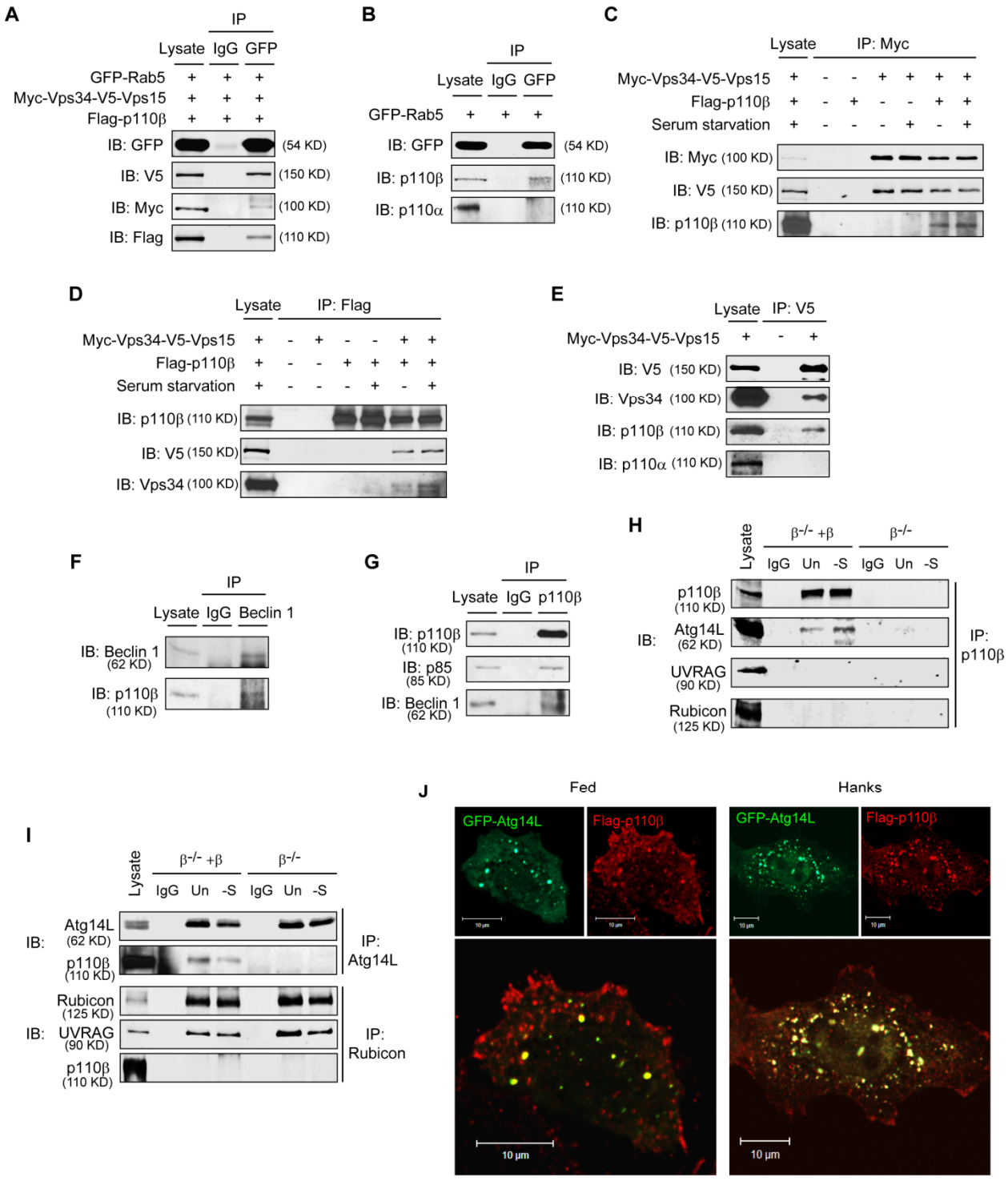

Figure 10. p110β is a component of the Vps34-Vps15-Beclin 1-Atg14L complex.

(A) HEK293T cells were transfected with indicated plasmids. Cell lysates were subjected to immunoprecipitation using IgG control or GFP antibody. The lysates and precipitates were analyzed with indicated antibodies. (B) GFP-Rab5 transfected HEK293T cells were subjected to immunoprecipitation, and the precipitates were immunoblotted with indicated antibodies. (C-E) HEK293T cells were transfected with indicated plasmids. Cells were either cultured in complete medium, or in serum-free medium for 12 h. Cell extracts were made and subjected to immunoprecipitation using Myc, Flag, or V5 antibodies. The precipitates together with lysates were subjected to immunoblotting with indicated antibodies. (F and G) 293T (F) or MCF10A (G) cell lysates were subjected to immunoprecipitation using IgG, Beclin 1, or p110β antibodies. The precipitates together with cell lysates were analyzed with indicated antibodies. (H and I) $\beta^{-/-}$ and p110β-reconstituted $\beta^{-/-}$ MEFs were cultured in complete medium, or in serum-free medium for 6 h. Cell extracts were subjected to immunoprecipitation using IgG control, p110β antibody (H), or Atg14L and Rubicon antibodies (I). The precipitates and cell lysates were analyzed with indicated antibodies. (J) HeLa cells were transfected with Flag-p110β together with GFP-Atg14L constructs. Cells were left untreated or starved in Hanks buffer for 4 h. The cells were fixed and stained with Flag and Alexa594-conjugated antibodies, and observed under a confocal fluorescence microscope. Representative images with green, red, or merged channels are shown. This figure was published in Journal of Cell Biology (Dou et al., 2010).

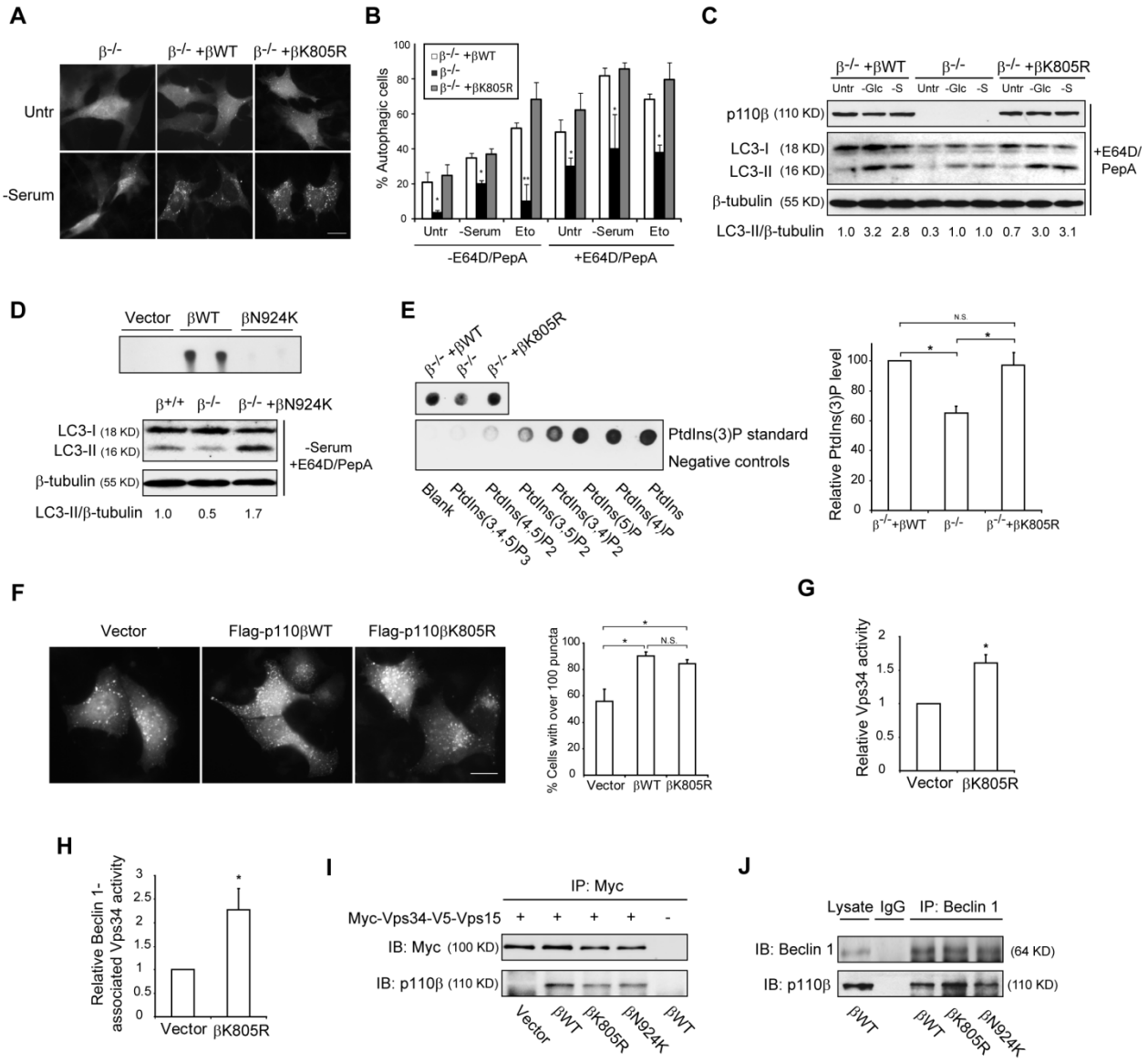

Figure 11. p110β promotes autophagy independently of its kinase activity.

(A) $\beta^{-/-}$ MEFs stably expressing GFP-LC3 were stably reconstituted with construct expressing p110βWT or p110βK805R mutant. Cells were left untreated or serum-starved for 6 h. Cells were fixed and imaged under a deconvolution fluorescence microscope. Representative images are shown. Scale bar: 20 μm. (B) Quantification of autophagic cell percentage of GFP-LC3 expressing MEFs upon indicated treatments. Data shown are averages of five blind countings + S.D.; * $p<0.05$, ** $p<0.005$. (C) The three cell lines were cultured in complete medium, glucose-free medium (12 h), or serum-free medium (6 h), in the presence of E64D and PepA. Cell lysates were immunoblotted with indicated antibodies. Quantification of LC3-II/ β-tubulin is shown at bottom. (D) (Top) HEK293 cells were transfected with empty vector, or constructs expressing Flag-tagged p110βWT or p110βN924K. p110β PI3K activity was assayed in Flag-

immunoprecipitates. Results show an autoradiograph from duplicate assays. (Bottom) $\beta^{+/+}$, $\beta^{-/-}$, and $\beta^{-/-}$ MEFs reconstituted with p110βN924K mutant were cultured in serum-free medium for 6 h, in the presence of E64D and PepA. Cell extracts were probed for LC3 and β-tubulin, and the ratio of LC3-II/ β-tubulin is shown. (E) MEFs with indicated genotypes were subject to protein-lipid overlay analysis for PI(3)P content. Quantification of total cellular PI(3)P normalized against total protein is shown on the right. Data shown are the mean values from three independent experiments. (* $p<0.05$, N.S., non-significant. Error bars: S.E.M.) (F) HeLa cells were transfected with GFP-FYVE, together with vector control, Flag-p110βWT, or Flag-p110βK805R construct. 48 h post transfection, cells were fixed and observed under a deconvolution fluorescence microscope. Scale bar: 20 μm. Cells with over 100 GFP puncta were quantified and presented. Data shown within each group are the average of at least 5 independent countings with over 200 cells. Error bars: S.D., * $p<0.05$, N.S.: non-significant. (G and H) HEK293T cells overexpressing Myc-Vps34-V5-Vps15, Beclin 1-GFP, together with vector control or Flag-p110βK805R were subjected to immunoprecipitation using an anti-Myc antibody (G) or a GFP antibody (H). Vps34 activity was determined. Data presented are the average of three independent experiments; error bars: S.E.M.; * $p<0.05$. (I) HEK293T cells were transfected with the Myc-Vps34-V5-Vps15 bicistronic plasmid, together with empty vector or constructs expressing wild-type or kinase-dead p110β mutants. Cell lysates were subject to immunoprecipitation using an anti-Myc antibody. The precipitates were immunoblotted for Myc and p110β. (J) HEK293T cells were transfected with constructs expressing wild-type or kinase-dead p110β mutants. Cell lysates were subject to immunoprecipitation using IgG or Beclin 1 antibody. The precipitates were probed for Beclin 1 and p110β. This figure was published in Journal of Cell Biology (Dou et al., 2010).

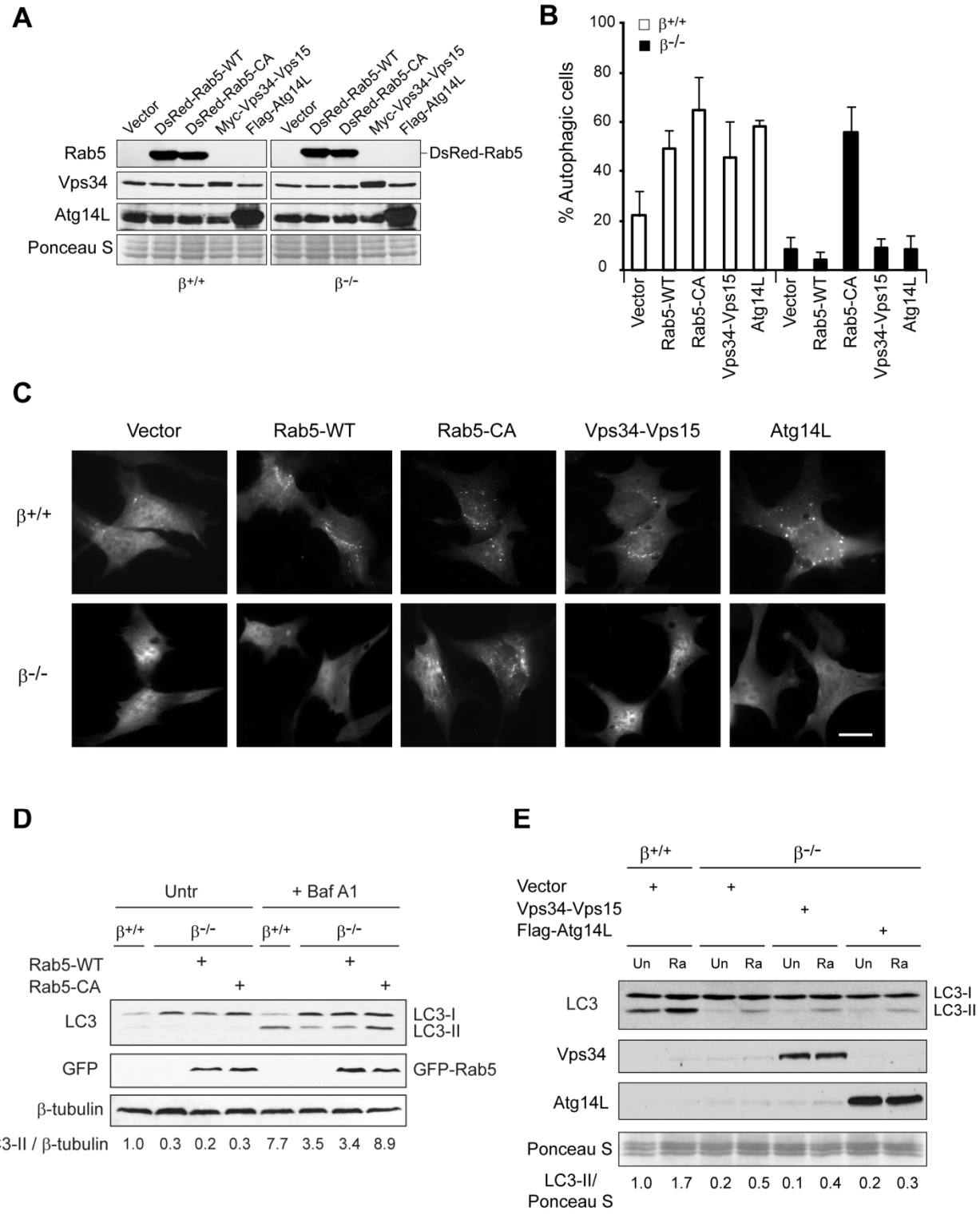

Figure 12. Rab5 plays a critical role in p110β-mediated autophagy.

(A-C) $\beta^{+/+}$ and $\beta^{-/-}$ MEFs were transfected with GFP-LC3 together with vector, DsRed-Rab5-WT, DsRed-Rab5-CA, Myc-Vps34-Vps15, or Flag-Atg14L expression constructs. (A) Western blots of cell lysates were probed with the indicated antibodies. Ponceau S staining shows equal protein loading. (B) Cells were fixed and imaged under a deconvolution microscope, and autophagic cells were quantified. Cells with more than 10 cytosolic puncta and diminished nuclear GFP were considered as autophagic. Data are averages of at least 4 blind countings with over 200 cells. Error bars: SD. (C) Representative images of GFP-LC3 fluorescence in MEFs. Scale bar: 20 μm. (D) $\beta^{+/+}$ and $\beta^{-/-}$ MEFs were transfected with vector (control), GFP-Rab5-WT, or GFP-Rab5-CA. 48 h post transfection, cells were left untreated or treated with 50 nM bafilomycin A1 for 6 h. Immunoblots of cell lysates were probed with the indicated antibodies. Relative levels of LC3-II (expressed as normalized LC3-II/β-tubulin ratios) are shown. (F) $\beta^{+/+}$ and $\beta^{-/-}$ MEFs were transfected with vector control or expression constructs encoding the bicistronic Vps34-Vps15, or Flag-Atg14L. 48 h post transfection, cells were left untreated or treated with 50 nM rapamycin for 6h, in the presence of 50 nM bafilomycin A1. The cell lysates were subjected to immunoblotting with indicated antibodies. Ponceau S staining is shown for equal loading. The relative amount of LC3-II is shown at the bottom. This figure has been submitted for publication.

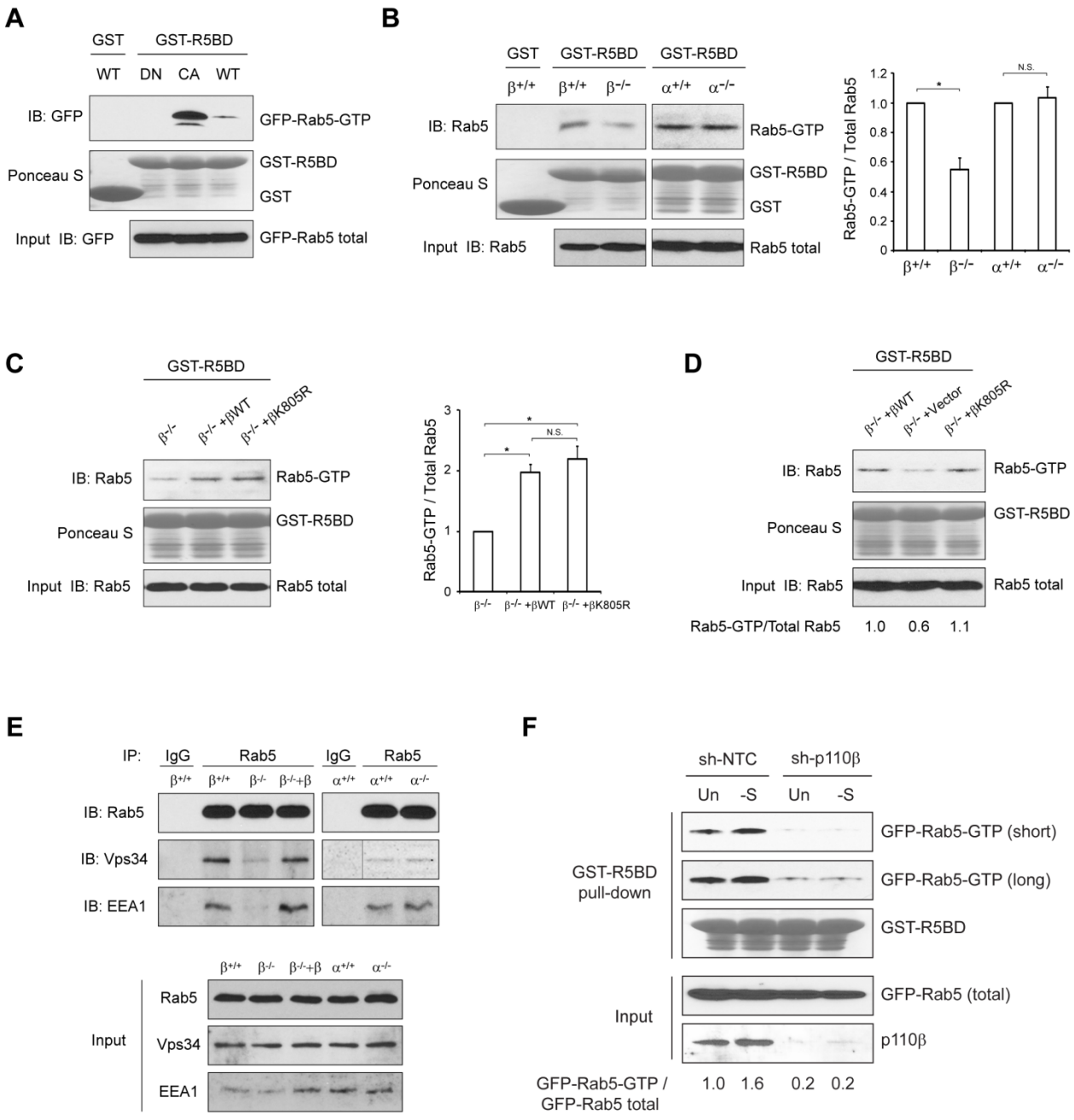

Figure 13. p110β promotes Rab5 activation.

(A) HEK293T cells were transfected with GFP-tagged Rab5-WT, Rab5-DN, or Rab5-CA. 48 h post transfection, cell lysates were subjected to pull-down with GST (control) or GST-R5BD beads. Western blots of precipitates and total cell lysates were probed with GFP antibody. Ponceau S staining shows GST and equal amounts of GST-R5BD used for the pull-downs. (B) Lysates of MEFs with the indicated genotypes were subjected to GST or GST-R5BD pull-down, and western blotting was used to analyze Rab5-GTP levels. Relative levels of Rab5-GTP (expressed as normalized Rab5-GTP/total Rab5 ratios) are shown on the right. Data are means

of three independent experiments ± SEM; * $p<0.05$; N.S., non-significant. (C) $\beta^{-/-}$ MEFs and those stably reconstituted with wild-type p110β or the kinase-dead K805R mutant were analyzed for Rab5-GTP by the GST-R5BD pull-down assay. Relative levels of Rab5-GTP are shown on the right. Data are average values of three independent experiments ± SEM; * $p<0.05$; N.S., non-significant. (D) $\beta^{-/-}$ MEFs were transfected with vector control, expression construct of p110β-WT or the kinase dead p110β-K805R mutant. 48 h post transfection, cell lysates were subjected to GST-R5BD pull-down for the amount Rab5-GTP. Relative Rab5-GTP against total Rab5 is shown. (E) MEFs with the indicated genotypes were subjected to immunoprecipitation with control IgG or Rab5 antibody. Immunoblots of the precipitates and the input were probed with the indicated antibodies. (F) HEK293T cells were stably infected with the tet-inducible shRNA control or that against p110β. Cells were treated with doxycycline (Dox, 1 μg/ml) for 3 d to reach a significant silencing of p110β. Cells were transfected with GFP-Rab5 after 1 d treatment of Dox. 2 d post transfection, cells were untreated or serum-deprived for 24 h (with Dox). Cell lysates were analyzed for the amount of GFP-Rab5-GTP using the R5BD pull-down assay. This figure has been submitted for publication.

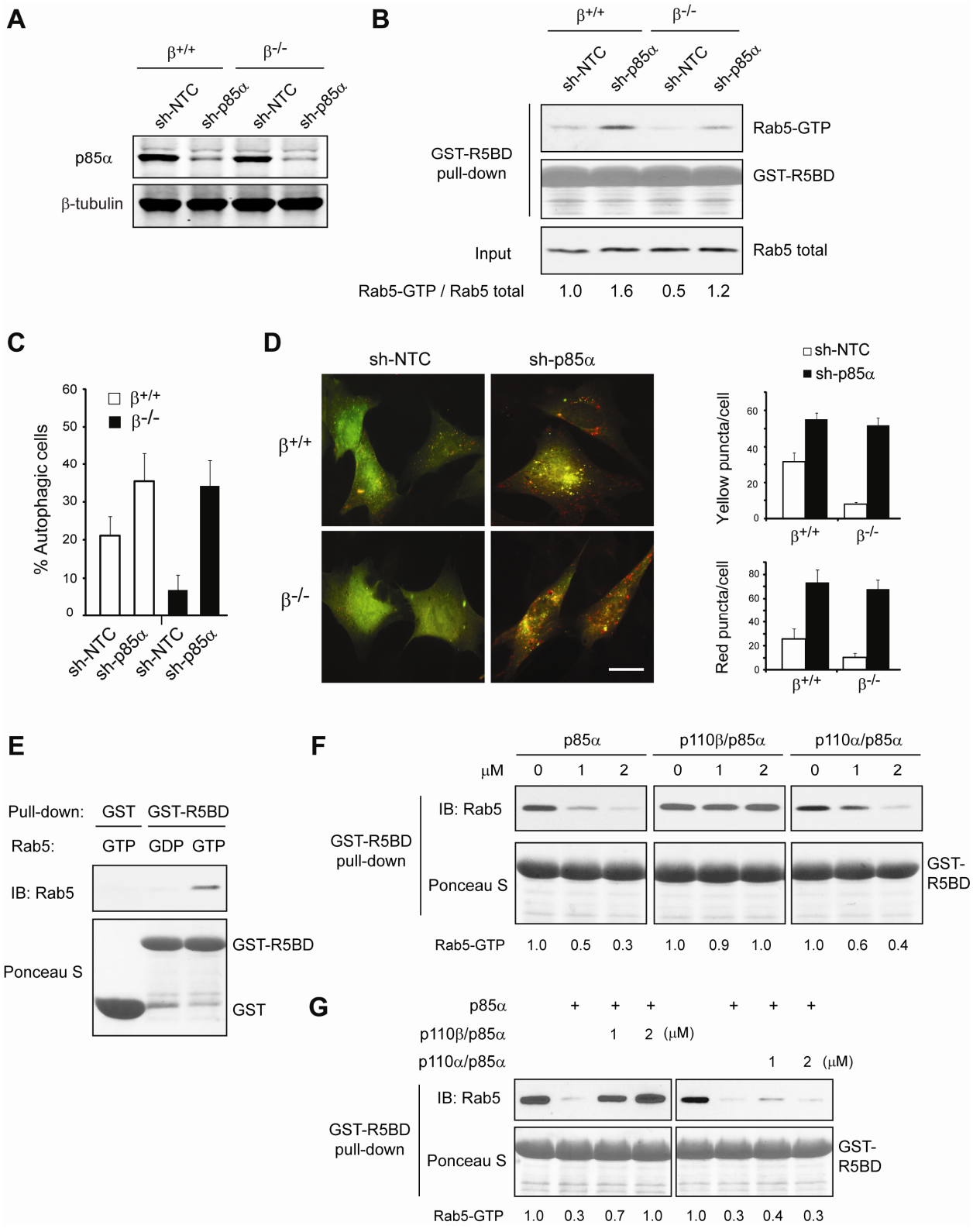

Figure 14. p110β suppresses the Rab5 GAP activity of p85α.

(A) $\beta^{+/+}$ and $\beta^{-/-}$ MEFs were stably infected with lentivirus encoding a non-targeting control shRNA or shRNA against p85α. Western blots of cell lysates were probed for p85α and β-tubulin (to show equal protein loading). (B) MEFs generated as in (A) were subjected to GST-R5BD pull-down assays to detect Rab5-GTP. Relative levels of Rab5-GTP (expressed as normalized ratios of Rab5-GTP/total Rab5) are shown. Note that p85α silencing leads to increased levels of Rab5-GTP. (C) MEFs generated as in (A) were transfected with GFP-LC3 and autophagic cells were quantified. The data are averages of at least four blind countings with over 200 cells. Error bars: SD. (D) MEFs generated as in (A) were transfected with mCherry-GFP-LC3. 48 h post transfection, cells were fixed and imaged under a deconvolution microscope. Images were taken, and yellow and red puncta were counted. Data are mean values of over 20 cells ± SEM. (E) Purified Rab5 (200 nM) was loaded with GDP or GTP and subjected to pull-down with GST or GST-R5BD beads. The precipitates were analyzed for Rab5-GTP. Ponceau S staining shows the amount of GST and GST-R5BD used for the pull-downs. (F) For *in vitro* Rab5 GAP assays, 200 nM Rab5-GTP was incubated with the indicated concentrations of purified p85α, p110β/p85α, or p110α/p85α. Rab5-GTP was then pulled down with GST-R5BD beads and quantified by immunoblotting. The relative amounts of Rab5-GTP are shown. (G) 200 nM Rab5-GTP was incubated with 2 μM p85α in the absence or presence of the indicated concentrations of p110β/p85α or p110α/p85α. Rab5 GAP activity was assessed as in (F). The relative amounts of Rab5-GTP are shown. This figure has been submitted for publication.

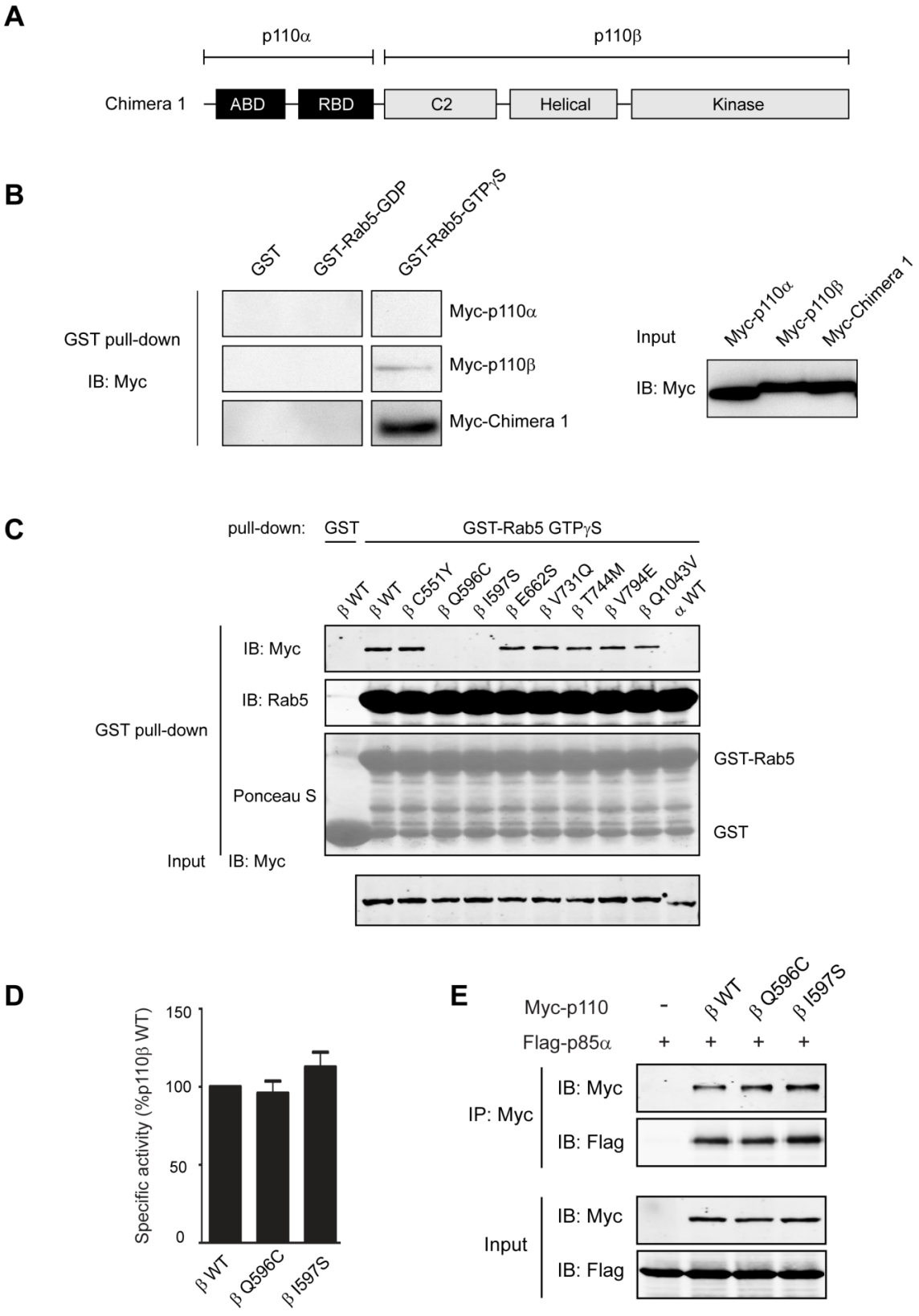

Figure 15. Characterization of p110β mutants defective in Rab5 association.

(A) Scheme of the chimera 1 construct that harbors a swapped ABD and RBD domain from p110α. (B) HEK293T cells were transfected with Myc-tagged p110α, p110β, or the chimera 1 construct together with p85. The cell lysates were subjected to pull-down with GST control, or GST-Rab5 loaded with GDP or GTPγS. Note that both p110β and the chimera 1 showed positive binding for Rab5, whereas p110α appeared negative. (C) HEK293T cells were transfected with Myc-tagged p110α or p110β constructs together with Flag-p85α. 48 h post transfection, cell lysates were subjected to pull-down with GST or GST-Rab5 loaded with GTPγS. Western blots of the precipitates and the input were probed with the indicated antibodies. Ponceau S staining shows GST and equal amounts of GST-Rab5 used for the pull-downs. (D) p110β-Q596C and p110β-I597S possess intact kinase activity. Data presented are the means of three independent experiments, normalized against that of p110β protein levels. Error bars: SEM. (E) HEK293T cells were transfected with Myc-tagged p110β-WT, p110β-Q596C or p110β-I597S together with Flag-p85α. 48 h post transfection, cell lysates were subjected to immunoprecipitation with Myc-antibody conjugated to agarose. Blots of the precipitates and the input were probed with Myc and Flag antibodies. The data in panel B and D were provided by Dr. Jonathan Backer's laboratory (Albert Einstein College of Medicine, NY). Panel C to E of this figure has been submitted for publication.

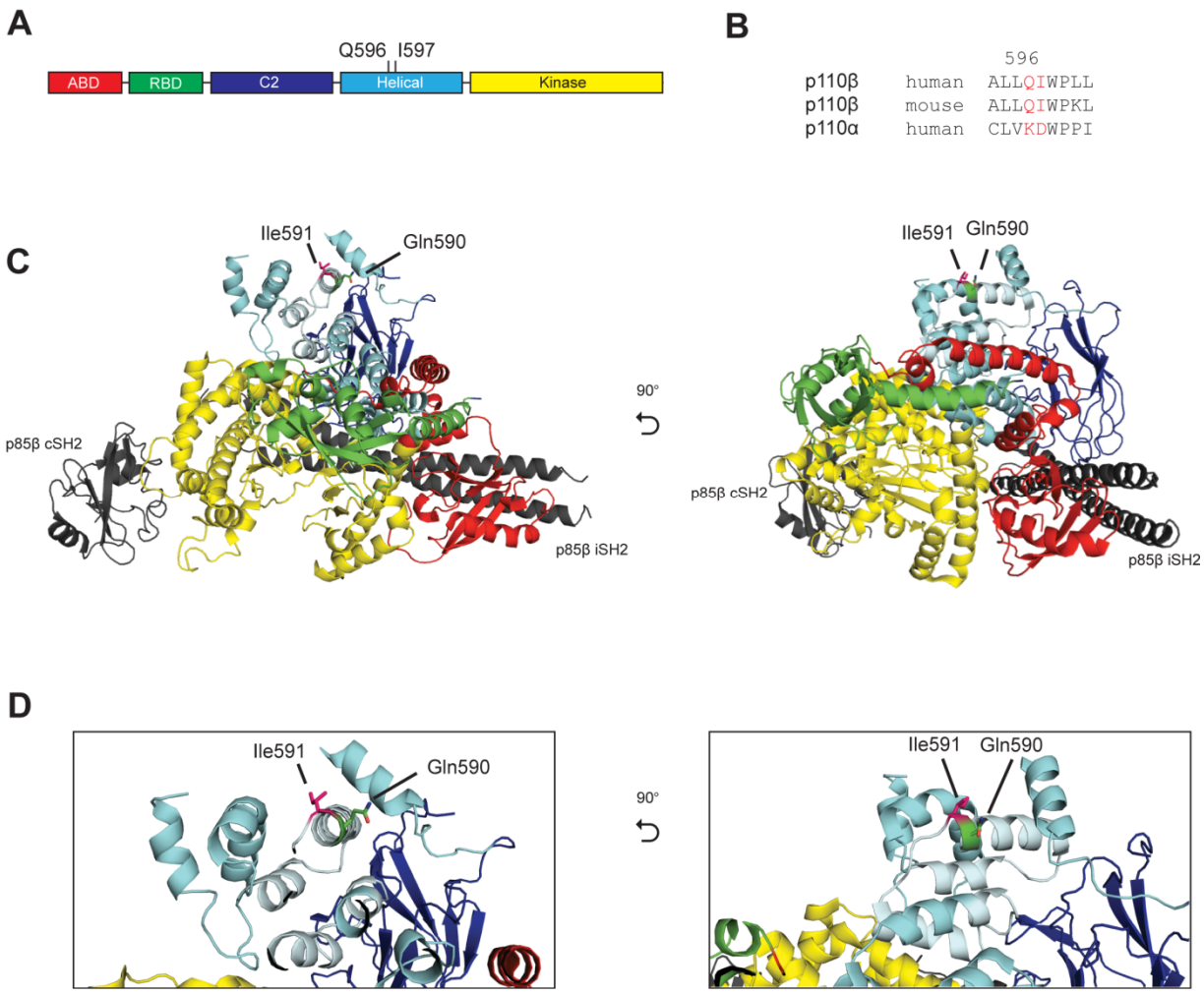

Figure 16. Structural analysis of p110β Q596 and I597 residues.

(A) Schematic domain organization of human p110β, highlighting residues Q596 and I597 in the helical domain. (B) Sequence alignment of amino acids 593 to 611 of the helical domain in p110α and p110β. 596 and 597 residues are noted in red. (C) Full view and side view (90° rotation) of mouse p110β complex with p85β iSH2 and cSH2 domains. p85β is labeled in dark gray. The Q596 and I597 residues corresponding to human sequence are highlighted. The residues for mouse p110β are Q590 and I591, respectively. (D) Detailed views of the two key residues in the helical domain. Structure is adapted from Zhang et al., 2011. This figure has been submitted for publication.

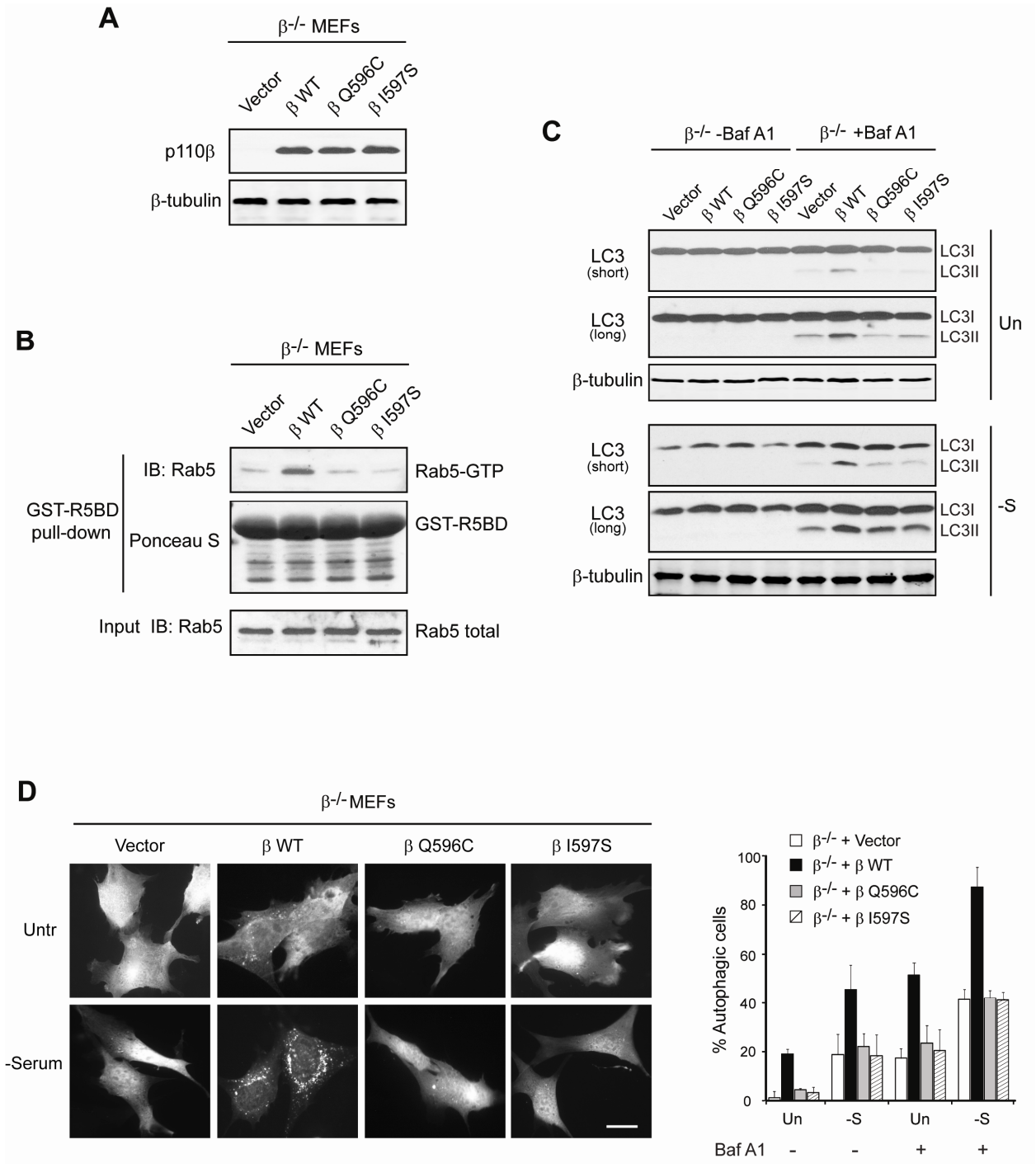

Figure 17. Association of p110β with Rab5 is required for Rab5 activity and autophagy.

(A) $\beta^{-/-}$ MEFs were stably reconstituted with vector (control), p110β-WT, p110β-Q596C or p110β-I597S. Cell lysates were analyzed for p110β expression levels. (B) Lysates of stably reconstituted MEFs were subjected to GST-R5BD pull-down assays to determine the amount of Rab5-GTP. (C) MEFs generated as in (A) were cultured in complete or serum-free medium for

6 h and treated with or without bafilomycin A1 (50 nM). Western blots of cell lysates were probed for LC3 and β-tubulin. (D) MEFs generated as in (A) were transfected with GFP-LC3. 48 h post transfection, the cells were cultured in complete or serum-free medium for 4 h, in the absence or presence of bafilomycin A1 (50 nM). Cells were observed under a deconvolution microscope; representative images of cells without bafilomycin A1 treatment are shown. Scale bar: 20 μm. Quantification of autophagic cells is shown on the right. Data are average values of at least 4 blind countings with over 200 cells. Error bars: SD. This figure has been submitted for publication.

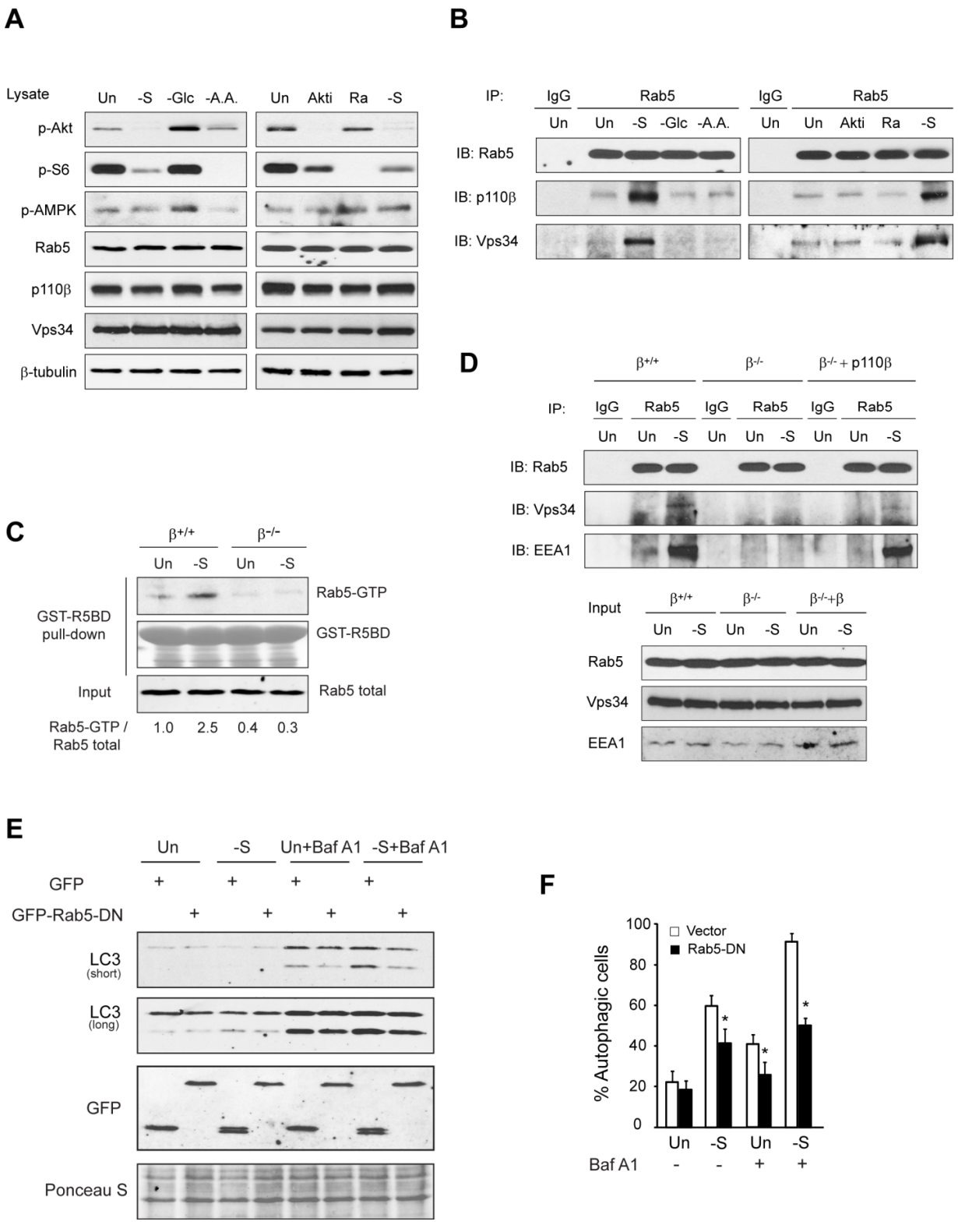

Figure 18. Withdrawal of trophic factors, but not nutrients, induces p110β-Rab5 binding and p110β-dependent Rab5 activation that stimulates autophagy.

(A) $\beta^{-/-}$ MEFs stably reconstituted with human p110β were left untreated, deprived of serum, glucose, or amino acids for 6 h, or treated with the Akt inhibitor (Akti, 10 μM) or rapamycin (Ra, 50 nM) overnight. Western blots of cell lysates were probed with the indicated antibodies to validate the effect of each treatment. (B) Lysates of cells treated as in (A) were subjected to immunoprecipitation with control IgG or Rab5 antibody. The precipitates were analyzed for Rab5, p110β, and Vps34. $\beta^{-/-}$ MEFs reconstituted with human p110β were used because the p110β antibody preferentially recognizes the human antigen. (C) $\beta^{+/+}$ and $\beta^{-/-}$ MEFs were left untreated or serum-deprived for 6 h. GST-R5BD pull-down assays were done to determine the amount of Rab5-GTP in cell lysates. (D) MEFs with the indicated genotypes were cultured in complete or serum-free medium for 6 h. Cell lysates were subjected to immunoprecipitation with IgG or Rab5 antibody. Western blots of the precipitates and input were probed with the indicated antibodies. (E) MEFs were transfected with indicated constructs. 48 h post transfection, cells were treated as indicated, and the lysates were probed for indicated antibodies. (F) MEFs were transfected with GFP-LC3 or DsRed vector or DsRed-Rab5 DN. Autophagic cells were analyzed. Data are average values of at least 4 blind countings with over 200 cells. Error bars: SD. *$p<0.05$. This figure has been submitted for publication.

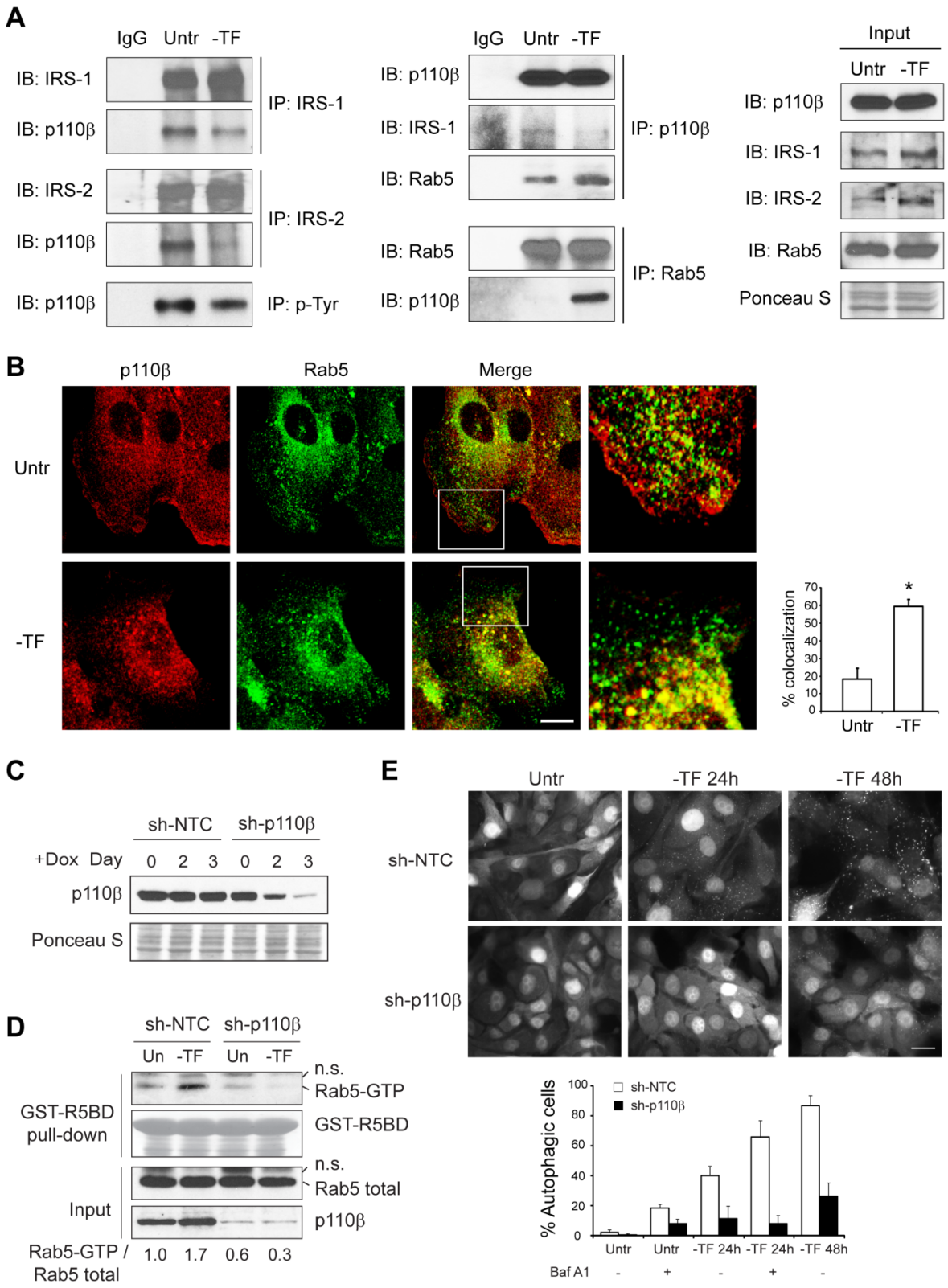

Figure 19. p110β dissociates from trophic factor receptor complexes and interacts with Rab5 upon trophic factor deprivation.

(A) MCF10A cells were grown in complete or basal (without trophic factors) medium for 24 h. Cell lysates were subjected to immunoprecipitation with the indicated antibodies or with phosphotyrosine antibody conjugated to agarose. Western blots of the precipitates and the input were probed with the indicated antibodies. (B) MCF10A cells were grown in complete or basal medium for 24 h. Immunofluorescence confocal microscopy was used to visualize p110β and Rab5 in fixed cells. Representative images are shown. Scale bar: 10 μm. The percentage of Rab5 colocalizing with p110β was quantified in over 50 cells and is shown on the right. Error bars: SEM. * $p<0.01$. (C) MCF10A cells were stably infected with lentiviruses encoding a tetracycline-inducible non-targeting control shRNA or shRNA against p110β. The two cell lines were treated in complete medium with doxycycline (Dox, 1 μg/ml) for the indicated times and then harvested for western blot analysis of p110β protein levels. (D) MCF10A cells generated as in (C) were treated with Dox for 3 d to silence p110β, then cultured in complete or basal medium for 24 h in the presence of Dox. Cell lysates were analyzed for the amount of Rab5-GTP using GST-R5BD pull-down assays. The input of Rab5 and p110β are shown. (E) Cells generated as in (C) stably expressing GFP-LC3 were left untreated or starved in basal medium for 24 or 48 h in the absence or presence of bafilomycin A1 (20 nM). The cells were then fixed and observed under a deconvolution microscope. Representative images of cells not treated with bafilomycin A1 are shown. Scale bar: 20 μm. Autophagic cells from the indicated culture conditions were quantified. Data are averages of at least 4 blind countings with over 500 cells. Error bars: SD. The quantification of autophagy in cells incubated for 48 h in the presence of bafilomycin A1 was not performed due to the cytotoxic effect of the drug. This figure has been submitted for publication.

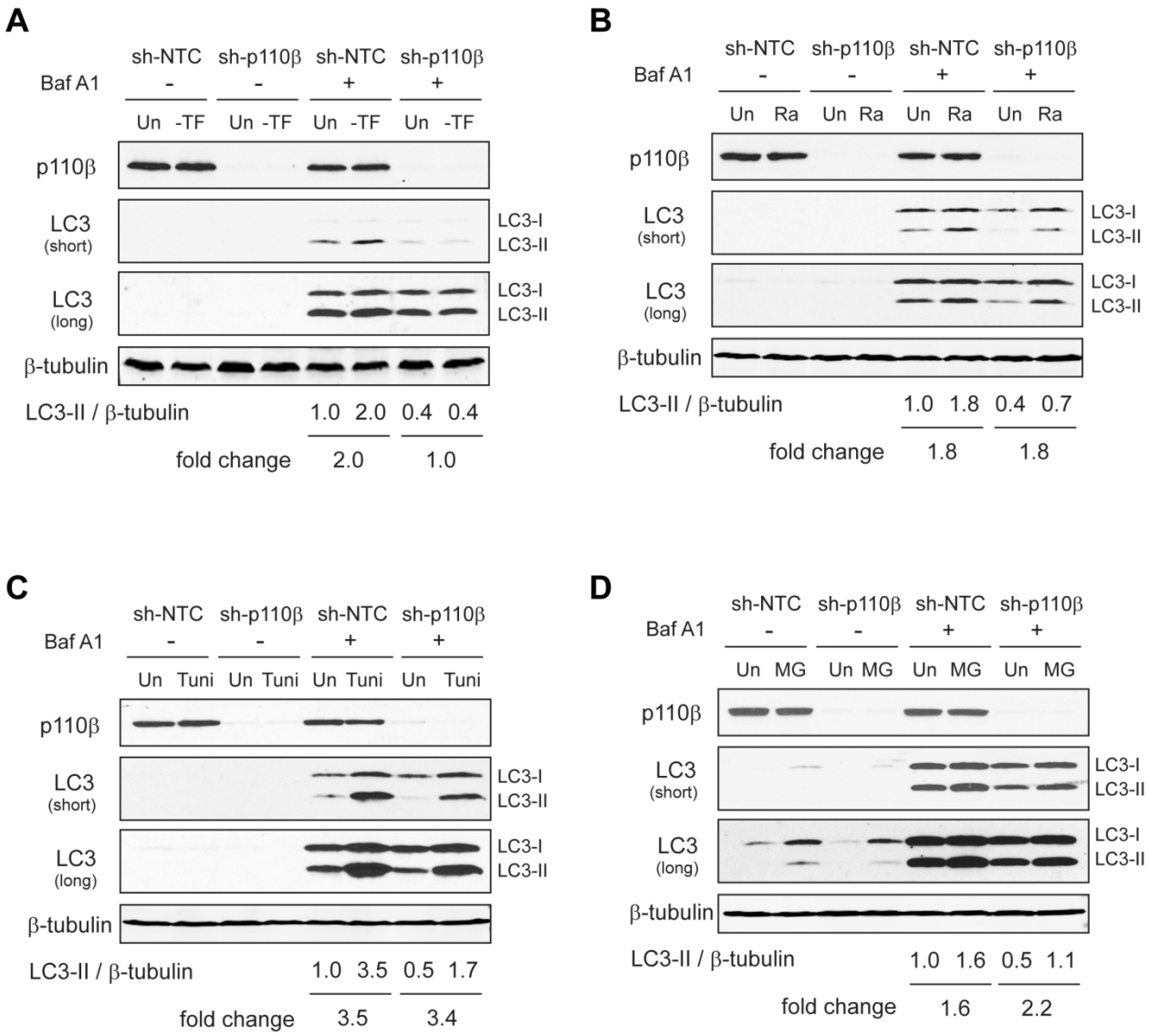

Figure 20. p110β plays a selective role in trophic factor limitation-induced autophagy.

(A-D) MCF10A cells were stably infected with tetracycline-inducible control shRNA or shRNA against p110β. Cells were treated with Dox for 3 d to allow knock-down of p110β. Cells were then left untreated, cultured in basal medium (A), or treated with rapamycin (Ra, 50 nM) (B), tunicamycin (0.1 μg/ml) (C), or MG132 (0.25 μM) (D) for 36 h in the absence or presence of bafilomycin A1 (20 nM). Cells were then harvested and lysates were subjected to immunoblotting for p110β, LC3, and β-tubulin. Short and long exposures of the LC3 immunoblots are shown. Relative amounts of LC3-II (expressed as normalized LC3-II/β-tubulin ratios) and fold change are shown at the bottom. Note that the trophic factor deprivation-induced increase in LC3-II was abolished in sh-p110β cells. While the basal level of LC3-II was lower in sh-p110β cells, the inducibility of LC3-II upon treatment with rapamycin, tunicamycin, or MG132 was intact. This figure has been submitted for publication.

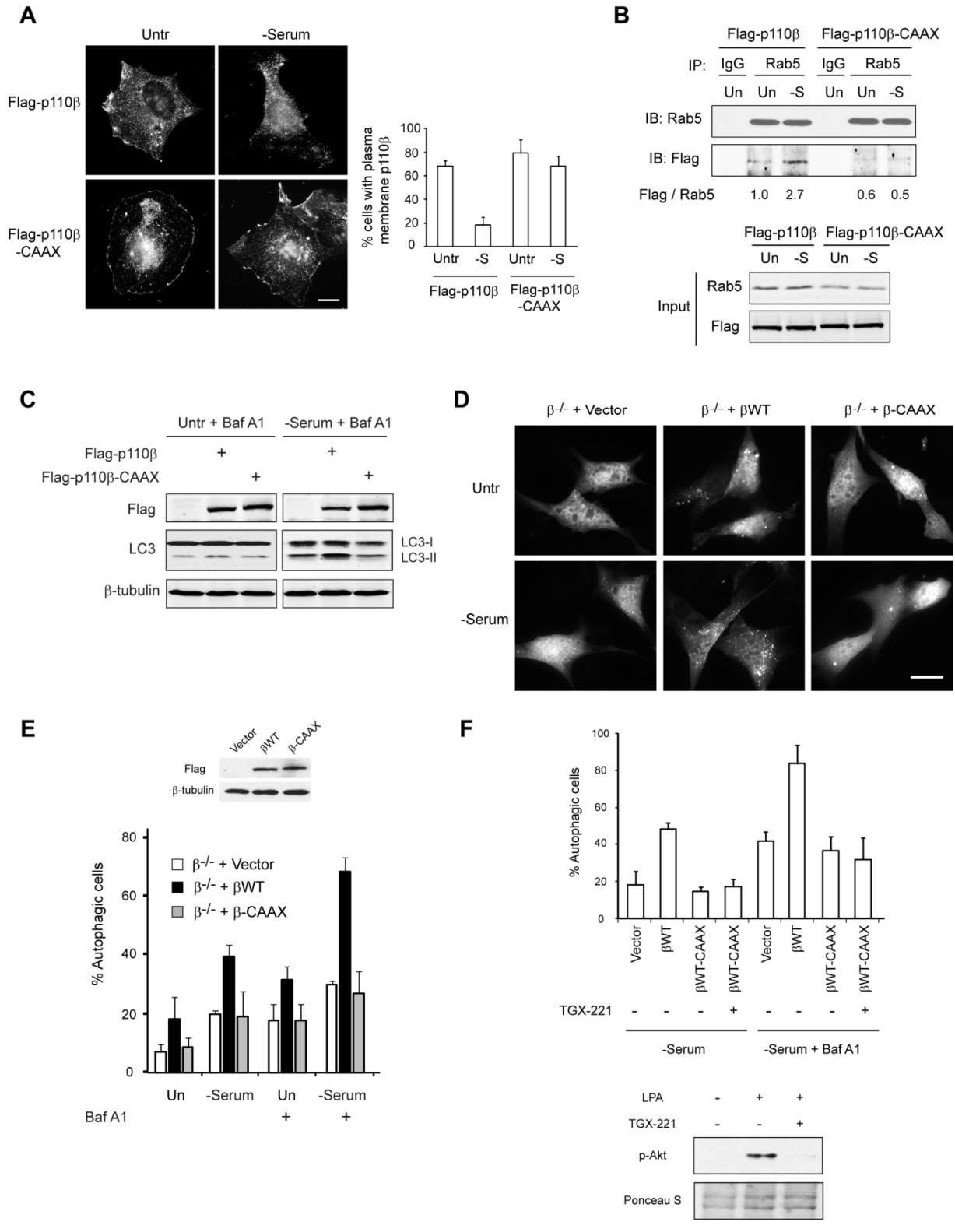

Figure 21. Cells with membrane-targeted p110β-CAAX display impaired Rab5 association and autophagy.

(A) Flag-p110β-WT or CAAX mutant were transfected into Hs578T cells. 48 h post transfection, cells were cultured in complete or serum-free medium for 6 h. Cells were then fixed and stained with Flag antibody, and observed under a deconvolution microscope. Representative images were taken. Scale bar: 20 μm. Note that serum deprivation led to decreased plasma membrane localization of p110β-WT but not p110β-CAAX. Quantification of cells with plasma membrane p110β was performed by counting a total of over 100 cells. Data presented are the mean values with SD. (B) HEK293T cells were transfected with wild-type Flag-p110β or Flag-p110β-CAAX. 48 h post transfection, the cells were left untreated or serum-deprived for 24 h. Cell lysates were subjected to immunoprecipitation with IgG or Rab5 antibody. The precipitates and input were analyzed for Rab5 and Flag. The normalized relative binding of Flag-p110β to Rab5 is shown. (C) $\beta^{-/-}$ MEFs were transfected with vector (control), wild-type Flag-p110β, or Flag-p110β-CAAX. 48 h post transfection, the cells were left untreated or serum-deprived in the presence of bafilomycin A1 (50 nM) for 6 h. Cell lysates were subjected to immunoblotting with the indicated antibodies. Note that p110β-WT but not p110β-CAAX increased the amount of LC3-II in $\beta^{-/-}$ cells. (D) $\beta^{-/-}$ MEFs were transfected with the indicated constructs together with GFP-LC3. 48 h post transfection, cells were left untreated or serum-deprived for 6 h, in the absence or presence of bafilomycin A1 (50 nM). The pictures shown are of cells in the absence of bafilomycin A1. Scale bar: 20 μm. Expression of the constructs and quantification of autophagic cells are shown in (E). Data are averages of at least 4 blind countings with over 200 cells. Error bars: SD. (F) $\beta^{-/-}$ MEFs were transfected with vector control or constructs encoding p110β-WT or CAAX mutant, together with GFP-LC3. 48 h post transfection, p110β-CAAX cells were treated with the p110β-specific kinase inhibitor TGX-221 (500 nM) for overnight. The cells were then serum-starved for 6 h, in the absence or presence of 50 nM bafilomycin A1. TGX-221 was present during the treatment. Cells were fixed and quantified for autophagy induction indicated by GFP-LC3 puncta. Data shown are the mean values of at least 4 blind countings with over 200 cells. Error bars: SD. (Bottom) Wild-type MEFs were serum-starved overnight, in the absence or presence of 500 nM TGX-221. The cells were then stimulated with 10 μM LPA for 5 min. TGX-221 was present during the stimulation. The cells were then harvested and the lysates were probed for pAkt T308 antibody. Ponceau S staining was shown as loading control. Note that TGX-221 blocked Akt phosphorylation. This figure has been submitted for publication.

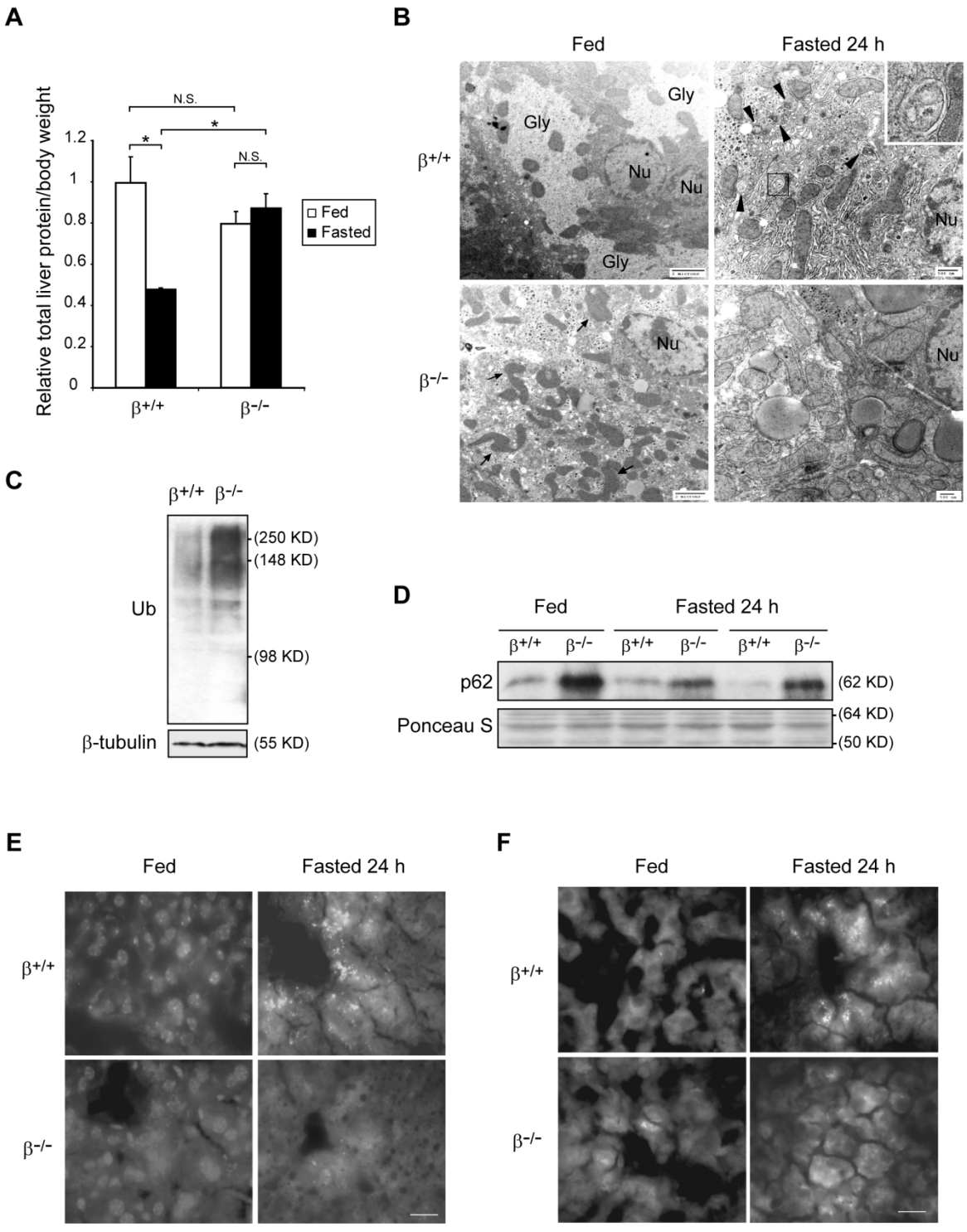

Figure 22. Autophagy is impaired in p110β-deficient liver.

(A) Gender and age-paired 8 to 10 week-old mice with indicated genotypes were fed or fasted for 24 h. Liver weight, body weight, and liver protein concentrations were measured. Data presented are the normalized average values + S.E.M.; n=5 within each group; * $p<0.05$; N.S.,

non-significant. (B) Electron micrographic images of livers from 8-week old fed or 24 h-fasted mice. Deformed mitochondria are indicated by arrow in the $\beta^{-/-}$ liver. In fasted livers, autophagosomes are labeled with arrowheads. Higher magnification view of a representative autophagosome is shown in the inset. Note the swollen mitochondria in fasted $\beta^{-/-}$ liver. Gly: glycogen area. Nu: nucleus. (C) Total lysates were made from $\beta^{+/+}$ and $\beta^{-/-}$ livers, and probed for ubiquitin and β-tubulin. Data shown are representative of three independent pairs of animals. (D) Total liver lysates from fed or 24 h-fasted mice with indicated genotypes were generated, and immunoblotted for p62. Ponceau S staining is shown for equal loading. (E) 8-week-old GFP-LC3 transgenic mice with indicated liver genotypes were fed or fasted for 24 h. Cryo-sections of the livers were observed under a deconvolution fluorescence microscope. Representative images are shown. Scale bar: 20 μm. (F) Beclin 1-GFP mice with $\beta^{+/+}$ or $\beta^{-/-}$ livers were left fed or fasted for 24 h. Liver cryo-sections were made and observed under a deconvolution fluorescence microscope. Representative images are shown. Scale bar: 20 μm. This figure was published in Journal of Cell Biology (Dou et al., 2010).

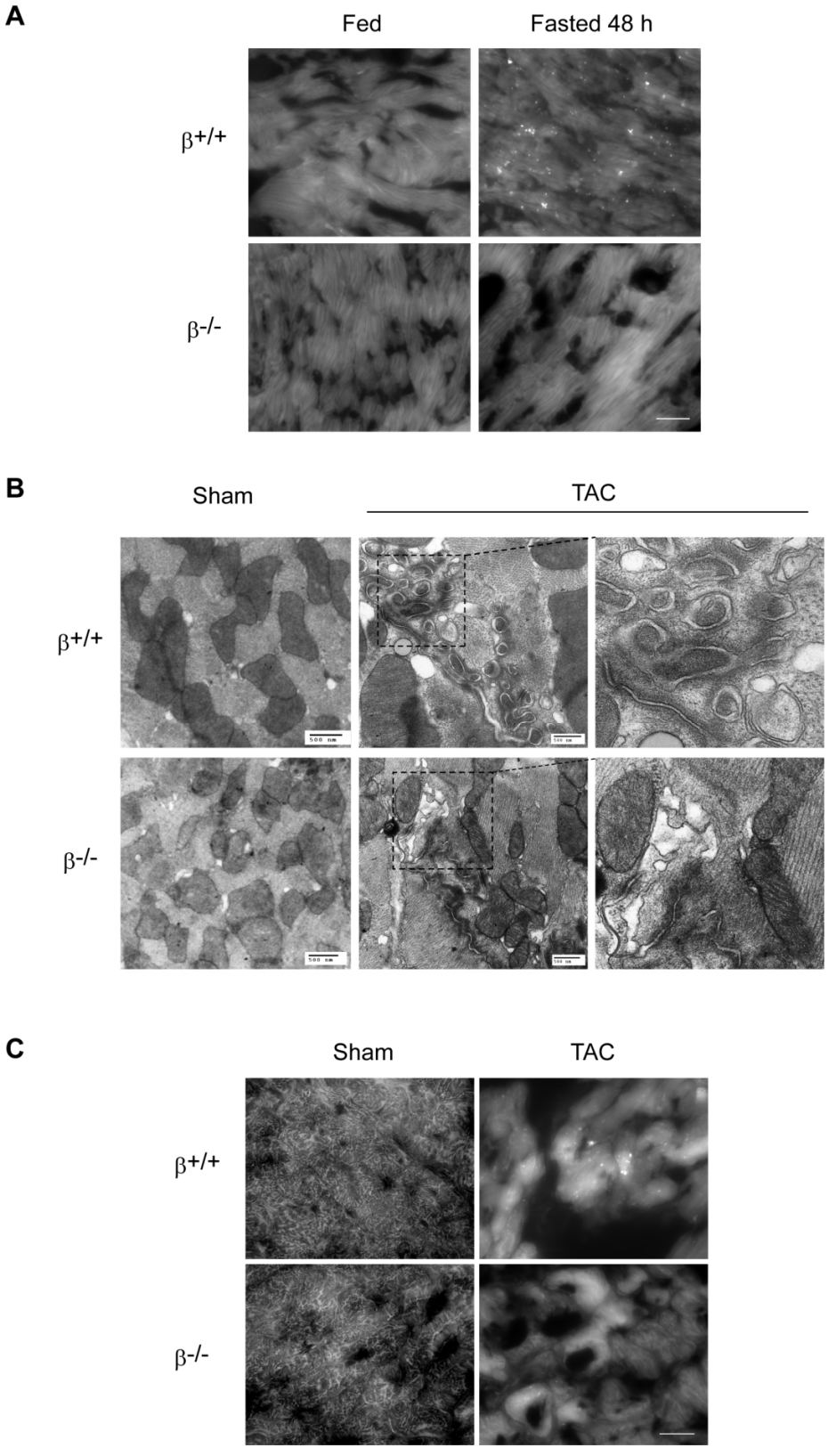

Figure 23. Autophagy is impaired in p110β-deficient heart.

(A) GFP-LC3 transgenic mice with indicated heart genotypes were fed or fasted for 48 h. Heart cryo-sections were observed and representative images are shown. Scale bar: 20 μm. Note the increase in GFP-LC3 puncta in fasted $\beta^{+/+}$ liver and heart, which are impaired in fasted $\beta^{-/-}$ mice. (B) At 8 weeks of age, MerCreMer;*p110β*$^{flox/flox}$ mice and their littermate *p110β*$^{flox/flox}$ controls were injected with 1 mg tamoxifen intraperitoneally daily for 28 days. Four weeks later, Transverse Aortic Constriction (TAC) or sham operation was performed on these tamoxifen-injected mice. 33 days later, hearts were harvested and sections were prepared for electron microscopy. Representative images are shown for each group of mice. Note the dramatic induction of autophagosomes in the $\beta^{+/+}$ heart, which is absent in the $\beta^{-/-}$ heart. (C) TAC or sham operation was performed on 10-12 week old MCK-*Cre*;GFP-LC3;*p110β*$^{flox/flox}$ mice and their littermate GFP-LC3;*p110β*$^{flox/flox}$ controls. 7 days later, hearts were harvested and frozen sections prepared. GFP-LC3 puncta in the heart sections were visualized under a deconvolution fluorescence microscope. Representative images with the same magnification are shown for each group of mice. Scale bar: 20 μm. The TAC surgery was performed by Dr. Ya-Ping Jiang in Dr. Richard Lin lab. This figure was published in Journal of Cell Biology (Dou et al., 2010).

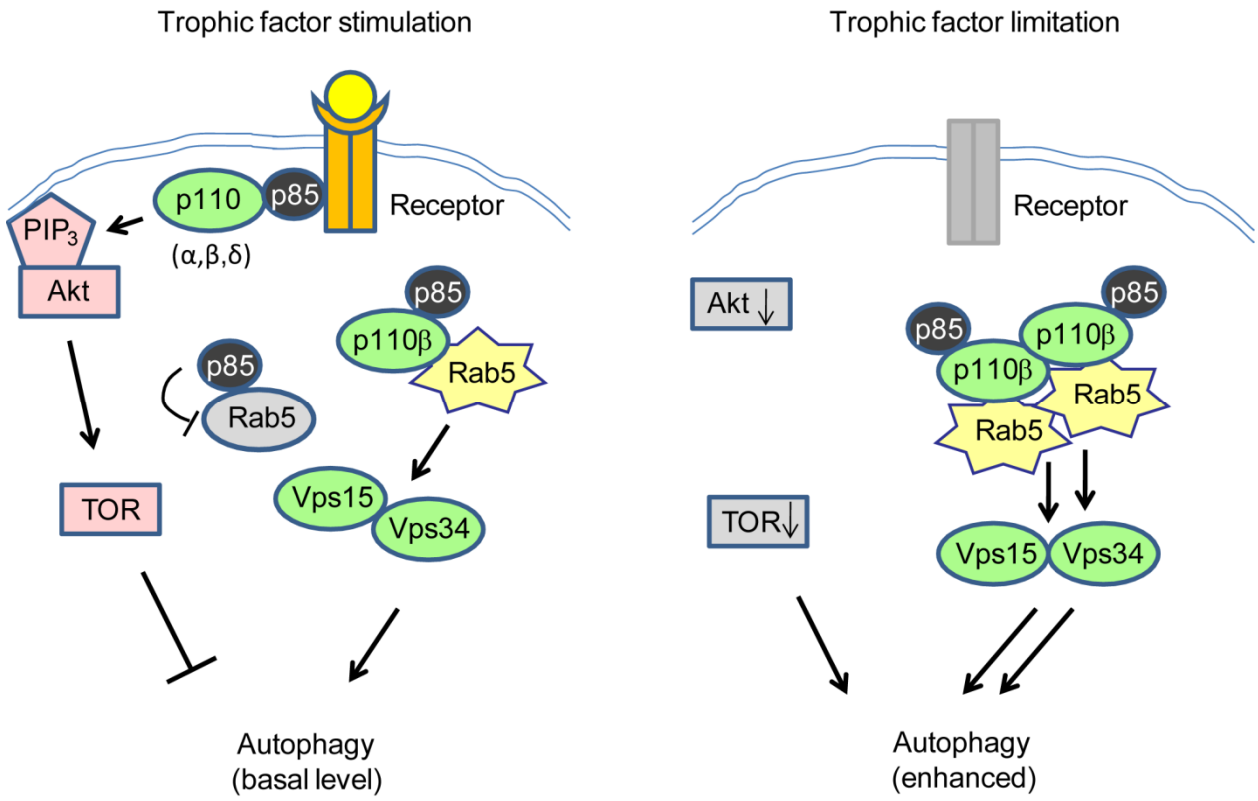

Figure 24. p110β is a positive regulator of autophagy.

The roles of p110β in the presence and absence of trophic factor conditions are depicted. (Left) Under trophic factor stimulation condition, the Class IA PI3K p110-p85 complex is recruited to the growth factor receptors and produces PI(3,4,5)P_3 that activates the Akt/TOR pathway which inhibits autophagy. Intracellularly, only p110β subunit interacts with Rab5 and is required for Rab5 activity and stimulation of Vps34 that contributes to basal level autophagy. (Right) Upon trophic factor deprivation, the p110-p85 complex dissociates from the trophic factor receptors, and Akt/TOR pathway activity is suppressed, which enhances autophagy. In addition, I discovered here that p110β translocates to the Rab5 compartment and stimulates Rab5 and Vs34 activity, leading to enhanced autophagy. This figure has been submitted for publication.

V. Materials and Methods

1) Mice

p110$\alpha^{+/+}$, p110$\alpha^{-/-}$, p110$\beta^{+/+}$, and p110$\beta^{-/-}$ mice were described elsewhere (Lu et al., 2009). Beclin 1-EGFP mice were a gift from Dr. Zhenyu Yue (Zhong et al., 2009). GFP-LC3 transgenic mice (Mizushima et al., 2004) were a gift from Dr. Noboru Mizushima. Albumin-Cre mice were purchased from The Jackson Laboratory. For fasting studies, mice were deprived of food while having free access to water. All mice were experimented in compliance with the Stony Brook University Institutional Animal Care and Use Committee guidelines.

2) Cell lines and culture

Primary mouse embryonic fibroblasts (MEFs) were generated from d 14-17 embryos from p110α (flox$^{+/-}$) or p110β (flox$^{+/-}$) matings (Lu et al., 2009). Early passage MEFs were immortalized by transfection of SV40 large T antigen-encoding plasmid. Immortalized MEFs were infected with either adenoviral GFP to generate $\alpha^{+/+}$ or $\beta^{+/+}$MEFs, or adenoviral Cre-GFP to generate $\alpha^{-/-}$ or $\beta^{-/-}$ MEFs.

MEFs, HEK293, HEK293T, BMK, HeLa, and Hs578T cells were cultured in DMEM supplemented with 10% fetal bovine serum (FBS), 100 units/ml penicillin, and 100 μg/ml streptomycin (Invitrogen), and transfected using Lipofectamine 2000 (Invitrogen). Glucose-free DMEM, Hank's buffer (with calcium and glucose), and dialyzed FBS were from Invitrogen. For short-term amino acid starvation, cells were incubated in Hank's buffer supplemented with 10% dialyzed FBS and 1% HEPES (Invitrogen). MCF10A cells were cultured in DMEM/F12 (Invitrogen) supplemented with 5% horse serum (Invitrogen), 20 ng/ml EGF (Sigma-Aldrich), 0.5 μg/ml hydrocortisone (Sigma-Aldrich), 100 ng/ml cholera toxin (Sigma-Aldrich), 10 μg/ml insulin (Sigma-Aldrich), 100 units/ml penicillin, and 100 μg/ml streptomycin. For growth factor removal experiments, MCF10A cells were cultured in basal medium (DMEM/F12 plus 5% horse serum, 100 units/ml penicillin, and 100 μg/ml streptomycin) for the indicated times.

3) Plasmids

GFP-LC3 constructs were described previously (Ullman et al., 2008). The bicistronic Myc-Vps34-V5-Vps15 (Yan et al., 2009) is a gift from Dr. Jonathan Backer. Beclin 1-GFP and GFP-Atg14L have been described previously (Zhong et al., 2009). GFP-DFCP1 is a gift from Dr. Nicholas Ktistakis. mCherry-GFP-LC3 is a gift from Dr. Terje Johanson (Pankiv et al., 2007). CMV 3×Flag constructs expressing Flag-p110β have been described previously (Ballou et al., 2007). The retroviral LPC-p110β was generated by cloning the p110β fragment from CMV 3×Flag-p110β into retroviral LPC vector. GFP-FYVE is a gift from Dr. Deborah Brown. GFP-Rab5-WT, GFP-Rab5-CA and GFP-Rab5-DN were a gift from Dr. Allan I. Levey (Volpicelli et al., 2001), and the Rab5 sequences were cloned into pDsRed vector. GST-R5BD was described elsewhere (Liu et al., 2007). GST-Rab5 was generated by cloning the Rab5 fragment into pGEX-2T. Myc-p110β, Myc-p110β-Q596C and Myc-p110β-I597S were subcloned into the retroviral LPC vector. The p110β-CAAX construct was made by using PCR to add sequences

encoding the carboxy-terminal 17 amino acids of K-Ras (KDGKKKKKKSKTKCVIM) to the 3' end of the p110β cDNA and cloning the fragment into pCMV-3xFlag.

4) Reagents and antibodies

DME, glucose-free DME, Hank's buffer, and LysoTracker red were purchased from Invitrogen; tunicamycin, E64D (used at 10 μg/ml), Akt inhibitor (Akti) from EMD; pepstatin A (used at 10 μg/ml), rapamycin, Ponceau S, and 3-methyladenine (3-MA, used at 1 mM) from Sigma-Aldrich; and etoposide from Takara Bio Inc. TGX-221 was described previously (Lu et al., 2009). The reagent concentrations are indicated in figure legends. Bafilomycin A1 was from Enzo; Ponceau S, GTP, GDP, GTPγS, and doxycycline were from Sigma-Aldrich. Tunicamycin, MG132, and LPA were from sources described in published literatures (Dou et al., 2010; Pan et al., 2011).

The following antibodies were used: rabbit polyclonal GFP, Atg14L, and Rubicon (Zhong et al., 2009). Phosphotyrosine peptide-conjugated agarose, p85, p110α, and p110β antibodies were described previously (Lu et al., 2009). The following antibodies were purchased commercially: p110β (Cell Signaling Technology), p62/SQSTM1 (Abnova), LC3 (Novus Biologicals; Cell Signaling Technology; MBL), ubiquitin (P4D1; Covance), β-tubulin (Sigma-Aldrich), Vps34 (Echelon Biosciences; Cell Signaling Technology), GFP (Santa Cruz Biotechnology, Inc.), Myc (9E10, Invitrogen), V5 (Invitrogen), Beclin 1 (Santa Cruz Biotechnology, Inc.), p-Akt 308 and 473 (Cell Signaling Technology), Flag (M2, Sigma-Aldrich), Atg5 (Abgent), UVRAG (MBL), PI(3)P (Echelon Biosciences), PI(3,4,5)P_3 (Echelon Biosciences), mouse and rabbit Rab5 (Santa Cruz Biotechnology), EEA1 (BD Biosciences), IRS-1 and IRS-2 (Santa Cruz Biotechnology), p-S6 S240/S244 (Cell Signaling Technology), p-AMPK T172 (Cell Signaling Technology), and Alexa 488- or Alexa 594-conjugated secondary antibodies (Invitrogen).

5) Retroviral and lentiviral infection

Stable cell lines were generated by retroviral infection. The lentiviral sh-p110β construct was purchased from Sigma-Aldrich. HEK293T cells were transfected with LPC-retroviral constructs together with helper virus construct, or lentiviral constructs and packaging plasmids. 24 h after transfection, the supernatant containing viral particles was supplemented with 10 μg/ml polybrene (Sigma-Aldrich), and filtered through a 0.45-μm filter. The supernatant was incubated with recipient cells in a 6-well plate. Infections were repeated twice, at 12- and 24-h intervals. For retrovirus-generated stable cell lines, 3 d after the first infection, infected recipient cells were selected with puromycin (InvivoGen).

To generate the tetracycline-inducible shRNA virus against p110β, we followed the procedure of the "all-in-one" system for the inducible expression of shRNA (Wiederschain et al., 2009). The Tet-pLKO-puro vector was purchased from Addgene. The oligo corresponding to the sh-p110β sequence was synthesized by Operon and inserted into the Tet-pLKO-puro vector. After lentiviral infection, cells were selected with puromycin, and the expression of shRNA was induced by addition of 1 μg/ml doxycycline.

6) Electron microscopy

Tissue samples were collected freshly and fixed in 4.0% PFA, 2.5% EM grade glutaraldehyde in 0.1 M PBS, pH 7.4. Cell samples were fixed in 2.5% EM-grade glutaraldehyde in 0.1 M PBS, pH 7.4. After fixation, samples were placed in 2% osmium tetroxide for tissues and 1% for cells in 0.1 M PBS, pH 7.4, dehydrated in a graded series of ethyl alcohol, and embedded in epon resin for tissues and Durcupan resin for cells. Ultra-thin sections of 80 nm were cut with an ultramicrotome (UltracutE; Reichert-Jung) and placed on formvar-coated slot copper grids. Sections were counterstained with uranyl acetate and lead citrate, and viewed with an electron microscope (Tecnai12 BioTwinG2; FEI). Images were acquired with a CCD digital camera system (model XR-60; Advanced Microscopy Techniques Corp.).

7) GFP-LC3 puncta observation and quantification

Quantification of GFP-LC3 was performed as described previously (Ullman et al., 2008). In brief, cells expressing GFP-LC3 were treated and fixed in 4% PFA in PBS and observed under an inverted microscope (Axiovert 200M; Carl Zeiss, Inc.) using the 63× oil objective. 50-200 cells were randomly selected and counted for autophagy induction. The cells with more than 10 green puncta and less nuclear GFP signal were considered autophagic.

For cryosections, the tissue was embedded directly in Optimal Cutting Temperature Compound (Sakura), stored at −80°C, and sectioned into 6-μm sections. GFP-LC3 and Beclin 1-GFP puncta were observed and imaged under an inverted microscope (Axiovert 200M; Carl Zeiss, Inc.) using the 63× oil objective.

8) Measurement of long-lived protein degradation

MEFs were plated into a 12-well plate. After overnight recovery, the cells were labeled with 0.5 μCi/ml ^{14}C-L-valine in L-valine-free medium (Invitrogen). 24 h after labeling, cells were washed three times with PBS and incubated in complete medium plus 10 mM unlabeled L-valine for 24 h to chase out short-lived proteins. The cells were washed again for three times with PBS, and cultured either in complete medium or in serum-free medium, both containing 10 mM unlabeled L-valine. The supernatant was taken at indicated time points, and precipitated with ice-cold trichloroacetic acid (TCA) at a final concentration of 10%. The TCA-soluble radioactivity was measured by liquid scintillation counting. At the end of the experiments, cells were precipitated with 10% ice-cold TCA, washed with 10% TCA, and dissolved in 0.2 N NaOH, and the radioactivity was measured. The degradation of long-lived protein was calculated by the radioactivity in TCA-soluble supernatant normalized against the total ^{14}C-radioactivity present in supernatants and cell pellets.

9) Flow cytometry

For PI(3)P and PI(3,4,5)P_3 flow cytometry analysis, 10^6 MEFs were washed with FACS buffer (PBS with 1.5% FBS) and fixed in 100 µl 1% PFA in PBS for 10 min at room temperature. After incubation with 0.03% saponin in PBS, cells were incubated with primary antibodies diluted in PBS with 0.3% saponin and 20% goat serum, for 30 min at 4°C. After another wash with 0.03% saponin in PBS, fluorophore-conjugated secondary antibodies were added to samples for 30 min at 4°C. The cells were washed twice with 0.03% saponin in PBS, once with FACS buffer, and resuspended in 0.5 ml FACS buffer. The samples were analyzed using a flow cytometer (FACSCalibur; BD).

10) Protein-lipid overlay assay

Total cellular PI(3)P measurement was performed using the PI(3)P Mass Strip kit (Echelon Biosciences). MEFs with ~80% confluency in 10-cm plates were harvested by trypsinization. 5-10% of the total cells were lysed, and the protein concentration determined by the BCA Protein Assay kit (Thermo Fisher Scientific). Cells with equal amounts of total protein were subjected to lipid extraction and protein-lipid overlay analysis following the manufacturer's protocol. PI(3)P samples and standards were visualized by ECL (Thermo Fisher Scientific) and quantified by ImageJ software (NIH, Bethesda, MD).

11) Immunoprecipitation

Cells were lysed with lysis buffer (20 mM Tris, pH 7.5, 137 mM NaCl, 1 mM $MgCl_2$, 1 mM $CaCl_2$, 1% NP-40, 10% glycerol, and 100 µM PMSF) supplemented with EDTA-free protease inhibitor cocktail (Roche). For cell lysates used for detecting phosphoproteins, 10 mM sodium pyrophosphate, 0.1 mM Na_3VO_4, 20 mM β-glycerolphosphate disodium, 10 mM NaF, and 1 mM $Na_4P_2O_7$ were added to the lysis buffer. Cell lysates were centrifuged at 17,000 *g* for 5 min; 500 µg to 1 mg of soluble protein was incubated with primary antibodies overnight at 4°C. Protein A- or protein G-agarose (Roche) was added the next day, and samples were incubated at 4°C for 2 h. The Myc, Flag, and phosphotyrosine immunoprecipitations were performed using anti-Myc, anti-Flag (Sigma-Aldrich), or anti-phosphotyrosine antibody (4G10)-conjugated agarose (Millipore) following the manufacturer's protocols. The precipitates were then washed 4-5 times with lysis buffer, boiled with 1× SDS sample buffer, and subjected to polyacrylamide gel electrophoresis and immunoblotting.

12) Immunofluorescence

Cells were fixed in 4% PFA in PBS for 20 min at room temperature. Cells were washed twice with PBS, and permeabilized with 0.1% Triton X-100 in PBS for 10 min. After washing two times, cells were blocked in 10% BSA in PBS for 2 h at room temperature. Cells were incubated with primary antibodies in 5% BSA in PBS overnight at 4°C. The next day, cells were washed four times with PBS containing 0.1% Tween 20 (PBST), each for 10 min, followed by incubation with fluorophore-conjugated secondary antibody in 5% BSA in PBST for 1 h at room temperature. Cells were then washed four times in PBST, twice with PBS, and mounted with Immu-Mount (Thermo Fisher Scientific). The slides were observed and imaged using an inverted deconvolution microscope (Axiovert 200M; Carl Zeiss, Inc.), or a two-photon laser

scanning confocal microscope (LSM 510 META NLO; Carl Zeiss, Inc.), and the colocalization was analyzed by the LSM software.

13) PI3K activity assays

For Vps34 kinase assays, HEK293T cells were transfected with indicated plasmids. 48 h after transfection, cells were harvested, and cell pellets were washed with 5 ml ice-cold PBS and 5 ml ice-cold wash buffer (20 mM Tris, pH 7.5, 137 mM NaCl, 1 mM $MgCl_2$, 1 mM $CaCl_2$, 100 mM sodium fluoride, and 10 mM sodium pyrophosphate). Vps34 activity lysis buffer (20 mM Tris, pH 7.5, 137 mM NaCl, 1 mM $MgCl_2$, 1 mM $CaCl_2$, 100 mM sodium fluoride, 10 mM sodium pyrophosphate, 100 µM orthovanadate, 1% NP-40, 10% glycerol, and 200 µM PMSF) was added and the cells were kept on ice for 10 min with frequent vortexing, followed by centrifugation at 18,000 *g* for 10 min at 4°C. Protein concentration of the supernatant was determined by Bradford assays (Bio-Rad Laboratories). Equal amounts of supernatant protein were gently mixed at 4°C overnight with Myc antibody-conjugated agarose (Invitrogen) or rabbit polyclonal GFP antibody. Protein A-agarose was added to GFP antibody-containing samples with further mixing for 2 h at 4°C. The beads were washed three times with 1 ml of lysis buffer for 5 min at 4°C, followed by two washes with 1 ml of Vps34 assay buffer (50 mM Hepeps, pH 7.5, 100 mM NaCl, 2 mM dithiothreitol, and 1 mM EGTA) without dithiothreitol. 75% of the beads were suspended in 40 µl of Vps34 assay buffer. Kinase assays were started by adding 5 µl of 2 mg/ml L-α-phosphatidylinositol (Sigma-Aldrich) sonicated in Vps34 assay buffer and 5 µl of reaction mix containing 400 µM ATP, 50 mM $MnCl_2$, and 0.25 µl of γ-[^{32}P]ATP (3,000 Ci/mmol; PerkinElmer) per assay in Vps34 assay buffer. Tubes were heated at 30°C for 15 min with shaking. The reactions were stopped with 120 µl of $CHCl_3/CH_3OH/HCl$ (10:20:0.2) and the tubes were put on a shaker for 10 min. After centrifuging for 5 min, 15 µl of the lower phase was spotted onto a silica gel thin-layer plate, and the reaction product was separated by chromatography for 1.5 h in $CHCl_3/CH_3OH/NH_4OH/H_2O$ (86:76:10:14). Radioactive spots containing PI(3)P were visualized by autoradiography, cut out of the plate, and quantified by scintillation counting. The other 25% of beads were boiled in SDS sample buffer and subjected to immunoblotting. Signals were quantified using the Odyssey Infrared Imaging System (LI-COR Biosciences). Vps34 activity was calculated as cpm normalized to the amount of Vps34 immunoprecipitated.

For p110β kinase assays, recombinant p110-β/p85α protein (Millipore) in 40 µl of PI3K assay buffer (20 mM Hepes, pH 7.5, 100 mM NaCl, and 0.5 mM EGTA) was mixed with 5 µl of 10 mg/ml L-α-phosphatidylinositol sonicated in PI3K assay buffer and 5 µl of reaction mix containing 400 µM ATP, 100 mM $MgCl_2$, and 0.25 µl of γ-[^{32}P]ATP per assay in PI3K assay buffer. Tubes were heated at 25°C for 20 min with shaking. The reactions were stopped and reaction products were analyzed as described above.

14) Transverse aortic constriction

Mice were anesthetized with 80 mg/kg ketamine and 10 mg/kg xylazine given intraperitoneally. The skin was cleaned with an iodine solution, and the operation was performed under sterile conditions. The surgical procedure was performed as described previously (Hu et

al., 2003) with modifications. In brief, mice were placed in a supine position and a horizontal skin incision ~1.0 cm in length was made at the level of the suprasternal notch. A 3-5-mm longitudinal cut was made in the proximal portion of the sternum. This allowed visualization of the aortic arch under low-power magnification. A wire with a snare on the end was passed under the aorta between the origin of the right innominate and left common carotid arteries. A 6-0 silk suture was snared with the wire and pulled back around the aorta. A bent 27-gauge needle was then placed next to the aortic arch, and the suture was snugly tied around the needle and the aorta. After ligation, the needle was quickly removed and the skin was closed. The sham procedure was identical except that the aorta was not ligated. The TAC experiments were performed by Dr. Ya-Ping Jiang in Dr. Richard Lin lab.

15) GST-Rab5 pull-down

GST-Rab5-GTPγS pull-downs were performed according to a published protocol (Christoforidis et al., 1999a) with slight modifications. pGEX-2T-Rab5 was transformed into BL21-CodonPlus *E. coli* and induced with 0.2 mM IPTG for 4 h at 28°C. Bacterial lysates were loaded onto glutathione agarose beads (Invitrogen), washed, and incubated with buffer containing 20 mM HEPES, 100 mM NaCl, 10 mM EDTA, 5 mM $MgCl_2$, 1 mM DTT, and 1 mM GTPγS (freshly made), pH 7.5, for 90 min at room temperature. The product was stabilized by washing the beads with the above buffer without EDTA for another 20 min at room temperature. The HEK293T cells were lysed in buffer containing 25 mM HEPES, 100 mM NaCl, 5 mM $MgCl_2$, 1 mM DTT, 1% NP-40, 10% glycerol, 100 μM PMSF, and EDTA-free protease inhibitor cocktail, pH 7.5. After centrifugation, supernatants of cell lysates were pre-cleared with GST beads, and then incubated with GST beads or GST-Rab5-GTPγS beads in the presence of 1 mM GTPγS for 2 h at 4°C. The beads were then washed 4 times with lysis buffer, boiled with 1× SDS sample buffer and subjected to immunoblotting.

16) GST-R5BD pull-down assay

The GST-R5BD construct and pull-down assays were described previously (Liu et al., 2007). Briefly, GST-R5BD was expressed in BL21-CodonPlus *E. coli* and purified with glutathione agarose beads. For pull-down of cell lysates, cells in 10-cm plates were lysed in buffer containing 25 mM HEPES, pH 7.4, 100 mM NaCl, 5 mM $MgCl_2$, 1% NP-40, 10% glycerol, 1 mM DTT, 100 μM PMSF, and EDTA-free protease inhibitor cocktail. After centrifugation, supernatants were incubated with GST-R5BD beads at 4°C, washed with lysis buffer, boiled in 1× SDS sample buffer and subjected to immunoblotting.

17) In vitro Rab5 GAP assays

Purified proteins for *in vitro* Rab5 GAP assays were purchased or prepared as follows. Rab5 was made by removing the protein from GST-Rab5 beads with thrombin (GE Healthcare). Purified p110β/p85α expressed in Sf21 cells was purchased from Millipore, and p110α/p85α was from Invitrogen. Free p85α was purified from Sf9 cells infected with baculovirus. Two days after infection, cells were lysed and low-speed supernatants were loaded onto a HiTrap Ni^{2+} column (Amersham Pharmacia Biotech). Free p85α was eluted by washing the column with 50 mM imidazole. Fractions containing p85α were loaded onto a HiTrap QFF column (Amersham

Pharmacia Biotech) and the proteins were eluted with a gradient of NaCl. p85α emerging at ~150-230 mM NaCl was pooled and concentrated, then purified by gel filtration on a Superdex 200 column (Amersham Pharmacia Biotech). Fractions containing highly purified p85α with little or no p110 were pooled, concentrated and stored at -20°C. The concentrations of p110β/p85α and p110α/p85α were normalized against that of p85α on immunoblots probed with p85α antibody. Signals were quantified using the Odyssey Infrared Imaging System (LI-COR Biosciences). For *in vitro* Rab5 GAP assays, 200 nM Rab5 was incubated with 200 nM GDP or GTP in loading buffer (20 mM Tris-HCl, pH 8, 2 mM EDTA, and 1 mM DTT) at 25°C for 30 min. Rab5-GTP hydrolysis was initiated by addition of p85α or the p110 complex in the presence of $MgCl_2$ at a final concentration of 10 mM. After 10 min at 25°C, the reactions were stopped by addition of ice cold buffer containing 25 mM HEPES, 100 mM NaCl, 5 mM $MgCl_2$, 1 mM DTT, and 0.1% NP-40. The samples were pre-cleared with GST beads and incubated with GST-R5BD beads. The beads were washed, boiled in 1× SDS sample buffer and subjected to immunoblotting.

18) Statistics

Student's *t* test was used to compare the differences between two groups. One-way ANOVA with Tukey's post-hoc test was used for comparisons between more than two groups. Results were considered significant when p was less than 0.05.

19) Image processing and densitometry measurements

Images captured by deconvolution and confocal microscopes were viewed and processed by AxioVision LE and Zeiss LSM image browser, respectively. Images were processed in Adobe Photoshop to enhance the brightness and contrast. Densitometry of immunoblot bands was determined by ImageJ software or by the Odyssey Infrared Imaging System.

VI. References

Ali, K., Bilancio, A., Thomas, M., Pearce, W., Gilfillan, A.M., Tkaczyk, C., Kuehn, N., Gray, A., Giddings, J., Peskett, E., *et al.* (2004). Essential role for the p110delta phosphoinositide 3-kinase in the allergic response. Nature *431*, 1007-1011.

Altomare, D.A., Wang, H.Q., Skele, K.L., De Rienzo, A., Klein-Szanto, A.J., Godwin, A.K., and Testa, J.R. (2004). AKT and mTOR phosphorylation is frequently detected in ovarian cancer and can be targeted to disrupt ovarian tumor cell growth. Oncogene *23*, 5853-5857.

Amaravadi, R.K., and Thompson, C.B. (2007). The roles of therapy-induced autophagy and necrosis in cancer treatment. Clin Cancer Res *13*, 7271-7279.

Amaravadi, R.K., Yu, D., Lum, J.J., Bui, T., Christophorou, M.A., Evan, G.I., Thomas-Tikhonenko, A., and Thompson, C.B. (2007). Autophagy inhibition enhances therapy-induced apoptosis in a Myc-induced model of lymphoma. J Clin Invest *117*, 326-336.

Arcaro, A., Zvelebil, M.J., Wallasch, C., Ullrich, A., Waterfield, M.D., and Domin, J. (2000). Class II phosphoinositide 3-kinases are downstream targets of activated polypeptide growth factor receptors. Mol Cell Biol *20*, 3817-3830.

Axe, E.L., Walker, S.A., Manifava, M., Chandra, P., Roderick, H.L., Habermann, A., Griffiths, G., and Ktistakis, N.T. (2008). Autophagosome formation from membrane compartments enriched in phosphatidylinositol 3-phosphate and dynamically connected to the endoplasmic reticulum. Journal of Cell Biology *182*, 685-701.

Backer, J.M. (2008). The regulation and function of Class III PI3Ks: novel roles for Vps34. Biochemical Journal *410*, 1-17.

Ballou, L.M., Selinger, E.S., Choi, J.Y., Drueckhammer, D.G., and Lin, R.Z. (2007). Inhibition of mammalian target of rapamycin signaling by 2-(Morpholin-1-yl) pyrimido 2,1-alpha isoquinolin-4-one. Journal of Biological Chemistry *282*, 24463-24470.

Barbieri, M.A., Li, G., Colombo, M.I., and Stahl, P.D. (1994). Rab5, an early acting endosomal GTPase, supports in vitro endosome fusion without GTP hydrolysis. J Biol Chem *269*, 18720-18722.

Beltran, L., Chaussade, C., Vanhaesebroeck, B., and Cutillas, P.R. (2011). Calpain interacts with class IA phosphoinositide 3-kinases regulating their stability and signaling activity. Proc Natl Acad Sci U S A *108*, 16217-16222.

Berger, Z., Ravikumar, B., Menzies, F.M., Oroz, L.G., Underwood, B.R., Pangalos, M.N., Schmitt, I., Wullner, U., Evert, B.O., O'Kane, C.J., *et al.* (2006). Rapamycin alleviates toxicity of different aggregate-prone proteins. Hum Mol Genet *15*, 433-442.

Bi, L., Okabe, I., Bernard, D.J., and Nussbaum, R.L. (2002). Early embryonic lethality in mice deficient in the p110beta catalytic subunit of PI 3-kinase. Mamm Genome *13*, 169-172.

Bose, S., Chandran, S., Mirocha, J.M., and Bose, N. (2006). The Akt pathway in human breast cancer: a tissue-array-based analysis. Mod Pathol *19*, 238-245.

Bruning, J.C., Michael, M.D., Winnay, J.N., Hayashi, T., Horsch, D., Accili, D., Goodyear, L.J., and Kahn, C.R. (1998). A muscle-specific insulin receptor knockout exhibits features of the metabolic syndrome of NIDDM without altering glucose tolerance. Mol Cell *2*, 559-569.

Bucci, C., Parton, R.G., Mather, I.H., Stunnenberg, H., Simons, K., Hoflack, B., and Zerial, M. (1992). The small GTPase rab5 functions as a regulatory factor in the early endocytic pathway. Cell *70*, 715-728.

Burman, C., and Ktistakis, N.T. (2010). Regulation of autophagy by phosphatidylinositol 3-phosphate. FEBS Lett *584*, 1302-1312.

Buzzai, M., Jones, R.G., Amaravadi, R.K., Lum, J.J., DeBerardinis, R.J., Zhao, F., Viollet, B., and Thompson, C.B. (2007). Systemic treatment with the antidiabetic drug metformin selectively impairs p53-deficient tumor cell growth. Cancer Res *67*, 6745-6752.

Cantley, L.C. (2002). The phosphoinositide 3-kinase pathway. Science *296*, 1655-1657.

Carpenter, C.L., Duckworth, B.C., Auger, K.R., Cohen, B., Schaffhausen, B.S., and Cantley, L.C. (1990). Purification and characterization of phosphoinositide 3-kinase from rat liver. J Biol Chem *265*, 19704-19711.

Castellano, E., and Downward, J. (2011). RAS Interaction with PI3K: More Than Just Another Effector Pathway. Genes Cancer *2*, 261-274.

Chagpar, R.B., Links, P.H., Pastor, M.C., Furber, L.A., Hawrysh, A.D., Chamberlain, M.D., and Anderson, D.H. (2010). Direct positive regulation of PTEN by the p85 subunit of phosphatidylinositol 3-kinase. Proc Natl Acad Sci U S A *107*, 5471-5476.

Chamberlain, M.D., Berry, T.R., Pastor, M.C., and Anderson, D.H. (2004). The p85alpha subunit of phosphatidylinositol 3'-kinase binds to and stimulates the GTPase activity of Rab proteins. J Biol Chem *279*, 48607-48614.

Chamberlain, M.D., Chan, T., Oberg, J.C., Hawrysh, A.D., James, K.M., Saxena, A., Xiang, J., and Anderson, D.H. (2008). Disrupted RabGAP function of the p85 subunit of phosphatidylinositol 3-kinase results in cell transformation. J Biol Chem *283*, 15861-15868.

Chamberlain, M.D., Oberg, J.C., Furber, L.A., Poland, S.F., Hawrysh, A.D., Knafelc, S.M., McBride, H.M., and Anderson, D.H. (2010). Deregulation of Rab5 and Rab4 proteins in p85R274A-expressing cells alters PDGFR trafficking. Cell Signal *22*, 1562-1575.

Chang, J.D., Sukhova, G.K., Libby, P., Schvartz, E., Lichtenstein, A.H., Field, S.J., Kennedy, C., Madhavarapu, S., Luo, J., Wu, D., *et al.* (2007). Deletion of the phosphoinositide 3-kinase p110gamma gene attenuates murine atherosclerosis. Proc Natl Acad Sci U S A *104*, 8077-8082.

Chattopadhyay, M., Selinger, E.S., Ballou, L.M., and Lin, R.Z. (2011). Ablation of PI3K p110-alpha prevents high-fat diet-induced liver steatosis. Diabetes *60*, 1483-1492.

Cheung, Z.H., and Ip, N.Y. (2009). The emerging role of autophagy in Parkinson's disease. Mol Brain *2*, 29.

Christoforidis, S., McBride, H.M., Burgoyne, R.D., and Zerial, M. (1999a). The Rab5 effector EEA1 is a core component of endosome docking. Nature *397*, 621-625.

Christoforidis, S., Miaczynska, M., Ashman, K., Wilm, M., Zhao, L., Yip, S.C., Waterfield, M.D., Backer, J.M., and Zerial, M. (1999b). Phosphatidylinositol-3-OH kinases are Rab5 effectors. Nat Cell Biol *1*, 249-252.

Ciraolo, E., Iezzi, M., Marone, R., Marengo, S., Curcio, C., Costa, C., Azzolino, O., Gonella, C., Rubinetto, C., Wu, H., *et al.* (2008). Phosphoinositide 3-kinase p110beta activity: key role in metabolism and mammary gland cancer but not development. Sci Signal *1*, ra3.

Comb, W.C., Hutti, J.E., Cogswell, P., Cantley, L.C., and Baldwin, A.S. (2012). p85alpha SH2 domain phosphorylation by IKK promotes feedback inhibition of PI3K and Akt in response to cellular starvation. Mol Cell *45*, 719-730.

Daitoku, H., Isida, J., Fujiwara, K., Nakajima, T., and Fukamizu, A. (2001). Dimerization of small GTPase Rab5. Int J Mol Med *8*, 397-404.

Dbouk, H.A., Pang, H., Fiser, A., and Backer, J.M. (2010). A biochemical mechanism for the oncogenic potential of the p110beta catalytic subunit of phosphoinositide 3-kinase. Proc Natl Acad Sci U S A *107*, 19897-19902.

Domin, J., Gaidarov, I., Smith, M.E., Keen, J.H., and Waterfield, M.D. (2000). The class II phosphoinositide 3-kinase PI3K-C2alpha is concentrated in the trans-Golgi network and present in clathrin-coated vesicles. J Biol Chem *275*, 11943-11950.

Domin, J., and Waterfield, M.D. (1997). Using structure to define the function of phosphoinositide 3-kinase family members. Febs Letters *410*, 91-95.

Dou, Z., Chattopadhyay, M., Pan, J.A., Guerriero, J.L., Jiang, Y.P., Ballou, L.M., Yue, Z., Lin, R.Z., and Zong, W.X. (2010). The class IA phosphatidylinositol 3-kinase p110-beta subunit is a positive regulator of autophagy. J Cell Biol *191*, 827-843.

Egan, D.F., Shackelford, D.B., Mihaylova, M.M., Gelino, S., Kohnz, R.A., Mair, W., Vasquez, D.S., Joshi, A., Gwinn, D.M., Taylor, R., *et al.* (2011). Phosphorylation of ULK1 (hATG1) by AMP-activated protein kinase connects energy sensing to mitophagy. Science *331*, 456-461.

Engelman, J.A., Luo, J., and Cantley, L.C. (2006). The evolution of phosphatidylinositol 3-kinases as regulators of growth and metabolism. Nature Reviews Genetics *7*, 606-619.

Falasca, M., and Maffucci, T. (2012). Regulation and cellular functions of class II phosphoinositide 3-kinases. Biochem J *443*, 587-601.

Fan, W., Nassiri, A., and Zhong, Q. (2011). Autophagosome targeting and membrane curvature sensing by Barkor/Atg14(L). Proc Natl Acad Sci U S A *108*, 7769-7774.

Fedorko, M. (1967). Effect of chloroquine on morphology of cytoplasmic granules in maturing human leukocytes--an ultrastructural study. J Clin Invest *46*, 1932-1942.

Fimia, G.M., Stoykova, A., Romagnoli, A., Giunta, L., Di Bartolomeo, S., Nardacci, R., Corazzari, M., Fuoco, C., Ucar, A., Schwartz, P., *et al.* (2007). Ambra1 regulates autophagy and development of the nervous system. Nature *447*, 1121-1125.

Flinn, R.J., Yan, Y., Goswami, S., Parker, P.J., and Backer, J.M. (2010). The late endosome is essential for mTORC1 signaling. Mol Biol Cell *21*, 833-841.

Foukas, L.C., Claret, M., Pearce, W., Okkenhaug, K., Meek, S., Peskett, E., Sancho, S., Smith, A.J., Withers, D.J., and Vanhaesebroeck, B. (2006). Critical role for the p110alpha phosphoinositide-3-OH kinase in growth and metabolic regulation. Nature *441*, 366-370.

Franke, T.F., Kaplan, D.R., Cantley, L.C., and Toker, A. (1997). Direct regulation of the Akt proto-oncogene product by phosphatidylinositol-3,4-bisphosphate. Science *275*, 665-668.

Fruman, D.A., Meyers, R.E., and Cantley, L.C. (1998). Phosphoinositide kinases. Annual Review of Biochemistry *67*, 481-507.

Fujita, N., Itoh, T., Omori, H., Fukuda, M., Noda, T., and Yoshimori, T. (2008). The Atg16L complex specifies the site of LC3 lipidation for membrane biogenesis in autophagy. Mol Biol Cell *19*, 2092-2100.

Fung, C., Lock, R., Gao, S., Salas, E., and Debnath, J. (2008). Induction of autophagy during extracellular matrix detachment promotes cell survival. Mol Biol Cell *19*, 797-806.

Furuya, T., Kim, M., Lipinski, M., Li, J., Kim, D., Lu, T., Shen, Y., Rameh, L., Yankner, B., Tsai, L.H., *et al.* (2010). Negative regulation of Vps34 by Cdk mediated phosphorylation. Mol Cell *38*, 500-511.

Gaidarov, I., Smith, M.E., Domin, J., and Keen, J.H. (2001). The class II phosphoinositide 3-kinase C2alpha is activated by clathrin and regulates clathrin-mediated membrane trafficking. Mol Cell *7*, 443-449.

Geering, B., Cutillas, P.R., Nock, G., Gharbi, S.I., and Vanhaesebroeck, B. (2007). Class IA phosphoinositide 3-kinases are obligate p85-p110 heterodimers. Proc Natl Acad Sci U S A *104*, 7809-7814.

Graupera, M., Guillermet-Guibert, J., Foukas, L.C., Phng, L.K., Cain, R.J., Salpekar, A., Pearce, W., Meek, S., Millan, J., Cutillas, P.R., *et al.* (2008). Angiogenesis selectively requires the p110alpha isoform of PI3K to control endothelial cell migration. Nature *453*, 662-666.

Green, A.J., Smith, M., and Yates, J.R. (1994). Loss of heterozygosity on chromosome 16p13.3 in hamartomas from tuberous sclerosis patients. Nat Genet *6*, 193-196.

Guillermet-Guibert, J., Bjorklof, K., Salpekar, A., Gonella, C., Ramadani, F., Bilancio, A., Meek, S., Smith, A.J., Okkenhaug, K., and Vanhaesebroeck, B. (2008). The p110beta isoform of phosphoinositide 3-kinase signals downstream of G protein-coupled receptors and is functionally redundant with p110gamma. Proc Natl Acad Sci U S A *105*, 8292-8297.

Gulati, P., Gaspers, L.D., Dann, S.G., Joaquin, M., Nobukuni, T., Natt, F., Kozma, S.C., Thomas, A.P., and Thomas, G. (2008). Amino acids activate mTOR complex 1 via Ca2+/CaM signaling to hVps34. Cell Metab *7*, 456-465.

Gupta, S., Ramjaun, A.R., Haiko, P., Wang, Y., Warne, P.H., Nicke, B., Nye, E., Stamp, G., Alitalo, K., and Downward, J. (2007). Binding of ras to phosphoinositide 3-kinase p110alpha is required for ras-driven tumorigenesis in mice. Cell *129*, 957-968.

Hancock, J.F., Cadwallader, K., Paterson, H., and Marshall, C.J. (1991). A CAAX or a CAAL motif and a second signal are sufficient for plasma membrane targeting of ras proteins. EMBO J *10*, 4033-4039.

Harada, K., Truong, A.B., Cai, T., and Khavari, P.A. (2005). The class II phosphoinositide 3-kinase C2beta is not essential for epidermal differentiation. Mol Cell Biol *25*, 11122-11130.

Harris, D.P., Vogel, P., Wims, M., Moberg, K., Humphries, J., Jhaver, K.G., DaCosta, C.M., Shadoan, M.K., Xu, N., Hansen, G.M., *et al.* (2011). Requirement for class II phosphoinositide 3-kinase C2alpha in maintenance of glomerular structure and function. Mol Cell Biol *31*, 63-80.

He, C., Bassik, M.C., Moresi, V., Sun, K., Wei, Y., Zou, Z., An, Z., Loh, J., Fisher, J., Sun, Q., *et al.* (2012). Exercise-induced BCL2-regulated autophagy is required for muscle glucose homeostasis. Nature *481*, 511-515.

Hemelaar, J., Lelyveld, V.S., Kessler, B.M., and Ploegh, H.L. (2003). A single protease, Apg4B, is specific for the autophagy-related ubiquitin-like proteins GATE-16, MAP1-LC3, GABARAP, and Apg8L. J Biol Chem *278*, 51841-51850.

Herman, P.K., and Emr, S.D. (1990). Characterization of VPS34, a gene required for vacuolar protein sorting and vacuole segregation in Saccharomyces cerevisiae. Mol Cell Biol *10*, 6742-6754.

Hu, P., Zhang, D., Swenson, L., Chakrabarti, G., Abel, E.D., and Litwin, S.E. (2003). Minimally invasive aortic banding in mice: effects of altered cardiomyocyte insulin signaling during pressure overload. Am J Physiol Heart Circ Physiol *285*, H1261-1269.

Inami, Y., Waguri, S., Sakamoto, A., Kouno, T., Nakada, K., Hino, O., Watanabe, S., Ando, J., Iwadate, M., Yamamoto, M., *et al.* (2011). Persistent activation of Nrf2 through p62 in hepatocellular carcinoma cells. J Cell Biol *193*, 275-284.

Inoue, Y., and Klionsky, D.J. (2010). Regulation of macroautophagy in Saccharomyces cerevisiae. Semin Cell Dev Biol *21*, 664-670.

Isakoff, S.J., Engelman, J.A., Irie, H.Y., Luo, J., Brachmann, S.M., Pearline, R.V., Cantley, L.C., and Brugge, J.S. (2005). Breast cancer-associated PIK3CA mutations are oncogenic in mammary epithelial cells. Cancer Res *65*, 10992-11000.

Itakura, E., Kishi, C., Inoue, K., and Mizushima, N. (2008). Beclin 1 forms two distinct phosphatidylinositol 3-kinase complexes with mammalian Atg14 and UVRAG. Mol Biol Cell *19*, 5360-5372.

Itakura, E., and Mizushima, N. (2010). Characterization of autophagosome formation site by a hierarchical analysis of mammalian Atg proteins. Autophagy *6*, 764-776.

Jaber, N., Dou, Z., Chen, J.S., Catanzaro, J., Jiang, Y.P., Ballou, L.M., Selinger, E., Ouyang, X., Lin, R.Z., Zhang, J., *et al.* (2012). Class III PI3K Vps34 plays an essential role in autophagy and in heart and liver function. Proc Natl Acad Sci U S A *109*, 2003-2008.

Jaeschke, A., Hartkamp, J., Saitoh, M., Roworth, W., Nobukuni, T., Hodges, A., Sampson, J., Thomas, G., and Lamb, R. (2002). Tuberous sclerosis complex tumor suppressor-mediated S6 kinase inhibition by phosphatidylinositide-3-OH kinase is mTOR independent. J Cell Biol *159*, 217-224.

Jia, S.D., Liu, Z.N., Zhang, S., Liu, P.X., Zhang, L., Lee, S.H., Zhang, J., Signoretti, S., Loda, M., Roberts, T.M., *et al.* (2008). Essential roles of PI(3)K-p110 beta in cell growth, metabolism and tumorigenesis. Nature *454*, 776-U102.

Johnson, E.E., Overmeyer, J.H., Gunning, W.T., and Maltese, W.A. (2006). Gene silencing reveals a specific function of hVps34 phosphatidylinositol 3-kinase in late versus early endosomes. J Cell Sci *119*, 1219-1232.

Jung, H.S., Chung, K.W., Won Kim, J., Kim, J., Komatsu, M., Tanaka, K., Nguyen, Y.H., Kang, T.M., Yoon, K.H., Kim, J.W., *et al.* (2008). Loss of autophagy diminishes pancreatic beta cell mass and function with resultant hyperglycemia. Cell Metab *8*, 318-324.

Kabeya, Y., Mizushima, N., Ueno, T., Yamamoto, A., Kirisako, T., Noda, T., Kominami, E., Ohsumi, Y., and Yoshimori, T. (2000). LC3, a mammalian homologue of yeast Apg8p, is localized in autophagosome membranes after processing. EMBO J *19*, 5720-5728.

Kamada, Y., Funakoshi, T., Shintani, T., Nagano, K., Ohsumi, M., and Ohsumi, Y. (2000). Tor-mediated induction of autophagy via an Apg1 protein kinase complex. J Cell Biol *150*, 1507-1513.

Kamada, Y., Yoshino, K., Kondo, C., Kawamata, T., Oshiro, N., Yonezawa, K., and Ohsumi, Y. (2010). Tor directly controls the Atg1 kinase complex to regulate autophagy. Mol Cell Biol *30*, 1049-1058.

Kihara, A., Kabeya, Y., Ohsumi, Y., and Yoshimori, T. (2001a). Beclin-phosphatidylinositol 3-kinase complex functions at the trans-Golgi network. Embo Reports *2*, 330-335.

Kihara, A., Noda, T., Ishihara, N., and Ohsumi, Y. (2001b). Two distinct Vps34 phosphatidylinositol 3-kinase complexes function in autophagy and carboxypeptidase Y sorting in Saccharomyces cerevisiae. J Cell Biol *152*, 519-530.

Kim, J., Kundu, M., Viollet, B., and Guan, K.L. (2011). AMPK and mTOR regulate autophagy through direct phosphorylation of Ulk1. Nat Cell Biol *13*, 132-141.

Klionsky, D.J., Abeliovich, H., Agostinis, P., Agrawal, D.K., Aliev, G., Askew, D.S., Baba, M., Baehrecke, E.H., Bahr, B.A., Ballabio, A., *et al.* (2008). Guidelines for the use and interpretation of assays for monitoring autophagy in higher eukaryotes. Autophagy *4*, 151-175.

Kodaki, T., Woscholski, R., Hallberg, B., Rodriguez-Viciana, P., Downward, J., and Parker, P.J. (1994). The activation of phosphatidylinositol 3-kinase by Ras. Curr Biol *4*, 798-806.

Komatsu, M., Waguri, S., Ueno, T., Iwata, J., Murata, S., Tanida, I., Ezaki, J., Mizushima, N., Ohsumi, Y., Uchiyama, Y., *et al.* (2005). Impairment of starvation-induced and constitutive autophagy in Atg7-deficient mice. Journal of Cell Biology *169*, 425-434.

Kraft, C., Deplazes, A., Sohrmann, M., and Peter, M. (2008). Mature ribosomes are selectively degraded upon starvation by an autophagy pathway requiring the Ubp3p/Bre5p ubiquitin protease. Nature Cell Biology *10*, 602-610.

Kuma, A., Hatano, M., Matsui, M., Yamamoto, A., Nakaya, H., Yoshimori, T., Ohsumi, Y., Tokuhisa, T., and Mizushima, N. (2004). The role of autophagy during the early neonatal starvation period. Nature *432*, 1032-1036.

Kundu, M., Lindsten, T., Yang, C.Y., Wu, J.M., Zhao, F.P., Zhang, J., Selak, M.A., Ney, P.A., and Thompson, C.B. (2008). Ulk1 plays a critical role in the autophagic clearance of mitochondria and ribosomes during reticulocyte maturation. Blood *112*, 1493-1502.

Kurosu, H., and Katada, T. (2001). Association of phosphatidylinositol 3-kinase composed of p110beta-catalytic and p85-regulatory subunits with the small GTPase Rab5. J Biochem *130*, 73-78.

Lee, I.H., Kawai, Y., Fergusson, M.M., Rovira, II, Bishop, A.J., Motoyama, N., Cao, L., and Finkel, T. (2012). Atg7 modulates p53 activity to regulate cell cycle and survival during metabolic stress. Science *336*, 225-228.

Lee, J.Y., Chiu, Y.H., Asara, J., and Cantley, L.C. (2011). Inhibition of PI3K binding to activators by serine phosphorylation of PI3K regulatory subunit p85alpha Src homology-2 domains. Proc Natl Acad Sci U S A *108*, 14157-14162.

Levine, B., and Kroemer, G. (2008). Autophagy in the pathogenesis of disease. Cell *132*, 27-42.
Levine, B., Mizushima, N., and Virgin, H.W. (2011). Autophagy in immunity and inflammation. Nature *469*, 323-335.

Li, J., Yen, C., Liaw, D., Podsypanina, K., Bose, S., Wang, S.I., Puc, J., Miliaresis, C., Rodgers, L., McCombie, R., *et al.* (1997). PTEN, a putative protein tyrosine phosphatase gene mutated in human brain, breast, and prostate cancer. Science *275*, 1943-1947.

Liang, C., Feng, P., Ku, B., Dotan, I., Canaani, D., Oh, B.H., and Jung, J.U. (2006). Autophagic and tumour suppressor activity of a novel Beclin1-binding protein UVRAG. Nat Cell Biol *8*, 688-699.

Liang, C., Lee, J.S., Inn, K.S., Gack, M.U., Li, Q., Roberts, E.A., Vergne, I., Deretic, V., Feng, P., Akazawa, C., *et al.* (2008). Beclin1-binding UVRAG targets the class C Vps complex to coordinate autophagosome maturation and endocytic trafficking. Nat Cell Biol *10*, 776-787.

Liang, X.H., Jackson, S., Seaman, M., Brown, K., Kempkes, B., Hibshoosh, H., and Levine, B. (1999). Induction of autophagy and inhibition of tumorigenesis by beclin 1. Nature *402*, 672-676.

Lin, S.Y., Li, T.Y., Liu, Q., Zhang, C., Li, X., Chen, Y., Zhang, S.M., Lian, G., Ruan, K., Wang, Z., *et al.* (2012). GSK3-TIP60-ULK1 signaling pathway links growth factor deprivation to autophagy. Science *336*, 477-481.

Lindmo, K., and Stenmark, H. (2006). Regulation of membrane traffic by phosphoinositide 3-kinases. Journal of Cell Science *119*, 605-614.

Lipinski, M.M., Hoffman, G., Ng, A., Zhou, W., Py, B.F., Hsu, E., Liu, X., Eisenberg, J., Liu, J., Blenis, J., *et al.* (2010). A genome-wide siRNA screen reveals multiple mTORC1 independent signaling pathways regulating autophagy under normal nutritional conditions. Dev Cell *18*, 1041-1052.

Liu, J., Lamb, D., Chou, M.M., Liu, Y.J., and Li, G. (2007). Nerve growth factor-mediated neurite outgrowth via regulation of Rab5. Mol Biol Cell *18*, 1375-1384.

Liu, J., Xia, H., Kim, M., Xu, L., Li, Y., Zhang, L., Cai, Y., Norberg, H.V., Zhang, T., Furuya, T., *et al.* (2011). Beclin1 controls the levels of p53 by regulating the deubiquitination activity of USP10 and USP13. Cell *147*, 223-234.

Livesey, K.M., Tang, D., Zeh, H.J., and Lotze, M.T. (2009). Autophagy inhibition in combination cancer treatment. Curr Opin Investig Drugs *10*, 1269-1279.

Lu, Z.J., Jiang, Y.P., Wang, W., Xu, X.H., Mathias, R.T., Entcheva, E., Ballou, L.M., Cohen, I.S., and Lin, R.Z. (2009). Loss of Cardiac Phosphoinositide 3-Kinase p110 alpha Results in Contractile Dysfunction. Circulation *120*, 318-325.

Lum, J.J., DeBerardinis, R.J., and Thompson, C.B. (2005). Autophagy in metazoans: Cell survival in the land of plenty. Nature Reviews Molecular Cell Biology *6*, 439-448.

Maffucci, T., Cooke, F.T., Foster, F.M., Traer, C.J., Fry, M.J., and Falasca, M. (2005). Class II phosphoinositide 3-kinase defines a novel signaling pathway in cell migration. J Cell Biol *169*, 789-799.

Maier, U., Babich, A., and Nurnberg, B. (1999). Roles of non-catalytic subunits in gbetagamma-induced activation of class I phosphoinositide 3-kinase isoforms beta and gamma. J Biol Chem *274*, 29311-29317.

Masiero, E., Agatea, L., Mammucari, C., Blaauw, B., Loro, E., Komatsu, M., Metzger, D., Reggiani, C., Schiaffino, S., and Sandri, M. (2009). Autophagy is required to maintain muscle mass. Cell Metab *10*, 507-515.

Mathew, R., Karantza-Wadsworth, V., and White, E. (2007a). Role of autophagy in cancer. Nat Rev Cancer *7*, 961-967.

Mathew, R., Karp, C.M., Beaudoin, B., Vuong, N., Chen, G.H., Chen, H.Y., Bray, K., Reddy, A., Bhanot, G., Gelinas, C., *et al.* (2009). Autophagy Suppresses Tumorigenesis through Elimination of p62. Cell *137*, 1062-1075.

Mathew, R., Kongara, S., Beaudoin, B., Karp, C.M., Bray, K., Degenhardt, K., Chen, G., Jin, S., and White, E. (2007b). Autophagy suppresses tumor progression by limiting chromosomal instability. Genes Dev *21*, 1367-1381.

Matsunaga, K., Morita, E., Saitoh, T., Akira, S., Ktistakis, N.T., Izumi, T., Noda, T., and Yoshimori, T. (2010). Autophagy requires endoplasmic reticulum targeting of the PI3-kinase complex via Atg14L. J Cell Biol *190*, 511-521.

Matsunaga, K., Saitoh, T., Tabata, K., Omori, H., Satoh, T., Kurotori, N., Maejima, I., Shirahama-Noda, K., Ichimura, T., Isobe, T., *et al.* (2009). Two Beclin 1-binding proteins, Atg14L and Rubicon, reciprocally regulate autophagy at different stages. Nature Cell Biology *11*, 385-U369.

Mizushima, N., Levine, B., Cuervo, A.M., and Klionsky, D.J. (2008). Autophagy fights disease through cellular self-digestion. Nature *451*, 1069-1075.

Mizushima, N., Noda, T., Yoshimori, T., Tanaka, Y., Ishii, T., George, M.D., Klionsky, D.J., Ohsumi, M., and Ohsumi, Y. (1998). A protein conjugation system essential for autophagy. Nature *395*, 395-398.

Mizushima, N., Yamamoto, A., Matsui, M., Yoshimori, T., and Ohsumi, Y. (2004). In vivo analysis of autophagy in response to nutrient starvation using transgenic mice expressing a fluorescent autophagosome marker. Mol Biol Cell *15*, 1101-1111.

Mizushima, N., Yoshimori, T., and Levine, B. (2010). Methods in mammalian autophagy research. Cell *140*, 313-326.

Mizushima, N., Yoshimori, T., and Ohsumi, Y. (2011). The role of Atg proteins in autophagosome formation. Annu Rev Cell Dev Biol *27*, 107-132.

Moreau, K., Ravikumar, B., Renna, M., Puri, C., and Rubinsztein, D.C. (2011). Autophagosome precursor maturation requires homotypic fusion. Cell *146*, 303-317.

Moreira, P.I., Santos, R.X., Zhu, X., Lee, H.G., Smith, M.A., Casadesus, G., and Perry, G. (2010). Autophagy in Alzheimer's disease. Expert Rev Neurother *10*, 1209-1218.

Morselli, E., Maiuri, M.C., Markaki, M., Megalou, E., Pasparaki, A., Palikaras, K., Criollo, A., Galluzzi, L., Malik, S.A., Vitale, I., *et al.* (2010). Caloric restriction and resveratrol promote longevity through the Sirtuin-1-dependent induction of autophagy. Cell Death Dis *1*, e10.

Murray, J.T., Panaretou, C., Stenmark, H., Miaczynska, M., and Backer, J.M. (2002). Role of Rab5 in the recruitment of hVps34/p150 to the early endosome. Traffic *3*, 416-427.

Nair, U., Jotwani, A., Geng, J., Gammoh, N., Richerson, D., Yen, W.L., Griffith, J., Nag, S., Wang, K., Moss, T., *et al.* (2011). SNARE proteins are required for macroautophagy. Cell *146*, 290-302.

Nakai, A., Yamaguchi, O., Takeda, T., Higuchi, Y., Hikoso, S., Taniike, M., Omiya, S., Mizote, I., Matsumura, Y., Asahi, M., *et al.* (2007). The role of autophagy in cardiomyocytes in the basal state and in response to hemodynamic stress. Nat Med *13*, 619-624.

Nemoto, T., Tanida, I., Tanida-Miyake, E., Minematsu-Ikeguchi, N., Yokota, M., Ohsumi, M., Ueno, T., and Kominami, E. (2003). The mouse APG10 homologue, an E2-like enzyme for Apg12p conjugation, facilitates MAP-LC3 modification. J Biol Chem *278*, 39517-39526.

Ohya, T., Miaczynska, M., Coskun, U., Lommer, B., Runge, A., Drechsel, D., Kalaidzidis, Y., and Zerial, M. (2009). Reconstitution of Rab- and SNARE-dependent membrane fusion by synthetic endosomes. Nature *459*, 1091-1097.

Opipari, A.W., Jr., Tan, L., Boitano, A.E., Sorenson, D.R., Aurora, A., and Liu, J.R. (2004). Resveratrol-induced autophagocytosis in ovarian cancer cells. Cancer Res *64*, 696-703.

Pan, J.A., Ullman, E., Dou, Z., and Zong, W.X. (2011). Inhibition of Protein Degradation Induces Apoptosis through a Microtubule-Associated Protein 1 Light Chain 3-Mediated Activation of Caspase-8 at Intracellular Membranes. Mol Cell Biol *31*, 3158-3170.

Pankiv, S., Clausen, T.H., Lamark, T., Brech, A., Bruun, J.A., Outzen, H., Overvatn, A., Bjorkoy, G., and Johansen, T. (2007). p62/SQSTM1 binds directly to Atg8/LC3 to facilitate degradation of ubiquitinated protein aggregates by autophagy. J Biol Chem *282*, 24131-24145.

Petiot, A., Ogier-Denis, E., Blommaart, E.F.C., Meijer, A.J., and Codogno, P. (2000). Distinct classes of phosphatidylinositol 3 '-kinases are involved in signaling pathways that control macroautophagy in HT-29 cells. Journal of Biological Chemistry *275*, 992-998.

Pickford, F., Masliah, E., Britschgi, M., Lucin, K., Narasimhan, R., Jaeger, P.A., Small, S., Spencer, B., Rockenstein, E., Levine, B., *et al.* (2008). The autophagy-related protein beclin 1 shows reduced expression in early Alzheimer disease and regulates amyloid beta accumulation in mice. J Clin Invest *118*, 2190-2199.

Polson, H.E., de Lartigue, J., Rigden, D.J., Reedijk, M., Urbe, S., Clague, M.J., and Tooze, S.A. (2010). Mammalian Atg18 (WIPI2) localizes to omegasome-anchored phagophores and positively regulates LC3 lipidation. Autophagy *6*.

Postic, C., and Magnuson, M.A. (2000). DNA excision in liver by an albumin-Cre transgene occurs progressively with age. Genesis *26*, 149-150.

Ravikumar, B., Duden, R., and Rubinsztein, D.C. (2002). Aggregate-prone proteins with polyglutamine and polyalanine expansions are degraded by autophagy. Hum Mol Genet *11*, 1107-1117.

Ravikumar, B., Imarisio, S., Sarkar, S., O'Kane, C.J., and Rubinsztein, D.C. (2008). Rab5 modulates aggregation and toxicity of mutant huntingtin through macroautophagy in cell and fly models of Huntington disease. J Cell Sci *121*, 1649-1660.

Ruck, A., Attonito, J., Garces, K.T., Nunez, L., Palmisano, N.J., Rubel, Z., Bai, Z., Nguyen, K.C., Sun, L., Grant, B.D., *et al.* (2011). The Atg6/Vps30/Beclin 1 ortholog BEC-1 mediates endocytic retrograde transport in addition to autophagy in C. elegans. Autophagy *7*, 386-400.

Santos, R.X., Cardoso, S., Correia, S., Carvalho, C., Santos, M.S., and Moreira, P.I. (2010). Targeting autophagy in the brain: a promising approach? Cent Nerv Syst Agents Med Chem *10*, 158-168.

Sarbassov, D.D., Ali, S.M., and Sabatini, D.M. (2005). Growing roles for the mTOR pathway. Current Opinion in Cell Biology *17*, 596-603.

Sarkar, S., Davies, J.E., Huang, Z., Tunnacliffe, A., and Rubinsztein, D.C. (2007). Trehalose, a novel mTOR-independent autophagy enhancer, accelerates the clearance of mutant huntingtin and alpha-synuclein. J Biol Chem *282*, 5641-5652.

Sartore-Bianchi, A., Martini, M., Molinari, F., Veronese, S., Nichelatti, M., Artale, S., Di Nicolantonio, F., Saletti, P., De Dosso, S., Mazzucchelli, L., *et al.* (2009). PIK3CA mutations in colorectal cancer are associated with clinical resistance to EGFR-targeted monoclonal antibodies. Cancer Res *69*, 1851-1857.
Shin, H.W., Hayashi, M., Christoforidis, S., Lacas-Gervais, S., Hoepfner, S., Wenk, M.R., Modregger, J., Uttenweiler-Joseph, S., Wilm, M., Nystuen, A., *et al.* (2005). An enzymatic cascade of Rab5 effectors regulates phosphoinositide turnover in the endocytic pathway. Journal of Cell Biology *170*, 607-618.

Simonsen, A., and Tooze, S.A. (2009). Coordination of membrane events during autophagy by multiple class III PI3-kinase complexes. Journal of Cell Biology *186*, 773-782.

Singh, R., Xiang, Y., Wang, Y., Baikati, K., Cuervo, A.M., Luu, Y.K., Tang, Y., Pessin, J.E., Schwartz, G.J., and Czaja, M.J. (2009). Autophagy regulates adipose mass and differentiation in mice. J Clin Invest *119*, 3329-3339.

Sopasakis, V.R., Liu, P., Suzuki, R., Kondo, T., Winnay, J., Tran, T.T., Asano, T., Smyth, G., Sajan, M.P., Farese, R.V., *et al.* (2010). Specific roles of the p110alpha isoform of phosphatidylinsositol 3-kinase in hepatic insulin signaling and metabolic regulation. Cell Metab *11*, 220-230.

Stenmark, H., Parton, R.G., Steele-Mortimer, O., Lutcke, A., Gruenberg, J., and Zerial, M. (1994). Inhibition of rab5 GTPase activity stimulates membrane fusion in endocytosis. EMBO J *13*, 1287-1296.

Sun, Q., Fan, W., Chen, K., Ding, X., Chen, S., and Zhong, Q. (2008). Identification of Barkor as a mammalian autophagy-specific factor for Beclin 1 and class III phosphatidylinositol 3-kinase. Proc Natl Acad Sci U S A *105*, 19211-19216.

Takahashi, Y., Meyerkord, C.L., Hori, T., Runkle, K., Fox, T.E., Kester, M., Loughran, T.P., and Wang, H.G. (2011). Bif-1 regulates Atg9 trafficking by mediating the fission of Golgi membranes during autophagy. Autophagy *7*, 61-73.

Takamura, A., Komatsu, M., Hara, T., Sakamoto, A., Kishi, C., Waguri, S., Eishi, Y., Hino, O., Tanaka, K., and Mizushima, N. (2011). Autophagy-deficient mice develop multiple liver tumors. Genes Dev *25*, 795-800.

Ullman, E., Fan, Y., Stawowczyk, M., Chen, H.M., Yue, Z., and Zong, W.X. (2008). Autophagy promotes necrosis in apoptosis-deficient cells in response to ER stress. Cell Death and Differentiation *15*, 422-425.

Urick, M.E., Rudd, M.L., Godwin, A.K., Sgroi, D., Merino, M., and Bell, D.W. (2011). PIK3R1 (p85alpha) is somatically mutated at high frequency in primary endometrial cancer. Cancer Res *71*, 4061-4067.

Vadas, O., Burke, J.E., Zhang, X., Berndt, A., and Williams, R.L. (2011). Structural basis for activation and inhibition of class I phosphoinositide 3-kinases. Sci Signal *4*, re2.

Vanhaesebroeck, B., Guillermet-Guibert, J., Graupera, M., and Bilanges, B. (2010). The emerging mechanisms of isoform-specific PI3K signalling. Nat Rev Mol Cell Biol *11*, 329-341.
Vanhaesebroeck, B., Stephens, L., and Hawkins, P. (2012). PI3K signalling: the path to discovery and understanding. Nat Rev Mol Cell Biol *13*, 195-203.

Velichkova, M., Juan, J., Kadandale, P., Jean, S., Ribeiro, I., Raman, V., Stefan, C., and Kiger, A.A. (2010). Drosophila Mtm and class II PI3K coregulate a PI(3)P pool with cortical and endolysosomal functions. J Cell Biol *190*, 407-425.

Vieira, O.V., Botelho, R.J., Rameh, L., Brachmann, S.M., Matsuo, T., Davidson, H.W., Schreiber, A., Backer, J.M., Cantley, L.C., and Grinstein, S. (2001). Distinct roles of class I and class III phosphatidylinositol 3-kinases in phagosome formation and maturation. J Cell Biol *155*, 19-25.

Volpicelli, L.A., Lah, J.J., and Levey, A.I. (2001). Rab5-dependent trafficking of the m4 muscarinic acetylcholine receptor to the plasma membrane, early endosomes, and multivesicular bodies. J Biol Chem *276*, 47590-47598.

Werner, E.D., Lee, J., Hansen, L., Yuan, M., and Shoelson, S.E. (2004). Insulin resistance due to phosphorylation of insulin receptor substrate-1 at serine 302. J Biol Chem *279*, 35298-35305.

Wheeler, M., and Domin, J. (2001). Recruitment of the class II phosphoinositide 3-kinase C2beta to the epidermal growth factor receptor: role of Grb2. Mol Cell Biol *21*, 6660-6667.

Wiederschain, D., Wee, S., Chen, L., Loo, A., Yang, G., Huang, A., Chen, Y., Caponigro, G., Yao, Y.M., Lengauer, C., *et al.* (2009). Single-vector inducible lentiviral RNAi system for oncology target validation. Cell Cycle *8*, 498-504.

Wong, E., and Cuervo, A.M. (2010). Autophagy gone awry in neurodegenerative diseases. Nat Neurosci *13*, 805-811.

Wu, C.Y., Jia, Z., Wang, W., Ballou, L.M., Jiang, Y.P., Chen, B., Mathias, R.T., Cohen, I.S., Song, L.S., Entcheva, E., *et al.* (2011). PI3Ks maintain the structural integrity of T-tubules in cardiac myocytes. PLoS One *6*, e24404.

Yan, Y., Flinn, R.J., Wu, H.Y., Schnur, R.S., and Backer, J.M. (2009). hVps15, but not Ca2+/CaM, is required for the activity and regulation of hVps34 in mammalian cells. Biochemical Journal *417*, 747-755.

Yu, J., Zhang, Y., McIlroy, J., Rordorf-Nikolic, T., Orr, G.A., and Backer, J.M. (1998). Regulation of the p85/p110 phosphatidylinositol 3'-kinase: stabilization and inhibition of the p110alpha catalytic subunit by the p85 regulatory subunit. Mol Cell Biol *18*, 1379-1387.

Yue, Z., Jin, S., Yang, C., Levine, A.J., and Heintz, N. (2003). Beclin 1, an autophagy gene essential for early embryonic development, is a haploinsufficient tumor suppressor. Proc Natl Acad Sci U S A *100*, 15077-15082.

Zerial, M., and McBride, H. (2001). Rab proteins as membrane organizers. Nat Rev Mol Cell Biol *2*, 107-117.

Zhang, H., Cicchetti, G., Onda, H., Koon, H.B., Asrican, K., Bajraszewski, N., Vazquez, F., Carpenter, C.L., and Kwiatkowski, D.J. (2003). Loss of Tsc1/Tsc2 activates mTOR and disrupts PI3K-Akt signaling through downregulation of PDGFR. J Clin Invest *112*, 1223-1233.

Zhang, X., Vadas, O., Perisic, O., Anderson, K.E., Clark, J., Hawkins, P.T., Stephens, L.R., and Williams, R.L. (2011). Structure of lipid kinase p110beta/p85beta elucidates an unusual SH2-domain-mediated inhibitory mechanism. Mol Cell *41*, 567-578.

Zhao, J.J., Cheng, H., Jia, S., Wang, L., Gjoerup, O.V., Mikami, A., and Roberts, T.M. (2006). The p110alpha isoform of PI3K is essential for proper growth factor signaling and oncogenic transformation. Proc Natl Acad Sci U S A *103*, 16296-16300.

Zhong, Y., Wang, Q.J., Li, X.T., Yan, Y., Backer, J.M., Chait, B.T., Heintz, N., and Yue, Z.Y. (2009). Distinct regulation of autophagic activity by Atg14L and Rubicon associated with Beclin 1-phosphatidylinositol-3-kinase complex. Nature Cell Biology *11*, 468-U262.

Zhou, X., Takatoh, J., and Wang, F. (2011). The mammalian class 3 PI3K (PIK3C3) is required for early embryogenesis and cell proliferation. PLoS One *6*, e16358.

Zhou, X., Wang, L., Hasegawa, H., Amin, P., Han, B.X., Kaneko, S., He, Y., and Wang, F. (2010). Deletion of PIK3C3/Vps34 in sensory neurons causes rapid neurodegeneration by disrupting the endosomal but not the autophagic pathway. Proc Natl Acad Sci U S A.

Zhu, H., Tannous, P., Johnstone, J.L., Kong, Y., Shelton, J.M., Richardson, J.A., Le, V., Levine, B., Rothermel, B.A., and Hill, J.A. (2007). Cardiac autophagy is a maladaptive response to hemodynamic stress. J Clin Invest *117*, 1782-1793.

Zoncu, R., Efeyan, A., and Sabatini, D.M. (2011). mTOR: from growth signal integration to cancer, diabetes and ageing. Nat Rev Mol Cell Biol *12*, 21-35.